University of Alberta

Nucleoside transport across mouse intestinal epithelium

by

Kelly Mitchell Kosheiff 

A thesis submitted to the Faculty of Graduate Studies and Research

in partial fulfillment of the requirements for the degree of

Master of Science

Department of Physiology

Edmonton, Alberta

Fall 2008

Your file Votre référence
ISBN: 978-0-494-47282-8
Our file Notre référence
ISBN: 978-0-494-47282-8

Abstract

Nucleosides formed by breakdown of dietary nucleotides and nucleic acids are absorbed across the intestinal epithelium, but the mechanism(s) by which this occurs are poorly understood. The current hypotheses of trans-epithelial fluxes of nucleosides favor models in which CNTs take up nucleosides from the intestinal lumen across the apical membrane, while ENTs release and/or take up nucleosides at the basolateral membrane. The specific types of CNTs and ENTs involved are unknown. Intact mouse intestinal epithelial tissue was used to examine the mechanism(s) by which particular radiolabelled nucleosides are transported trans-cellularly using the Ussing chamber experimental apparatus. Key findings are: (i) that both purine and pyrimidine nucleosides exhibit trans-epithelial transport, (ii) that the primary intestinal locus of this transport is jejunum, (iii) that the majority of this flux is Na^+-dependent and requires the presence of Na^+ at the apical membrane, and (iv) that cross-competition and CNT3 knock-out studies implicate broad specificity CNT3 in the process.

Table of Contents

List of Tables

List of Figures

Chapter 2

Chapter 3

List of abbreviations

5'DFUR	5'-deoxy-5-fluorouridine
Acylovir	9-(2-hydroxyethanoxymethyl)guanine ; ACV
ATP	adenosine 5'triphosphate
Balb/c	wildtype mice strain
cAMP	3', 5'- cyclic adenosine monophosphate
CDK	cyclin dependent kinase
CDKI	cyclin dependent kinase inhibitor
Capecitabine	*N*-[1-(5-deoxy-β-D-ribofuranosyl)-5-fluoro-1,2-dihydro-2-oxo-4-pyrimidyl]-*n*-pentylcarbamate ; Xeloda
CFTR	Cystic Fibrosis Transmembrane conductance Regulator
Ch^+ KHS	choline substituted, bicarbonate free Krebs-Henseleit solution
Cladribine	2-chloro-2'-deoxyadenosine
Clofarabine	2-chloro-9-(2'-deoxy-2'-fluoro-b-D-arabinofuranosyl) adenine, Cl-FaraA
CNT	concentrative nucleoside transporter
CNT3 (-/-)	homozygous FVB/N CNT3 null mice
CNT3 (+/+)	homozygous FVB/N wildtype mice
CPM	counts per minute
Ct	cycle threshold for PCR reactions
Cytarabine	1-(darabinofuranosyl)cytosine, AraC
Didanosine	2'3'-dideoxyinosine, ddI

Dilazep	3-[4-[3-(3,4,5-Trimethoxybenzoyl)oxypropyl]-1,4-diazepan-1-yl]propyl 3,4,5-trimethoxybenzoate
Dipyridamole	2-{[9-(bis(2-hydroxyethyl)amino)-2,7-bis(1-piperidyl)-3,5,8,10-tetrazabicyclo[4.4.0]deca-2,4,7,9,11-pentaen-4-yl]-(2-hydroxyethyl)amino}ethanol
Draflazine	2-aminocarbonyl-N-(4-amino-2,6-dichlorophenyl)-4-(5,5-bis(4-fluorophenyl)-pentyl)-1-piperazineacetamide
ENT	equilibrative nucleoside transporter
ENT3	equilibrative nucleoside transporter 3
ENT4	equilibrative nucleoside transporter 4
Fludarabine	2-fluoro-2'-deoxyadenosine
Ganciclovir	9-[(1,3-dihydroxy-2-propoxy)methyl]guanine
GAPDH	glyceraldehyde phosphate dehydrogenase
Gemcitabine	2', 2'-difluoro-2'-deoxycytine
G_s	stimulatory G protein
hCNT1	human concentrative nucleoside transporter 1
hCNT2	human concentrative nucleoside transporter 2
hCNT3	human concentrative nucleoside transporter 3
hENT1	human equilibrative nucleoside transporter 1
hENT2	human equilibrative nucleoside transporter 2
HEPES	*N*-2-hydroxyethylpiperazine-*N*'-2-ethanesulfonic acid
hRPTC	human renal proximal convoluted tubule cells
I_{sc}	short circuit current
KHS	Krebs-Henseleit solution
K_m	Michalis-Menten constant for kinetic analysis measure of affinity
Lamivudine	3'-thiacytidine ; 3TC

LSC	liquid scintillation cocktail
mCNT1	mouse concentrative nucleoside transporter 1
mCNT2	mouse concentrative nucleoside transporter 2
mCNT3	mouse concentrative nucleoside transporter 3
mENT1	mouse equilibrative nucleoside transporter 1
mENT2	mouse equilibrative nucleoside transporter 2
Na^+ KHS	sodium containing, bicarbonate free Krebs-Henseleit solution
NBMPR	nitrobenzylmercaptopurine ribonucleoside, nitrobenzylthioinosine, 6-[(4-nitrobenzyl)thio]-9-(β-D-ribofuranosyl)purine
NT	nucleoside transporter
OCTN2	organic cation/carnitine transporter 2
PCT	proximal convoluted tubule
R	linear correlation coefficient
rCNT1	rat concentrative nucleoside transporter 1
rCNT2	rat concentrative nucleoside transporter 2
rCNT3	rat concentrative nucleoside transporter 3
rENT1	rat equilibrative nucleoside transporter 1
rENT2	rat equilibrative nucleoside transporter 2
Rf	retention factor for TLC migration
Ribavirin	1--β-D-ribofuranosyl-1,2,4-triazole-3-carboxamide
RT-PCR	reverse transcriptase polymerase chain reaction
SEM	standard error of mean
SLC28	solute carrier family 28; concentrative nucleoside transporter

SLC28a3	solute carrier family 28 isoform a3; CNT3
SLC29	solute carrier family 29; equilbrative nucleoside transporter
Stavudine	2', 3'-didehydro-3'-deoxythymidine ; d4T
TER	transepithelial resistance
TLC	thin layer chromatography
UMP	uridine monophosphate
V_{max}	velocity of transport with maximum amount of substrate
Zalcitabine	2', 3'-dideoxycytidine, ddC
Zidovudine	3'-azido-2', 3'-dideoxythymidine, ZDV, AZT

Chapter 1 Introduction

1.1 Ussing Chamber

In the early 1950s Hans Ussing developed an apparatus designed to measure electrical currents across isolated frog skin. He discovered, using $^{24}Na^{+}$, that short-circuit current recordings across frog skin were due to the movement of Na^{+} ions across the epithelium (Ussing and Zerahn, 1951). Ussing continued to use his apparatus to characterize the transport of other ions across epithelia. The value of the Ussing chamber system was soon recognized by the wider scientific community, spawning its use in a variety of different experimental situations. These included the use of this system to study transport across intestinal epithelial tissues to compliment previous discoveries made concerning intestinal epithelial transport (Frizzell and Schultz, 1979; Schultz *et al.*, 1985).

The power of the Ussing chamber lies in its ability to separate the basolateral and apical surfaces of the epithelium. This also allows different incubating media to be applied to the apical and basolateral membranes and different drugs and mediators to be added independently to the apical and basolateral surfaces (Ghanem *et al.*, 2004; Lam *et al.*, 2004; Li *et al.*, 2004). Furthermore, the defining characteristics of epithelial tissue are polarity and tightness. The Ussing chamber allows both of these properties to be maintained; polarity due to having separate apical and basolateral chambers, and tightness due to maintenance of tight junctions. Maintenance of tight junction integrity throughout Ussing chamber experiments is demonstrated by constant paracellular permeability to mannitol (Polentarutti *et al.*, 1999). Another advantage of Ussing

chambers is that various electrical parameters such as transepithelial resistance, potential difference, impedance and short circuit current can be recorded over the duration of experiments (Polentarutti *et al.*, 1999; Li *et al.*, 2004; van de Kerkhof *et al.*, 2006). These electrical parameters have value in assessing tissue viability and functional activity of ion transport (Polentarutti *et al.*, 1999; Lam *et al.*, 2003; Ghanem *et al.*, 2004; Lam *et al.*, 2004; van de Kerkhof *et al.*, 2006). More recently, the Ussing chamber has been used to study the transport of radiolabelled substances across epithelial cell layers (Ungell *et al*, 1997; Kato *et al.*, 2000; Errasti-Murugarren *et al.*, 2007). Intestinal epithelium can be isolated from attached smooth muscle and connective tissue, thereby allowing only the epithelium to be studied in transepithelial flux experiments (Lam *et al*, 2003, Lam *et al*, 2004; Kato *et al.*, 2006; Hayashi *et al.*, 2007; Zhang *et al.*, 2007a).

The most common applications of Ussing chambers have been measurements of short circuit current (I_{sc}). Typically, a specific drug is added to either the basolateral or apical chambers, and the resulting I_{sc} is recorded. This is carried out under various conditions, which can lead to conclusions concerning epithelial function. For example, Lam *et al.* (2003) used mouse colon epithelium to study Cl^- transport using Ussing chamber experiments. It was shown that the α_2 adrenergic receptor antagonist, UK 14,304, caused a reduction in transepithelial (I_{sc}) current recording, illustrating that the Ussing chamber can detect electrical differences upon application of certain drugs. Furthermore, it was shown that the reason for the reduction in transepithelial current was due to inhibition of Cl^- secretion through CFTR (Cystic Fibrosis Transmembrane Conductance Regulator), because (i) the UK 14,304-induced reduction of current still occurred in the presence of drugs blocking apical Na^+ and K^+ channels (ii) the UK 14,304

effect was lost in Cl^- free media (iii) the effect was lost in mouse tissue lacking the CFTR Cl^- channel, and (iv) there was a decrease in $^{36}Cl^-$ basolateral-to-apical, but not apical-to-basolateral flux, in the presence of UK 14,304. These experiments demonstrate the variety of applications that the Ussing chamber can have. Since substances remain in the circulating media for the duration of the experiment, drugs can be added sequentially in order to discover the drug's mechanism of action. Moreover, buffering media can be altered to include or exclude various electrolytes. Different tissues can also be used, including tissues with particular channels or transporters knocked out. Finally, tracer radiolabelled substances can be added to one side of the Ussing chamber and sampled from the opposite side to show transepithelial flux of the substance under various conditions. When all of the above applications are put together, an accurate depiction of a physiological process can be determined.

In the experiments undertaken and described in this thesis, the above uses of the Ussing chamber were adapted to examine radiolabelled nucleoside transport across mouse intestinal epithelial cells. The difference between our experiments, involving nucleoside flux determinations, and the experiments completed by Lam *et al.* (2003), for example, was that the latter experiments involved relatively large ion fluxes through ion channels, whereas the thesis experiments assessed the slower movement of larger molecules across the epithelium using transporters. The evaluation of transepithelial transporter-mediated processes in epithelia has been examined both for mouse intestinal tissue and for nucleoside transporters, but not both together. The Ussing chamber apparatus, for example, was used to analyze the role of the organic cation/carnitine transporter, OCTN2, in carnitine transport across the mouse small intestine epithelium.

This involved addition of ^{3}H-carnitine to the apical chamber and sampling from the basolateral chamber under various conditions, such as with or without Na^{+} in the buffering medium, and using tissue from wild-type or OCTN2 null mice (Kato *et al.*, 2006). Transepithelial fluxes of radiolabelled nucleosides have also been examined, but only in transwell cell culture experiments using either human colonic Caco-2 cells (He *et al.*, 1994), rat small intestinal IEC-6 cells (He *et al.*, 1994; Aymerich *et al.*, 2004), a murine proximal tubule cell line (PCT) (Errasti-Murugarren *et al.*, 2007), or primary cultures of human proximal tubule epithelium (Damaraju *et al.*, 2007; Elwi *et al.*, 2008).

As described in this thesis, adapting Ussing chamber methodology to studies of transepithelial nucleoside fluxes proved to be a very effective and versatile way of investigating the mechanism of transfer of nucleosides across mouse intestinal epithelial cells. Not only was this a novel application of the Ussing chamber apparatus, and more physiologically relevant than transwell cell culture studies, the method proved advantageous over other previous attempts to characterize intestinal nucleoside transport employing isolated enterocytes, purified brush-boarder and basolateral membrane vesicles, or intestinally-derived recombinant transporters produced in *Xenopus* oocytes, each of which resulted in a loss of polarity of the epithelial cells (Vijayalakshmi and Belt, 1988; Jarvis, 1989; Betcher *et al.*, 1990; Roden *et al.*, 1991; Huang *et al.*, 1993; 1994; Patil and Unadkat, 1997).

1.2 Handling of nucleosides in the intestine

1.2.1 Source of nucleosides supplied to the intestine

The nucleosides used by the intestine come from the intestinal lumen and the blood stream. The supply from the lumen is from two sources; epithelial cells that have sloughed off from the rest of the epithelium and from the diet (Young *et al*, 2001). Enterocytes are produced at the crypts of the intestinal epithelium, migrate toward the villus tip, differentiating along the way, and are continuously released from the surface of the intestinal epithelium into the lumen. This process takes place over a span of 2 – 4 days, by which means the epithelium is in a continual state of renewal (Cheng and Bjerknes, 1985; Potten and Loeffler, 1987; Young *et al.*, 2001). Free enterocytes in the intestinal lumen are then degraded releasing nucleoproteins which, in combination with dietary nucleoproteins, are degraded to nucleic acids by proteases. The combined enzymatic activity of pancreatic nucleases and apical alkaline phosphatase produces nucleosides (Valdes *et al.*, 2000; Young *et al.*, 2001).

Energetically expensive to make, and in a tissue with limited *de novo* biosynthetic capability, exogenous nucleosides are readily and necessarily taken up into enterocytes in order to allow for the rapid growth that is a defining characteristic of these cells (Valdes *et al.*, 2000). Nucleosides are required for growing cell populations because they are direct precursors of nucleotides, including ATP, which in turn determines the cell's energy levels and is required for protein, RNA and DNA synthesis and, therefore, cellular division (King *et al.*, 2006). Hydrophilic in nature, passage of nucleosides across enterocyte plasma membranes is mediated by specialized nucleoside transporter (NT) proteins (Uauy *et al.*, 1990, Aymerich *et al.*, 2005; Pastor-Anglada *et al.*, 2007).

1.2.2 Metabolism of intestinal nucleosides

Early studies of intestinal nucleoside metabolism found that nucleosides are extensively metabolized and released in the form of various metabolites. Such studies, using isolated rat intestinal loops, determined that pyrimidine nucleosides were metabolized to the corresponding free nucleobase, and that purine nucleosides were metabolized more extensively to uric acid (Bronk and Hastewell, 1988; Stow and Bronk, 1992). In contrast, Vijayalakshmi and Belt (1988) found that 60% of the pyrimidine nucleoside, thymidine, remained in its nucleoside form, and that 95 % of the poorly metabolized purine nucleoside formycin B remained in its nucleoside form following uptake into enterocytes. On the other hand, transwell studies carried out using differentiated Caco-2 cultured cells found that no purine nucleosides were collected from the basolateral side in their nucleoside form, following transepithelial flux, but instead were in the form of uric acid and nucleobases (He *et al.*, 1994). Pyrimidine nucleosides were also found to be mostly converted to nucleobases; however, there was a small component (20 %) that was still in their nucleoside form (He *et al.*, 1994). In vascularly perfused rat jejunum, most uridine was converted to uracil, with some moving across the epithelium as intact uridine (Young *et al.*, 2001) because of the relatively high activity of uridine phosphorylase, which converts uridine to uracil. When the uridine phosporylase gene was deleted in mice, there was more than five times higher gut uridine levels than in wildtype mice, indicating that uridine is metabolized to uracil in wild-type animals (Cao *et al.*, 2005). This study also found that in the absence of uridine phosphorylase, intestinal nucleotide levels increased. Because intestinal nucleoside and nucleotide levels were measured using whole tissue extracts, and because of the complexity of metabolic effects observed with the deletion of the uridine phosporylase gene, it was difficult to

make precise conclusions concerning uridine metabolism within enterocytes (Cao *et al.*, 2005).

Thus, the literature has proved to be quite varied concerning nucleoside metabolism within the intestinal epithelium, a variation that is the result of the different *in vitro* systems used, how well they mimic *in vivo* enzymatic activity, and because the nucleoside enzymatic machinery is regulated by exogenous factors such as nutrition (Young *et al.*, 2001). Despite these differences, the consensus is that purine nucleosides are more extensively metabolized than pyrimidine nucleosides, and that both types of nucleosides are found mostly in their respective nucleobase forms following transport in and/or through intestinal epithelial cells.

1.2.3 Nucleosides as regulatory molecules of proliferation and differentiation in the intestine

Nucleosides act upon the intestinal epithelium to regulate cell proliferation and differentiation (Sanderson and He, 1994). As previously mentioned, the intestinal epithelium undergoes rapid turnover of its cells. This involves division of intestinal crypt cells, yielding enterocytes which mature as they migrate to the villus tip where they undergo apoptosis and are released into the intestinal lumen (Cheng and Bjerknes, 1985, Potten and Loeffler, 1987, Young *et al.*, 2001, Stehr *et al.*, 2005). The processes of division, differentiation and apoptosis all depend upon regulation of the cell cycle which, in turn, depends on regulatory molecules such as cyclin-dependent kinases (CDK). CDKs are regulated by cyclin-dependent kinase inhibitors (CDKI), which have been found to control the differentiation processes in enterocytes (Stehr *et al.*, 2005). Furthermore, novel nucleoside analogue anticancer drugs are pharmacological CDKIs

(Schang *et al.*, 2005). The precise mechanism by which CDKIs influence enterocyte differentiation is not currently known; however, it is possible that the supply of nucleosides to the intestine influences the growth and differentiation of enterocytes through intetacting with CDKs and the cell cycle. This is plausible because it has been observed that in both Caco-2 and IEC-6 intestinal cell lines there was increased enterocyte proliferation upon addition of nucleosides (Sanderson and He, 1994). It should be noted that in these studies, the nucleoside supply was provided as nucleotides. For Caco-2 cells the effect was only present when the cells were deprived of glutamine and non-essential amino acids (Sanderson and He, 1994). However, regardless of conditions, IEC-6 intestinal cells showed increased growth in the presence of nucleosides (Sanderson and He, 1994). Furthermore, IEC-6 is a non-differentiated crypt-like cell line, but differentiates into enterocytes when grown on a collagen matrix. These cells displayed increased differentiation with the addition of nucleosides (given as nucleotides) as evidenced by increased alkaline phoshatase and sucrase activity (Sanderson and He, 1994).

Another effect that nucleosides have on the intestinal epithelium is regulation of the expression of intestinal nucleoside transporters (NT). It has been demonstrated that rats subjected to 48 h fasting had elevated amounts of concentrative nucleoside transporter 1 (CNT1) protein in jejunum brush-border vesicle preparations, and a corresponding increase in thymidine uptake into the vesicles (Valdes *et al.*, 2000). The effect of fasting was mimicked when rats were given nucleotide-deprived diets (Valdes *et al.*, 2000). Therefore, the presence of nucleosides in the intestine impacts the expression and activity of NTs.

In sum, nucleosides have been shown to influence enterocyte proliferation as well as differentiation, through process that are unknown, but potentially through interaction with various cyclin-dependent kinases. Nucleosides also influence the expression of NTs in the intestine.

1.2.4 Nucleoside interactions with intestinal purinergic receptors

Adenosine, a purine nucleoside, has been found to stimulate chloride secretion in the small intestine, indicated by changes in short circuit current (I_{sc}) (Mun *et al.,* 1998; Ghanem *et al.*, 2005). There are several types of adenosine (purinergic) receptors expressed in the intestine, including A_1, A_{2a}, A_{2b}, and A_3. In the mouse jejunal epithelium, A_{2b} had much greater expression than A_{2a} and A_3, both of which were more abundant than A_1 (Mun *et al.,* 1998). Here, A_{2b} receptors at the basolateral membrane have been shown to activate Cl^- secretion through a G_s-cAMP-adenylate cyclase (isoform 6) pathway, whereas A_{2a} receptor activation in mouse colon inhibits Cl^- secretion (Mun *et al.*, 1998; Lam *et al.*, 2003; Ghanem *et al.*, 2005; Kolachala *et al.*, 2006). Because A_{2b} is the most abundant adenosine receptor in the jejunum, and because activation of this receptor leads to Cl^- secretion, the predominant role of adenosine in the small intestine is to stimulate Cl^- and therefore fluid secretion. Furthermore, the presence of luminal adenosine in mouse jejunal epithelium preparations can also activate Cl^- and fluid secretion via A_1 receptor activation (Ghanem *et al.*, 2005). The extent of activation of the basolateral A_{2b} and the apical A_1 receptors leading to Cl- secretion will depend upon availability of adenosine to these receptors. The interaction between adenosine receptors and nucleoside transporters has been examined in T84 intestinal epithelial cells, with the observation that nucleoside transporters control the amount of adenosine available to

activate its receptors (Mun *et al.*, 1998). It has also been established in rabbit ileum epithelial cells that when Na^+-independent equilibrative nucleoside transporter 1 (ENT1) was inhibited by dipyridimole or NBMPR (nitrobenzylthioinosine, S-(4-nitrobenzyl)-6-thioinosine, nitrobenzylmercaptopurine ribonucleoside), there was a corresponding substantial increase in Cl^- secretion (Dobbins *et al.*, 1984). Taken together, these observations suggest that nucleoside transporters have a role in controlling Cl^- secretion in the intestine.

1.2.5 Nucleoside transport in the intestine

Nucleosides play crucial roles in the intestinal mucosa, including involvement in metabolism, cell proliferation, cell differentiation and control of signaling molecules (Sections 1.2.1 - 1.2.4). All of these essential functions require nucleosides to be taken up into intestinal epithelial cells through nucleoside transporters (NTs). Knowledge of the nature and mechanisms of intestinal nucleoside transport is, therefore, required in order to fully understand the physiological effects that nucleosides have on the intestinal epithelium. Such an understanding is not presently available. Current hypotheses favour the view that nucleoside transport across the intestinal epithelium follows the same general model as intestinal glucose transport, in that there are Na^+-dependent concentrative transport processes at the apical membrane for uptake into the enterocyte, and Na^+-independent equilibrative transport processes at the basolateral membrane for exit from the cell (Ngo *et al.*, 2001; Young *et al.*, 2001). Early evidence confirmed this hypothesis by showing that uptake of adenosine into rabbit ileum apical (brush-border) membrane vesicles was dependent upon Na^+ being present in the bathing medium, and that uptake could be stimulated by applying an inwardly negative electrical gradient

(Betcher *et al.*, 1990). This suggested that nucleosides were transported across the apical membrane through an electrogenic, Na^+-coupled process. Other studies using brush border membrane vesicle preparations from rabbit ileum, rabbit jejunum and human jejunum produced similar observations (Williams *et al.*, 1989; Roden *et al.*, 1991; Patil and Unadkat, 1997). In addition to finding that the apical membrane transported nucleosides in a concentrative and Na^+-dependent manner, these studies were also able to provide data supporting that the Na^+:nucleoside coupling ratio was 1:1, and that at least two distinct Na^+-dependent transport processes with different permeant specificities were involved (Patil and Unadkat, 1997). These two types of Na^+-dependent transport were termed N1 or *cif* and N2 or *cit*, and were purine nucleoside specific and pyrimidine nucleoside specific, respectively (nomenclature for nucleoside transporters is described in detail in Section 1.3.1). The presence of at least two separate concentrative Na^+-dependent nucleoside transport processes at the apical membrane in intestinal epithelial cells has also been demonstrated in studies of isolated mouse enterocytes (Vijayalakshmi and Belt, 1988). Thymidine, a pyrimidine nucleoside, and formycin B, a purine nucleoside, were both taken up in a Na^+-dependent manner. However, thymidine uptake was inhibited by other pyrimidine nucleosides, but not by purine nucleosides (with the exception of uridine), and formycin B uptake was inhibited by other purine nucleosides, but not by pyrimidine nucleosides. This suggested that purine and pyrimidine nucleosides, with the exception of uridine, used different nucleoside transporters (Vijayalakshmi and Belt, 1988). Apparent inconsistencies with the notion of two separate nucleoside transport processes were observations that purine nucleosides adenosine and its derivatives tubercidin and deoxyadenosine could inhibit the supposedly

pyrimidine nucleoside specific nucleoside transporter (Vijayalakshmi and Belt, 1988). Thus, uridine, adenosine and adenosine analogues seemingly shared otherwise functionally separate purine and pyrimidine nucleoside transport systems.

Additional complexity with regard to mechanisms of concentrative nucleoside transport in intestine was revealed by the discovery of a novel broad specificity Na^+-dependent nucleoside transport process for both purine and pyrimidine nucleosides in *Xenopus* oocytes microinjected with rat jejunal enterocyte mRNA (Huang *et al.*, 1993), a process also revealed in rabbit choroid plexus and human myeloid cell lines, and termed the N3 or *cib* transport process (Wu *et al.*, 1992; Belt *et al.*, 1993).

Beginning in 1994 with the cDNA cloning of rat (r) CNT1 from a rat jejunal cDNA library (Huang *et al.*, 1994), the proteins responsible for each of the three concentrative nucleoside transport processes present in human and other mammalian cells and tissues have been identified and characterized, and are designated CNT1 (*cit*), CNT2 (*cif*) and CNT3 (*cib*) (please see Section 1.3 for details).

Complementary to investigations of nucleoside uptake into apical membrane vesicles, Betcher *et al.* (1990) also examined nucleoside uptake into rabbit ileum basolateral membrane vesicles. Combined with parallel investigations of basolateral membrane vesicles from rabbit renal outer cortex (Williams *et al.*, 1989), these studies showed that basolateral nucleoside transporters did not depend upon Na^+, and could be inhibited by the equilibrative (*es*-type) nucleoside transport inhibitor NBMPR. As detailed in Section 1.3, the nucleoside transport protein responsible for *es*-type functional activity is designated ENT1, while that responsible for a corresponding equilibrative

nucleoside transport process that is insensitive to inhibition by NBMPR (*ei*) is designated ENT2.

The use of isolated enterocytes and brush border and basolateral membrane vesicles, or investigation of intestinally-derived recombinant nucleoside transporters produced in *Xenopus* oocytes, however, does not accurately depict physiological nucleoside transport in the intact epithelium. Formycin B uptake into and transepithelial flux across intact rabbit jejunal epithelium was examined by Roden *et al.* (1991). The use of this more physiological preparation confirmed that uptake of nucleosides at the apical membrane was dependent on Na^+, and that at the basolateral was Na^+-independent. It was further shown that the transepithelial flux across the jejunum was greater in the apical-to-basolateral direction than in the basolateral-to-apical direction, indicating vectorial flux of nucleosides (Roden *et al*, 1991).

Other approaches towards characterization of intestinal nucleoside transport have involved use of cultured cell lines. These studies report a variety of results, likely due to significant differences in origin and behavior of the different cell lines used, and between cultured cells and native cells, as well as the requirement of cultured cells to mature and reach confluence (Young *et al.*, 2001; Aymerich *et al.*, 2004). In particular, nucleoside transport has been studied in three intestinal epithelial cell lines: Caco-2, IEC-6 and T84. Caco-2 and T84 are derived from human colon, while IEC-6 is derived from rat small intensine. Marked differences in reported nucleoside transport rates (*e.g.* Caco-2 > IEC-6) (Sanderson and He, 1994) point to the variability in transporter expression between the different cell lines. Jakobs and Paterson (1986) found that uptake of formycin B in IEC-6 cells was largely dependent upon the presence of Na^+, and efflux from the cells was

inhibited by the addition of NBMPR. These observations therefore provided support to the hypothesis that uptake of nucleosides into intestinal epithelial cells is coupled with Na^+, and that efflux was *via* equilibrative nucleoside transporters. Subsequent studies have established that Na^+-dependent nucleoside transport activity in IEC-6 cells is largely purine nucleoside-selective *via* CNT2, with little involvement of CNT1, while equilibrative nucleoside transport activity is largely *via* ENT1 (Aymerich *et al.*, 2004). Transepithelial fluxes of nucleosides were examined across Caco-2 cells grown on filter inserts (He *et al.*, 1994). The results showed greater apical-to-basolateral than basolateral-to-apical transfer of cytidine and guanosine, providing evidence of vectorial transport; however, whether these fluxes were Na^+-dependent was not investigated (He *et al.*, 1994). Analysis of RNA transcript levels in Caco-2 and T84 cells by RT-PCR revealed message for ENT1 and ENT2, but not for CNT1 or CNT2 (Ward and Tse, 1999). Furthermore, uridine uptake into monolayers of these cell lines proved to be independent of Na^+, was not completely inhibited by the potent ENT1 inhibitor, NBMPR, but was blocked by NBMPR in combination of dipyridimole, an inhibitor of both ENT1 and ENT2 (Ward and Tse, 1999). This indicated the presence of Na^+-independent nucleoside transport by a combination of ENT1 and ENT2 in both Caco-2 and T84 cell lines. Mun *et al.* (1998) also found adenosine transport in T84 cells to be Na^+-independent. Therefore, it is evident that nucleoside uptake studies using intestinal cell lines are poor predictors of *in vivo* intestinal nucleoside transport.

In view of the incomplete and often contradictory nature of the existing intestinal nucleoside transport literature, and because of inherent limitations in existing methodologies to study the problem, the experiments described in this thesis attempted to

characterize intestinal nucleoside transport using whole, intact epithelial preparations obtained from mice, this species being chosen because of the present and future availability of strains deficient in particular nucleoside transporter functional activities.

1.3 Nucleoside Transporters

1.3.1 Classification

Functional studies using various tissue preparations or isolated cells in combination with molecular biological approaches have identified two types of nucleoside transporters in humans and other mammalian species. One is the concentrative nucleoside transporter (CNT) family, designated in humans as SLC28; the other is the equilibrative nucleoside transporter (ENT) family, designated in humans as SLC29 (Griffith and Jarvis, 1996; Cass *et al.*, 1998; Young *et al.*, 2001; Kong *et al.*, 2004; Yao *et al.*, 2007). CNTs are Na^+-dependent inwardly-directed secondary active transporters which, as suggested by their name, are able to accumulate nucleosides within cells by transporting molecules against their concentration gradient. ENTs, on the other hand, passively transport nucleosides bi-directionally down their concentration gradients (Cass *et al.*, 1998; Young *et al.*, 2001; Kong *et al.*, 2004).

Prior to their molecular identification, nucleoside transporters were named based upon functional characteristics. Three major functional concentrative processes have been described (Griffith and Jarvis, 1996; Cass *et al.*, 1998; Young *et al.*, 2001). The *cit, cif,* and *cib* processes are all insensitive to inhibition by NBMPR (as indicated by "*i*"), but have different permeant preferences. The *cit* process selectively transports pyrimidine nucleosides (and, to a lesser extent, adenosine), the *'t'* in *cit* designating

thymidine as a specific permeant that was involved in the system's initial discovery. The *cif* process transports purine nucleosides as well as uridine, *'f'* designating formycin B as a specific permeant involved in the system's initial discovery. The *cib* transport process does not show nucleoside permeant preference, the *'b'* indicating broad nucleoside selectivity for both purine and pyrimidine nucleosides. A contemporary and parallel numerical designation had N1 equivalent to *cif*, N2 equivalent to *cit*, and N3 equivalent to *cib*.

Once each nucleoside transporter was cloned, a new nomenclature system was employed. This designated *cit* (N2) as CNT1 (concentrative nucleoside transporter 1), *cif* (N1) as CNT2 (concentrative nucleoside transporter 2) and *cib* (N3) as CNT3 (concentrative nucleoside transporter 3) (Young *et al.*, 2001; Damaraju *et al.*, 2003; Gray *et al.*, 2004; Kong *et al.*, 2004; Podgorska *et al.*, 2005; Elwi *et al.*, 2006).

There are two major equilibrative nucleoside transport processes, *es* and *ei*. Both transport purine and pyrimidine nucleosides. The *es* process stands for equilibrative-sensitive because it is inhibited by nanomolar concentrations of NBMPR, while the *ei* process stands for equilibrative-insensitive because it is insensitive to inhibition by NBMPR (Yao *et al.*, 1997; Cass *et al.*, 1998; Young *et al.*, 2001; Damaraju *et al.*, 2003; Baldwin *et al.*, 2004, Kong *et al.*, 2004; Elwi *et al.*, 2006; King *et al*, 2006). The *es* process corresponds to cloned transporter ENT1 (equilibrative nucleoside transporter 1), while *ei* corresponds to ENT2 (equilibrative nucleoside transporter 2) (Young *et al.*, 2001; Baldwin *et al.*, 2004). There have been two more ENTs cloned recently, ENT3 and ENT4 (Baldwin *et al.*, 2004).

ENTs and CNTs belong to different membrane protein families, are structurally

unrelated to each other, and have different topological arrangements within the membrane. For the remainder of this thesis, nucleoside transporters will be referred to as CNT1-3 and ENT1-4.

1.3.2 CNT1

The cDNA of the first mammalian nucleoside transporter to be identified was isolated by functional expression screening of a rat jejunum cDNA library in *Xenopus* oocytes (Huang *et al.*, 1994). The protein responsible for the observed Na^+-dependent uptake of uridine was termed rat (r) CNT1. This 648 amino acid residue transporter, which functionally displayed *cit*-type behavior (pyrimidine-selective) transported uridine with a K_m value of 37 μM when produced in *Xenopus* oocytes (Huang *et al.*, 1994). Subsequently, human (h) CNT1 was homology cloned from human kidney (Ritzel *et al.*, 1997). hCNT1 has 650 amino acid residues, with uridine apparent K_m value in *Xenopus* oocytes similar to rCNT1. Although r/hCNT1 are pyrimidine nucleoside-selective, both bind and transport the purine nucleoside adenosine, the difference between adenosine and uridine transport kinetics being that adenosine has a much lower V_{max} value than uridine, giving adenosine the potential to act as a physiological CNT1 inhibitor (Yao *et al.*, 1996; Young *et al.*, 2001). hCNT1 has Na^+:nucleoside coupling ratio of 1:1 (Ritzel *et al.*, 1997; Smith *et al.*, 2007).

Rat and human CNT1 display 83% sequence identity, and have a common predicted membrane architecture with 13 putative transmembrane domains (TMs) (Hamilton *et al.*, 2000; Young *et al.*, 2001). rCNT1 protein was expressed predominantly in the epithelial brush-border membranes of rat jejunum and renal cortical tubule cells, and in the bile canalicular membranes of liver parenchymal cells (Hamilton *et al.*, 2000).

In addition to accepting physiological nucleosides, CNT1 also transports therapeutic nucleoside analogues. For example, the nucleoside antiviral drugs zidovudine (3'-azido-3'-deoxythymidine, AZT) and zalcitabine (2',3'-dideoxycytidine,ddC), in addition to the anticancer pyrimidine nucleoside analogues cytarabine (1-(β-D-arabinofuranosyl)cytosine, AraC), gemcitabine (2',2'-difluorodeoxycytidine, dFdC), and 5'-deoxy-5-fluorouridine (5'-dFUR, a metabolite of capecitabine (*N*-[1-(5-deoxy-β-D-ribofuranosyl)-5-fluoro-1,2-dihydro-2-oxo-4-pyrimidyl]-*n*-pentylcarbamate)) are all hCNT1 permeants to varying degrees (Huang *et al.*, 1994; Yao *et al.*, 1996; Ritzel *et al.*, 1997; Graham *et al.*, 2000; Lostao *et al.*, 2000; Damaraju *et al.*, 2003; Gray *et al.*, 2004; Elwi *et al.*, 2006). hCNT1 showed the greatest affinity for gemcitabine amongst nucleoside drugs tested, as observed by 90% inhibition of uridine transport upon addition of 500 μM gemcitabine (Graham *et al.*, 2000).

1.3.3 CNT2

cDNAs encoding the CNT2 protein have been obtained from four different species. First isolated from a rat liver cDNA library (Che *et al.*, 1995), the CNT2 protein was subsequently cloned from human kidney, human small intestine, rabbit small intestine and mouse spleen using homology cloning RT-PCR techniques (Wang *et al.*, 1997; Ritzel *et al.*, 1998; Gerstin *et al.*, 2000; Patel *et al.*, 2000). Rat, rabbit and human CNT2 were functionally characterized in *Xenopus* oocytes and displayed Na^+-dependent *cif*-like behavior (Che *et al.*, 1995; Wang *et al.*, 1997; Ritzel *et al.*, 1998; Gerstin *et al.*, 2000). Recombinant mouse CNT2 function was also investigated in Cos-1 cells, where formycin B (an inosine analogue) showed substantially greater fluxes than thymidine, and where uridine, adenosine and inosine, but not thymidine or cytidine, could inhibit the

formycin B transport (Patel *et al.*, 2000). Although purine nucleoside-selective, CNT2 transporters also transported the pyrimidine nucleoside uridine. However for hCNT2, for example, the apparent affinity for inosine transport (K_m of 5 μM in *Xenopus* oocytes) was much greater than that for uridine (K_m of 40-80 μM in *Xenopus* oocytes) (Wang *et al.*, 1997; Ritzel *et al.*, 1998). Kinetic analysis of hCNT2 has also been undertaken using a yeast heterologous expression system, giving an apparent K_m value of 28 μM for uridine (Zhang *et al.*, 2005). The stoichiometry of Na:nucleoside coupling for CNT2 is, like CNT1, 1:1 (Smith *et al.*, 2007). Despite functional similarities between different species CNT2 isoforms there were slight structural differences. With similar functional characteristics, mCNT2, rCNT2 and hCNT2 share 80 - 93 % sequence identity (Wang *et al.*, 1997; Ritzel *et al.*, 1998; Patel *et al.*, 2000). hCNT2 has broader tissue distribution than hCNT1 (Wang *et al.*, 1997; Ritzel *et al.*, 1998). Similar to CNT1, CNT2 has 13 TM predicted membrane architecture.

As anticipated by their different selectivities for physiological nucleosides, hCNT2 and hCNT1 also differ with respect to transport of therapeutic nucleoside drugs. The antiviral nucleoside analogue didanosine (2'3'-dideoxyinosine, ddI) used in the treatment of HIV, for example, is transported by hCNT2 but not by hCNT1 (Ritzel *et al.*, 1998). Anticancer nucleoside analogue drugs transported by hCNT2 include clofarabine (2-chloro-9-(2'-deoxy-2'-fluoro-β-D-arabinofuranosyl) adenine, Cl-FaraA) which, for example is used for acute lymphocytic leukemia (Damaraju *et al.*, 2003).

1.3.4 CNT3

The third CNT isoform to be identified, mouse and human CNT3 (mCNT3 and hCNT3) were cloned from human mammary gland, differentiated human myeloid HL-60

cells and mouse liver (Ritzel *et al.*, 2001). With 79% sequence identity, hCNT3 and mCNT3 contain 691 and 703 amino acid residues, respectively (Ritzel *et al.*, 2001). Functional activity corresponding to the *cib* transport process was confirmed by functional characterization of h/mCNT3 produced in *Xenopus* oocytes. Both transporters exhibited robust Na^+-dependent uptake of uridine, cytidine, thymidine, adenosine, guanosine and inosine, indicating an ability to transport both purine and pyrimidine nucleosides (Ritzel *et al.*, 2001). Kinetic analysis of hCNT3 revealed apparent K_m values of 15 – 53 μM, with cytidine and adenosine (15 μM) having the lowest values, followed by uridine (22 μM) and thymidine (21 μM), and then by guanosine (43 μM) and inosine (53 μM) (Ritzel *et al.*, 2001). Corresponding mCNT3 apparent K_m values are: uridine (18 μM), adenosine (26 μM), thymidine (30 μM), cytidine (35 μM), guanosine (37 μM) and inosine (49 μM) (Drs. SK Loewen and SY Yao, personal communication). Human CNT3 transcripts have been found in pancreas, bone marrow, trachea, intestine, mammary gland, and smaller amounts in liver, brain, heart and kidney (Ritzel *et al.*, 2001). More recently, Damaraju *et al.* (2007) have used immunostaining to demonstrate the presence of hCNT3 protein in the apical membranes of kidney proximal tubule cells. Corresponding apical hCNT3 functional activity has been demonstrated in human renal proximal tubule cell (hRPTC) cultures (Damaraju *et al.*, 2007; Elwi *et al.*, 2008). In marked contrast to CNT1/2, h/mCNT3 have a 2:1 Na^+:nucleoside coupling ratio. It has also been discovered that CNT3 can substitute H^+ for Na^+ (Ritzel *et al.*, 2001; Smith *et al.*, 2007). Similar to CNT1/2, the CNT3 isoform also has 13 TM predicted membrane architecture.

Since hCNT3 transports both purine and pyrimidine nucleosides, it also can accept purine and pyrimidine nucleoside analogue drugs. Specifically, h/mCNT3 have been shown to transport the anticancer pyrimidine nucleoside drugs 5-fluorouridine, 5-fluoro-2'deoxyuridine, zebularine and gemcitabine, as well as the purine nucleoside drugs fludarabine (2-fluoro-2'-deoxyadenosine) and cladribine (2-chloro-2'-deoxyadenosine) (Ritzel *et al.*, 2001; Elwi *et al.*, 2008; Drs SK Loewen and SY Yao, personal communication). To a lesser extent, the antiviral nucleoside drugs zidovudine, zalcitabine (pyrimidine nucleoside analogues) and didanosine (purine nucleoside analogue) are also transported by h/mCNT3 (Ritzel *et al.*, 2001; Drs SK Loewen and SY Yao, personal communication).

1.3.5 The ENT family

The ENT family of nucleoside transporters consists of 4 isoforms, ENT1, ENT2, ENT3 and ENT4. ENT1 and ENT2 are the best described, and are known to transport nucleosides bidirectionally into and out of cells down their concentration gradients (Cass *et al.*, 1998; Young *et al.*, 2001; Damaraju *et al.*, 2003; Baldwin *et al.*, 2004; Kong *et al.*, 2004; Elwi *et al.*, 2006; King *et al*, 2006).

The ENT1 protein was identified and its DNA was first cloned from human placenta (Griffiths *et al.*, 1997a). When produced in *Xenopus* oocytes, hENT1 showed functional activity consistent with the lack of Na^+-dependence, broad nucleoside specificity, and sensitivity to inhibition by NBMPR characteristic of the *es* nucleoside transport process (Griffiths *et al.*, 1997a). The K_i for NBMPR inhibition of uridine transport was 2 nM, indicating high affinity binding of NBMPR to hENT1. hENT1 accepts various nucleoside drugs as permeants, such as cladribine, cytarabine,

fludararabine and gemcitabine, and inhibited by vasodilator drugs such as dilezep, draflazine and dipyridimole (Cass *et al.*, 1998; Young *et al.*, 2001; Damaraju *et al.*, 2003; Baldwin *et al.*, 2004; Kong *et al.*, 2004; Elwi *et al.*, 2006; King *et al*, 2006). In contrast to hCNTs the antiviral nucleoside drugs, zidovudine, zalcitabine and didanosine, are not transported by hENT1, due to the absence of the ribose 3'-hydroxyl group, which is required for *es*-type transport (Gati *et al.*, 1984; Young *et al.*, 2001). The apparent K_m of uridine influx by recombinant hENT1 produced in *Xenopus* oocytes was 0.24 mM (Griffiths *et al.*, 1997a). Other nucleosides display a variety of apparent K_m values ranging from from 50 μM for adenosine to 680 μM for cytidine (Baldwin *et al.*, 2004). The human ENT1 isoform has 456 residues compared to 460 residues in mENT1 and 457 residues in rENT1 (Griffiths *et al.*, 1997a; Yao *et al.*, 1997; Kiss *et al.*, 2000). Human and mouse, and human and rat ENT1 are 79 and 78 % identical in amino acid sequence, respectively. Both rodent proteins transport nucleosides similarly to hENT1 (Griffiths *et al.*, 1996; Yao *et al.*, 1997; Kiss *et al.*, 2000; Baldwin *et al.*, 2004). There are, however, inhibitor differences between species, dilezep and dipyridimole inhibiting hENT1 and mENT1, but having limited effect against rENT1 (Yao *et al.*, 1997; Kiss *et al*, 2000). In contrast to the 13 TMs of CNTs, ENT1 and other ENT isoforms have a predicted 11 TM membrane topology (Sundaram *et al*, 2001b).

ENT1 is present in most, possibly all cell types and, in particular, has been found in various epithelia including intestine, kidney and others. Initially thought to be restricted to basolateral membranes, there is increasing evidence in kidney showing apical localization (Damaraju *et al.*, 2007).

The DNA encoding hENT2 was also cloned from human placenta, and exhibits *ei*-type nucleoside transport activity, including low sensitivity to inhibition by NBMPR, when produced in *Xenopus* oocytes (Griffiths *et al.*, 1997b). Furthermore, hENT2, and subsequently isolated r/mENT2, are less sensitive to inhibition by dilezep and dipyridimole than hENT1 (Griffiths *et al.*, 1997a; 1997b; Yao *et al*, 1997; Kiss *et al.*, 2000). hENT2 transports both purine and pyrimidine nucleosides with a uridine apparent K_m value (0.2 mM) only slightly lower than hENT1 (0.24 mM) (Griffiths *et al.*, 1997a; 1997b). The one exception to this broad permeant selectivity is cytidine, which is poorly transported by hCNT2 with an apparent K_m value > 5 mM compared to 0.5 mM for hENT1(Griffiths *et al.*, 1997b; Yao *et al.*, 1997). Similarly, the anticancer cytidine nucleoside analogue, gemcitabine, has lower affinity for hENT2 than for hENT1 (Mackey *et al.*, 1999). In the opposite direction, antiviral nucleoside drugs lacking 3'-hydroxyl groups that could not be transported by hENT1 (zidovudine, zalcitabine and didanosine) are transported by hENT2 (Yao *et al.*, 2001). Physiologically, the most important functional difference between hENT2 and hENT1 is the ability of hENT2 to also transport purine and pyrmidine nucleobases (apparent K_m values 0.7 - 2.6 mM) (Yao *et al.*, 2002).

Both rENT2 and mENT2 have been characterized (Yao *et al.*, 1997; Kiss *et al.*, 2000). Both of these transporters display similar functional and structural properties to hENT2, except that mENT2 has been reported to lack the ability to transport pyrimidine nucleobases (Nagai *et al.*, 2007). The latter still bind to the transporter, and act as non-transported mENT2 inhibitors. mENT2 does, however, transport purine nucleobases

(Nagai *et al.*, 2007). h/r/mENT2 each have 456 amino acid residues, and r/mENT2 show 88% sequence identity to hENT2 (Baldwin *et al.*, 2004).

Two additional human and mouse ENT isoforms, h/mENT3 and h/mENT4, have recently been characterized (Baldwin *et al.*, 2005; Barnes *et al.*, 2006). Both are activated at acidic pH: h/mENT3 are broad specificity, intracellular transporters possibly located in lysosomal membranes, whereas h/mENT4 are adenosine/adenine-specific and found predominantly in CNS and the heart. Neither isoform is inhibited by dilezep, dipyridimole or NBMPR (Baldwin *et al.*, 2005; Barnes *et al.*, 2006).

1.4 Role of the intestine in nucleoside drug therapy

As described in previous sections, various anticancer and antiviral nucleoside drugs are bound by nucleoside transporters, the therapeutic efficacy of these drugs depending upon CNT/ENT-mediated transport into cells of targeted tissues. Increasingly, there are specific examples where nucleoside transporter content in the cancer cells of patients predicts cytotoxicity and therapeutic outcome (Gati *et al.*, 1998; Damaraju *et al.*, 2003; Elwi *et al.*, 2006; Zhang *et al.*, 2007b). In addition to requiring nucleoside transporters for uptake into target cells in antiviral and anticancer chemotherapy, orally administered drugs require transport into and across the intestinal epithelium in order to access the blood stream. This has implications for bioavailability (Young *et al.*, 2001). Some examples of nucleoside drugs that are orally administered and the pathologies that they are used to treat are: AIDS (zidovudine, didanosine, zalcitabine, stavudine, lamivudine), herpes simplex/zoster (acyclovir (9-(2-hydroxyethanoxymethyl)guanine ; ACV)), cytomegalovirus (ganciclovir (9-[(1,3-dihydroxy-2-propoxy)methyl]guanine)),

lymphoma and leukemia (cladribine), refractory breast cancer (capecitabine) and respiratory syncytial virus (RSV) (ribavirin (1-β-D-ribofuranosyl-1,2,4-triazole-3-carboxamide)) (Young *et al.*, 2001). Transport of only some of these drugs has been characterized in intestinal cell preparations. Ribavirin, for example, was studied using brush border membrane vesicles isolated from human intestine (Patil *et al.*, 1998). This showed ribivirin transport by hCNT2 (*cif*) with an apparent K_m of 19 μM. A typical 600 mg dose of ribarivin will reach concentrations of more than 1 mM in the intestinal lumen, thereby saturating CNT2 and potentially reducing bioavailability to less than 50 % (Patil *et al.*, 1998). Examples of orally-administered drugs which have yet to be investigated in intestine include acyclovir and ganciclovir, whose transport has been studied only in human erythrocytes (Mahony *et al.*, 1988), and stavudine and lamivudine, whose interactions with nucleoside transporters have yet to be established (Young *et al.*, 2001).

1.5 Hypotheses and aims

The presence of nucleoside transport activity in intestinal epithelium is well documented. However, these studies have focused on studying nucleoside transport and transporters using *in vitro* intestinal preparations that do not closely resemble the *in vivo* properties of the intestinal epithelium. Examples of these methods can be found in Section 1.2.5, and include brush border and basolateral membrane vesicles, isolated enterocytes and cultured cell monolayers. Furthermore, most of these experiments were uptake assays, with no information concerning the transepithelial movement of nucleosides across the intestinal epithelium. The research described in this thesis addresses this deficiency by using the Ussing chamber apparatus to demonstrate and

characterize nucleoside transport across the mouse intestinal epithelium. The Ussing chamber has been used to study transporter-mediated processes across epithelia in only a limited number of cases, and this was the first investigation to apply the technique to the study of intestinal transepithelial nucleoside fluxes. The ultimate goal of the studies described in this thesis is to functionally describe the molecular mechanism(s) responsible for transepithelial nucleoside and nucleoside drug transport across the intestinal epithelium.

Chapter 2 – Materials and Methods

2.1 Chemicals

^{3}H-uridine was obtained from GE Healthcare (Baie d'Urfe, Que., Canada). ^{3}H-formycin B, ^{14}C-uridine and ^{14}C-uracil were purchased from Moravek Biochemicals (Brea, CA., USA). ^{3}H-Mannitol came from Perkin-Elmer Life Sciences (Boston, MA., USA). The corresponding unlabelled nucleosides (uridine, thymidine, inosine and formycin B) were purchased from Sigma-Aldrich (Oakville, Ont., Canada). All other chemicals were of analytical grade.

2.2 Animals

Unless otherwise indicated, experiments were performed on Balb/c mice bred in a pathogen-free environment and housed by Health Sciences Laboratory Animal Services, University of Alberta. Feeding of all animals was not regulated.

2.3 Mouse Intestinal Tissue Preparation

Mice were euthanized by CO_2 narcosis and cervical dislocation of the spinal cord. The entire intestinal tract was removed, cut just below the stomach and just above the anus. The time of day for sacrifice was approximately 10:00 AM. The desired tissue region was then isolated (Fig. 2-1). The duodenum was considered to be the 4 cm segment immediately distal to the stomach. The jejunum was considered to be the next ~ 8 cm (the segment 4 cm distal from the stomach to ~ 4 cm proximal from the caecum). The next 4 cm was considered to be the ileum, which was the segment immediately

proximal to the caecum. Finally, the colon was dissected as the section of intestinal tissue from the caecum to the anus. Once collected, the desired tissue was flushed with approximately 10 ml of room temperature Na^+ KHS medium (Section 2.4.2). Next, the intestinal segment was cut longitudinally to obtain a rectangular piece of tissue. The smooth muscle layer, attached to the basolateral surface of the epithelium, was then dissected away leaving only the epithelium. The resulting epithelial preparation was cut into ~ 1 cm^2 sections, and mounted into the Ussing chambers, which had an aperture of 0.2 cm^2 (Fig. 2-2).

2.4 Ussing Chamber Experiments

2.4.1 Ussing chamber apparatus

The circulating water-jacketed Ussing chamber apparatus used in the present series of experiments was custom made in the workshop facilities of the Department of Chemistry, Faculty of Science, University of Alberta, and comprised of a U-shaped tubing system made of glass (Fig. 2-2). The epithelial tissue was located at the center of the U-shaped tube, thereby creating two chambers. Each chamber contained 10 ml of either Na^+ or Ch^+ KHS medium (Section 2.4.2). One of the 10 ml chambers was exposed to the apical surface of the epithelium and was therefore termed the apical chamber. Likewise, the opposite chamber was exposed to the basolateral surface of the epithelium and was termed the basolateral chamber. Both chambers were heated to 37 °C and bubbled with air in order to oxygenate the circulating medium and create a bubble lift in the solution. The U-shaped arrangement containing equal volumes of medium in the two

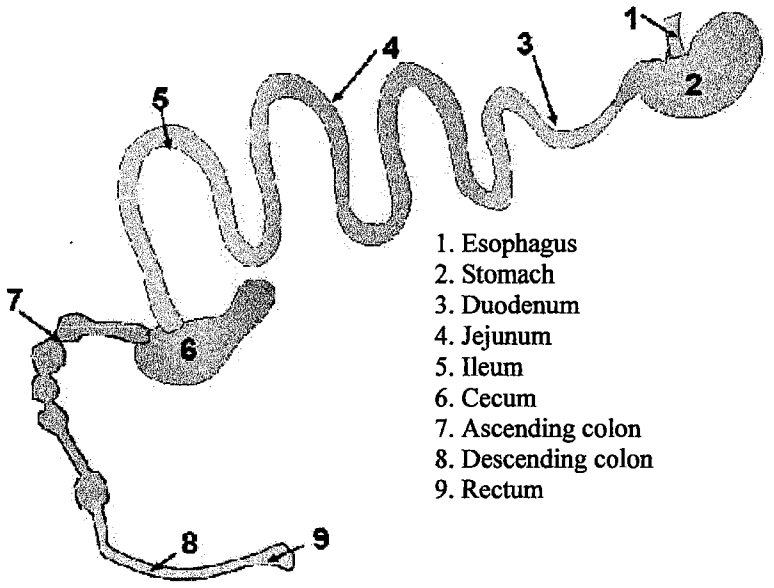

Figure 2-1 Schematic representation of the mouse gastrointestinal tract.
The segments of the intestine that were used in experiments described in this thesis were duodenum (3), jejunum (4) ileum (5) and the entire colon (7 and 8) (adapted from: *http://www3.niaid.nih.gov/labs/aboutlabs/cmb/InfectiousDiseasePathogenesisSection/mouseNecropsy/step6IntestinesStomachSpleenPancreas.htm*).

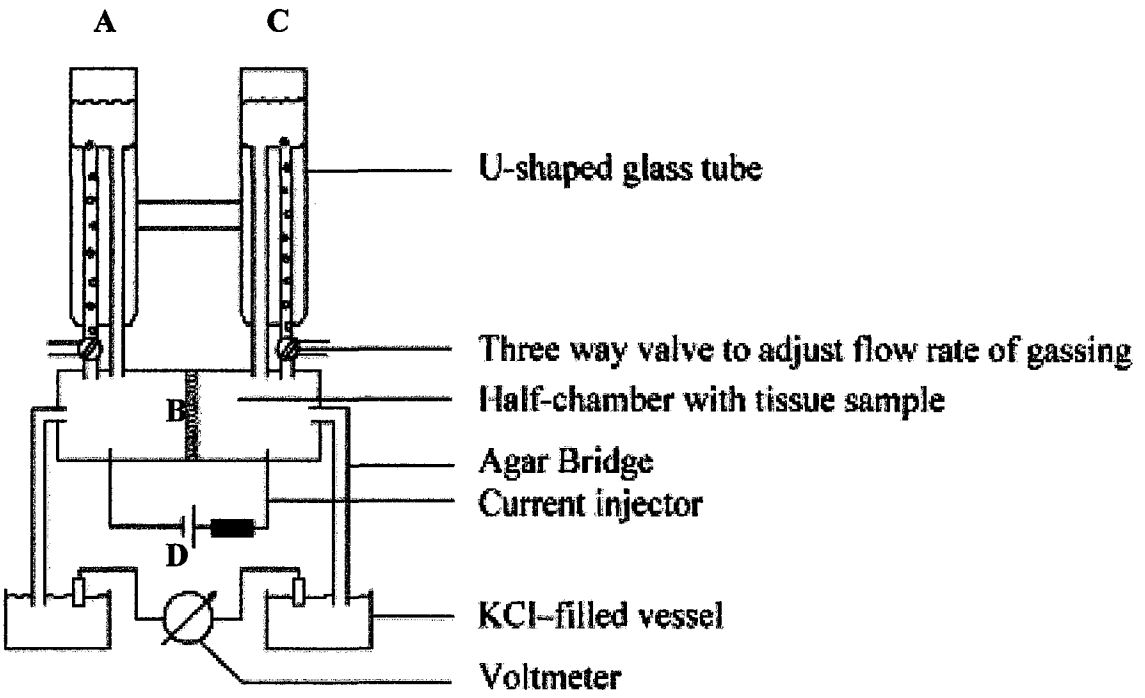

Figure 2-2 Ussing Chamber apparatus.
The left side of the apparatus (A) was the apical chamber; it contained Krebs-Henseleit solution (KHS) medium which bathed the apical side of the epithelial tissue (B). The tissue separated the apical chamber from the basolateral chamber (C). This chamber also contained KHS medium, which bathed the basolateral side of the mouse epithelial tissue. A schematic representation of the electrical measurement setup is also shown (D). The potential difference was kept at 0 mV by the current injector (amplifier). The amount of current injected is termed the short circuit current (I_{sc}).

chambers (10 ml each) allowed equal hydrostatic pressure on both sides of the epithelium and, therefore, avoided tissue damage by stretching (Li *et al.*, 2004). During the course of experiments, ^{3}H-nucleosides in the presence or absence of excess competing unlabelled nucleosides were added to one chamber, and timed samples were taken from the opposite chamber in order to determine the trans-epithelial flux. All substances remained in the solutions until the end of the experiment. Four identical Ussing chamber systems were constructed to enable four individual tissue samples to be analyzed simultaneously.

2.4.2 Media

Two modified Krebs-Henseleit solutions (KHS), both bicarbonate (HCO_3^-)-free, were used for Ussing chamber experiments. One contained a physiological concentration of Na^+ (Na^+ KHS medium). The other was Na^+ -free and employed choline$^+$ as Na^+ substitute (Ch^+ KHS medium). The Na^+ KHS medium contained (mM): 135.2 NaCl, 4.7 KCl, 2.5 $CaCl_2$, 1.2 $MgCl_2$, 10 HEPES (pH = 7.4), 1.2 KH_2PO_4, and 11.1 glucose. The Ch^+ KHS medium contained (mM): 135.2 choline chloride, 4.7 KCl, 2.5 $CaCl_2$, 1.2 $MgCl_2$, 10 HEPES (pH = 7.4), 1.2 KH_2PO_4, and 11.1 glucose.

2.4.3 Apical-to-basolateral nucleoside flux

Unless otherwise indicated, the ^{3}H-nucleoside (uridine or formycin B) was added to the apical chamber at time zero to create an initial extracellular concentration of 1 μM (1 μCi/ml) in that chamber. Every 10 min for 2 h, a 100 μl sample was taken from the basolateral chamber, added to 2.5 ml of liquid scintillation cocktail (LSC) (ScintiSafe Econo 2, Fisher Scientific, Ottawa, Ont., Canada), and counted for ^{3}H in a Beckman LS 6000 IC liquid scintillation counter (Beckman-Coulter, Mississauga, Ont., Canada). To

maintain equal hydrostatic pressure on both sides of the tissue, equal timed samples were also removed from the apical chamber and either counted for radioactivity or discarded. The appearance of ^{3}H on the basolateral side of the epithelium generated a transepithelial flux profile that was expressed as pmol ^{3}H-nucleoside transported per cm^2 of epithelial tissue as a function of time in min (Fig. 3-1).

Competing unlabelled nucleosides were added to the apical chamber either halfway through the experiment (after 50 minutes), or immediately before ^{3}H-nucleoside addition. Depending on the experiment (see Chapter 3), the concentration of unlabelled nucleoside was 1, 5 or 20 mM.

2.4.4 Basolateral-to-apical nucleoside flux

The majority of experiments assessed flux of nucleosides across mouse intestinal epithelium in the apical-to-basolateral direction (Section 2.4.3). However, some experiments assessed ^{3}H-uridine fluxes in the opposite direction from the basolateral side to the apical side. Specifications for these experiments were identical to those in Section 2.4.3 with the exception that (i) ^{3}H-uridine and competing unlabelled uridine were added to the basolateral chamber, and (ii) flux assay samples were removed from the apical chamber.

2.4.5 ^{3}H-mannitol flux

Mannitol fluxes were determined by the same procedure outlined in section 2.4.3, except that ^{3}H-mannitol was added to the apical chamber at time zero instead of ^{3}H-nucleoside.

2.4.6 Measurement of short circuit current and trans-epithelial resistance

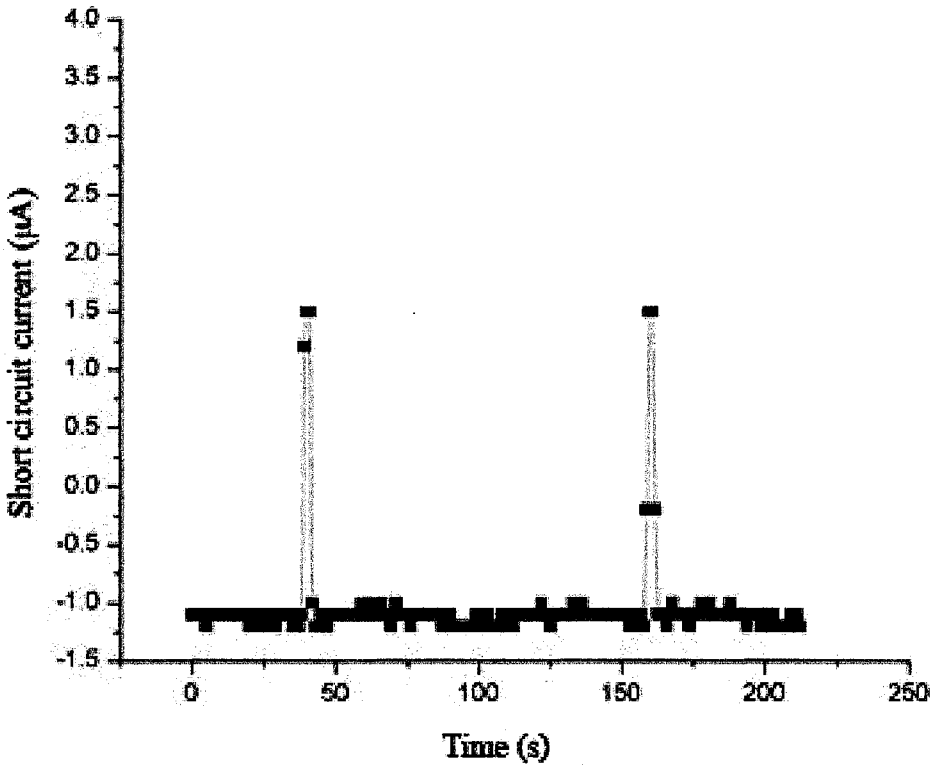

Figure 2-3 Transepithelial resistance.
Short circuit measurements were the amount of current required to maintain a 0 mV potential difference across the epithelium. These measurements were taken every 0.25 s. At discrete intervals, a 0.5 mV potential difference was added across the epithelium resulting in a change in current (μA) (shown as the spikes in this representative recording). This change in current, together with the 0.5 mV potential difference added, was used to calculate the transepithelial resistance using Ohm's Law (V=IR). Trans-epithelial resistance was a measure of tissue integrity.

During the course of the Ussing chamber experiments, the epithelium potential difference was clamped to 0 mV using a DVC 1000 amplifier (World Precision Instruments, Sarasota, FL., USA). Short circuit current (I_{sc}), the current required to keep the potential difference clamped at zero, was recorded every 0.25 s through Ag-AgCl electrodes and 3 M agarose bridges using a Powerlab 8SP series data acquisition system and Chart data acquisition software (AD Instruments, Colorado Springs, CO, USA). Accumet Ag-AgCl electrodes were from Fisher Scientific (Ottawa, Ont., Canada).

As a further measure of epithelium integrity, trans-epithelial resistance was also measured throughout the experiment. At discrete intervals, a 0.5 mV potential difference was applied across the tissue, creating a corresponding increase in I_{sc} (Fig. 2-2). Using Ohm's law, the resistance across the epithelium was calculated (Lam *et al.*, 2003).

2.5 Generation and genotyping of mCNT3 Null Mice

Cloned 129SvEvBrd Embryonic Stem cells (Lexicon Pharmaceuticals, Woodlands, TX, USA) containing a LacZ/neo cassette in the place of exons 4-6 of the Slc28a3 (mCNT3) gene (Fig. 2-4) were introduced into FVB/N mice to generate a breeding colony of mCNT3 null animals (FVB;129-CNT3) housed in the Vivarium of the Cross Cancer Institute (Edmonton, Alta., Canada). Wild-type FVB/N and homozygous mCNT3 null mice were genotyped by ear clip PCR as illustrated in Fig. 2-4, and are referred to as CNT3 (-/-) and CNT3 (+/+), respectively.

2.6 Relative Gene Expression of Nucleoside Transporters

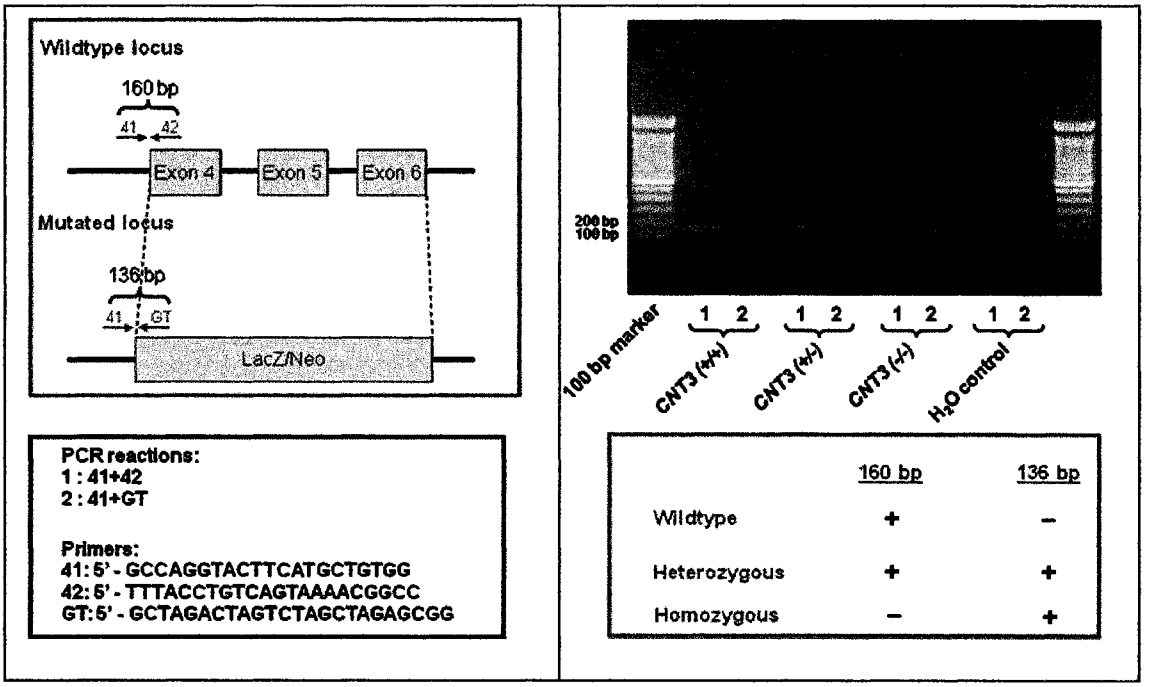

Figure 2-4 Generation and genotyping of mCNT3 knockout mice.
(A) The insertion site of a LacZ/Neo cassette in the place of exons 4-6 of the slc28a3 (mCNT3) gene is shown. Also indicated are the locations and sequences of the PCR primers used for genotyping, and sizes of each of the PCR products generated. (B) Representative Southern blots obtained for individual CNT3 (+/+), CNT3 (+/-) and CNT3 (-/-) mice.

TaqMan™ quantitative real time RT-PCR (Applied Biosystems, Streetsville, Ont., Canada) was used to quantify the relative abundance of transcripts for individual mCNT and mENT nucleoside transporters in mouse jejunal epithelium. TaqMan™ technology utilizes an oligonucleotide probe having a 5' fluorescent tag and a corresponding 3' quenching molecule. The probe is positioned between two PCR primers. Probe and primer sets used for mCNT1-3 and mENT1-4 were obtained from Applied Biosystems and are listed in Table 2-1. During the PCR reactions, Taq-polymerase 5'-nucleotidase cleaves the fluorescent tag from the 5' end in each PCR cycle. The amount of fluorescence detected in real time corresponds to the amount of transcript in the original sample (Ritzel *et al.*, 2001).

As shown in Chapter 3 (Fig. 3-15), the amount of gene expression is determined by the number of cycles required to achieve a certain threshold of fluorescence (Ct). Therefore, the smaller the Ct value the greater the expression of the gene because fewer cycles are required to give a particular amount of fluorescent signal.

Approximately 1 cm of mouse jejunal tissue with smooth muscle removed was collected, stored in RNAlater (0.5 ml) and mechanically lysed. The TaqMan™ reactions were performed as described previously (Rtizel *et al.*, 2001). RNA from the intestinal cells was reverse transcribed using the Taqman™ Gold RT-PCR kit. Next, real time-PCR cycles were undertaken using the Applied Biosystems 7700 Sequence Detection System and Applied Biosystems Taqman™ PCR Universal Master Mix kit. The amplification cycles were performed as followed: single cycles at 50 °C for 2 min and 95 °C for 10 min, followed by 40 cycles at 95 °C for 15 s and 1 min at 60 °C. The

Nucleoside Transporter	Location of Probes and Primers	Applied Biosystems Part Numbers
mCNT3	exon 6/7	Mm01338879_m1
mCNT2	exon 5/6	Mm00445488_m1
mCNT1	exon 13/14	Mm00671982_gH
mENT1	exon 2/3	Mm01270581_m1
mENT2	exon 2/3	Mm01231340_m1
mENT3	exon 5/6	Mm00469917_m1
mENT4	exon 6/7	Mm00525575

Table 2-1 List of probe and primer sets for real time RT-PCR of nucleoside transporters in mouse jejunal epithelium.
For each nucleoside transporter, the location on the respective gene where the probe and primer sets adhere is indicated. The Applied Biosystems reference numbers for each of the probe and prime sets are also given.

expression level in each sample was compared to glyceraldehyde 3-phosphate dehydrogenase (GAPDH) as an internal control, the reported ΔCt values representing the Ct value for that particular nucleoside transporter minus the corresponding GADPH Ct value in the same sample. The transcript expression levels for jejunum in Figure 3-16 are given as 1/ ΔCt.

2.7 Immunohistochemistry

Anti-mCNT3 polyclonal antibodies were developed against amino acids 61-84 of the protein. The antibodies were grown in rabbits and collected from rabbit serum. Specificity of the antibody for mCNT3 was demonstrated in yeast membranes expressing recombinant mCNT3 (results not shown). Immunohistochemistry of formalin-fixed paraffin-embedded sections (4-6 μm) of mouse jejunum was undertaken as described previously (Damaraju *et al.*, 2007) using Target Retrieval Solution high pH, Envision+ horseradish peroxidase-conjugated dextran polymer and diaminobenzidine obtained from DAKO (Carpentaria, CA, USA). Sections stained in the absence of primary antibody or in the presence of a 10X molar mass excess of peptide (aa 61-84) were used as controls. Slides were imaged through a Zeiss Axioskop2 plus Microscope with F fluar X40/1.3 oil immersion lens and Zeiss Axiocam 12 megapixel camera. Images were displayed using Zeiss Axiovision software.

2.8 Thin Layer Chromatography

Thin layer chromatography (TLC) was performed on Cellulose 300 plates (20X20 cm, 100 microns thick) purchased from SelectoScientific (Suwanee, GA, USA) and

eluted with 0.55 M LiCl in 0.2% (v/v) formic acid (Williams *et al.*, 1989; Williams and Jarvis, 1991). Samples (200 µl) of Na^+ KHS medium taken after 2 h from the basolateral chambers of apical-to-basolateral ^{3}H-uridine flux assays (Section 2.4.3) were passed through Amicon Ultra Centrifugal filter 10000 MWCO spin columns (Millipore, Bedford, MA, USA) to remove contaminating protein and directly spotted onto TLC plates. The spots were overlaid with 20 µl uridine (10 mM), 20 µl uracil (10 mM) and 20 µl UMP (10 mM) and developed alongside corresponding ^{14}C-uracil and ^{3}H-uridine standards for approximately 12 h. Plates were then dried and cut into 1 cm sections. Each section was soaked in 1 ml H_2O followed by the addition of 8 ml LSC. Radioactivity present in each 1 cm section was counted, and R_f values calculated.

2.9 ^{3}H Tissue Accumulation

At the end of jejunal ^{3}H-uridine and ^{3}H-formycin B flux experiments (Section 2.4.3), the epithelial tissue was removed from between the Ussing chambers and dissolved in 200 µl of 5% (w/v) SDS and 2.5% (w/v) NaOH for 12 h. Next, 2.5 ml LSC was added and the radioactivity trapped inside the jejunal epithelium was counted for ^{3}H.

2.10 Statistical Analysis

All nucleoside flux values and RT-PCR data are presented as mean ± standard error of the mean (SEM). The computation of fluxes was completed by linear regression analysis, giving slopes for the plot of flux versus time for each individual experiment. These slopes were averaged for each condition and presented as mean ± standard error of the mean (SEM). The flux plots were all approximately linear, having correlation

coefficients of $R > 0.90$. When comparing differences between two groups, a student's T-test was used where statistical significance was considered to be a p-value < 0.05. The number of experiments completed for each condition is represented as n.

Chapter 3 Results

3.1 Ussing Chamber Fluxes

3.1.1 Transport of uridine across mouse jejunum epithelial tissue

Sheets of mouse jejunum epithelial tissue were prepared as described in Section 2.3 and mounted between apical and basolateral chambers holding Na^+-containing (Na^+ KHS) medium. The general experimental procedure used to examine apical-to-basolateral uridine fluxes in mouse intestine is described in Section 2.3.2. As shown in Fig. 3-1, the flux across the jejunal epithelium in Na^+ KHS medium was approximately linear with time, and after 50 min had reached a value of 146 ± 43 pmol/cm^2 ($n = 5$). At this time, an excess of unlabelled uridine was added to the apical side of the tissue to give a final concentration of 20 mM in the apical chamber. Sampling was then continued from the basolateral side for a further 70 min. The flux continued to be approximately linear with time, and after 2 h the amount of uridine that had been transported across the jejunum epithelial tissue into the basolateral chamber was 191 ± 44 pmol/cm^2 ($n = 5$) (Fig. 3-1). Therefore, the majority of transepithelial movement across the jejunum occurred before unlabelled uridine was added. Prior to uridine addition, the rate of transport was 2.46 ± 0.77 pmol/cm^2/min, compared to 0.60 ± 0.05 pmol/cm^2/min after uridine addition ($n = 5$). As illustrated by the slopes of the lines drawn in Fig. 3-1, therefore, there was a marked 75 % decrease in transepithelial flux rate as a result of uridine addition to the apical chamber at the halfway point of the experiment ($p < 0.05$).

Corresponding uridine fluxes were also determined in the absence of Na^+ (Ch^+ KHS medium in both apical and basolateral chambers) (Fig.3-2). The resulting flux of

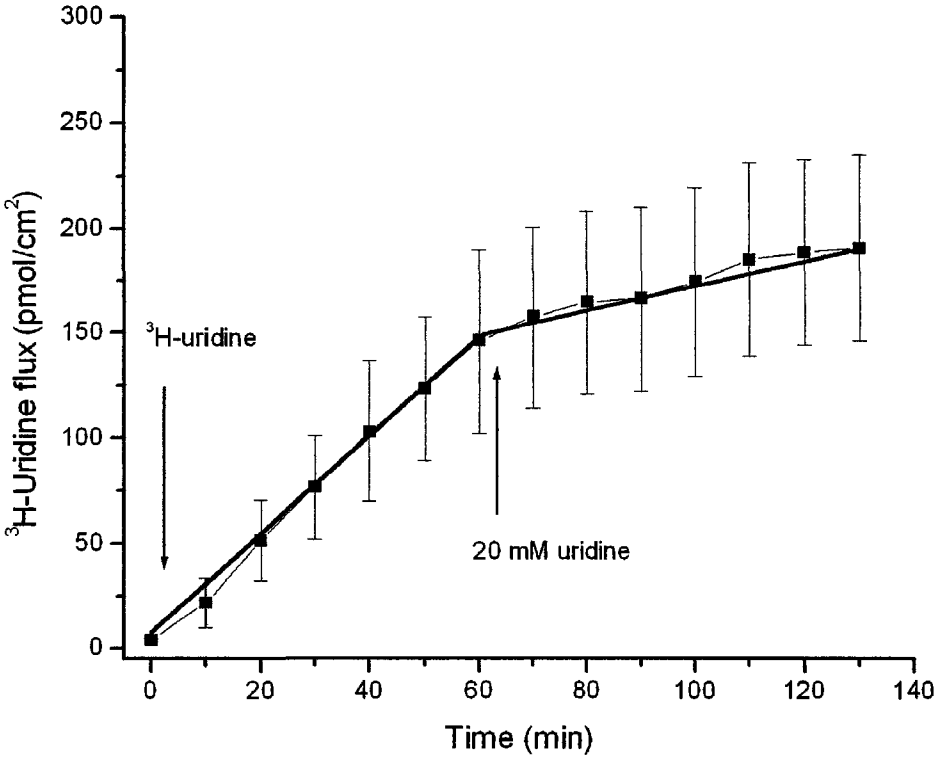

Figure 3-1 Transport of uridine across mouse jejunal epithelium.
Mouse jejunal epithelial tissue was bathed in Na^+ KHS medium on both the apical and basolateral sides of the tissue. ^{3}H-Uridine (1μM) was added to the apical chamber at time zero. At 10 min intervals, 100 μl samples were taken from the basolateral chamber to determine uridine flux. After 50 min, unlabelled uridine was added to the apical chamber (20 mM). As shown by the slopes of the regression lines, this substantially reduced the rate of uridine transport across the epithelium ($p < 0.05$) ($n = 5$) (error bars represent SEM).

^{3}H-uridine (1 μM) across the epithelium to the basolateral chamber was slower than in the presence of $Na^+$and, at 50 min before the addition of 20 mM apical unlabelled uridine, had reached a value of 31 ±1 pmol/cm^2 (n = 6). After uridine addition, the time course of appearance of ^{3}H in the basolateral chamber continued unaltered and reached a final value of 86 ± 2 pmol/cm^2 (n = 6) at 2 h (Fig. 3-2). As shown in histogram form in Fig. 3-3, calculated rates of ^{3}H-uridine transport before and after uridine addition (0.64 ± 0.01 and 0.70 ± 0.05 pmol/cm^2/min (n = 6), respectively) were not significantly different either from each other, or from the rate of transport in Na^+ KHS medium after addition of uridine. Na^+ removal therefore resulted in a 74 % decrease in ^{3}H-uridine transport rate ($p < 0.05$), the residual flux being unaffected by addition of unlabelled uridine. In consequence, therefore, and as illustrated diagrammatically by the slopes of the lines in Fig. 3-2, transepithelial movement of ^{3}H-uridine across the mouse jejunum was resolved into two components. The first and major component of transport was Na^+-dependent, and self-inhibited by excess unlabelled uridine. The second was Na^+-independent and unaffected by excess unlabelled nucleoside. Thus, in Na^+ KHS medium after uridine addition, the slope of the uptake curve decreased to become parallel to that in Ch^+ KHS medium. Representing approximately 25 % of the total ^{3}H-uridine transported in the presence of Na^+ (Fig. 3-3), the residual uridine-insensitive flux in Ch^+ KHS medium had the characteristics of non-mediated movement of permeant across the epithelium.

In parallel with sampling from the basolateral chamber, equal 100 μl aliquots of medium were removed every 10 min from the apical chamber. There was no significant change in apical uridine concentration either in the presence or absence of Na^+ over the incubation period of 2 h (data not shown).

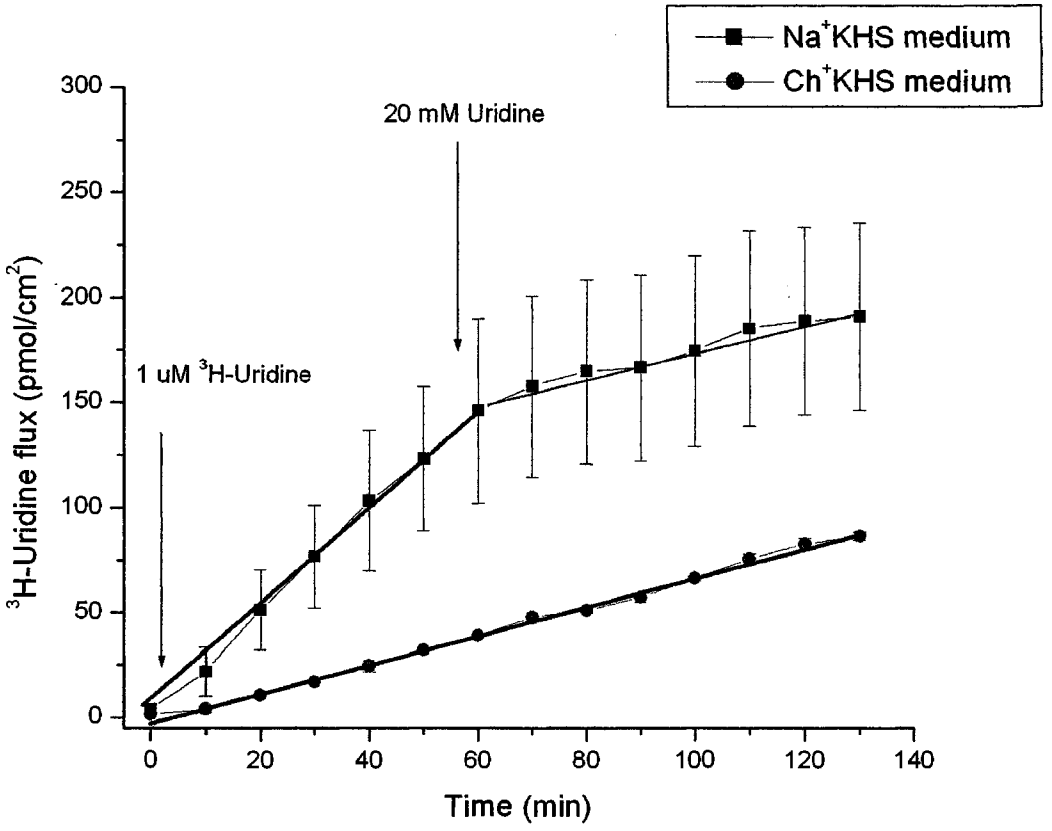

Figure 3-2 Na^+ dependent transport of uridine across mouse jejunal epithelium. Mouse jejunal epithelial tissue was subjected to either Na^+ KHS medium (*squares*) (n = 5) or Ch^+ KHS medium (*circles*) (n = 6). In each condition, ^{3}H-uridine (1 μM) was applied to the apical chamber and the resulting transepithelial flux measured by taking samples from the basolateral chamber every 10 min for 2 h. After 50 min, uridine (20 mM) was applied to the apical chamber. As shown by the slopes of the regression lines, uridine transport was much greater in the presence than in the absence of Na^+, and a high concentration of unlabelled uridine blocked the Na^+-dependent component of transepithelial uridine movement ($p < 0.05$) (error bars represent SEM). The data in Na^+ KHS medium are from Fig. 3-1.

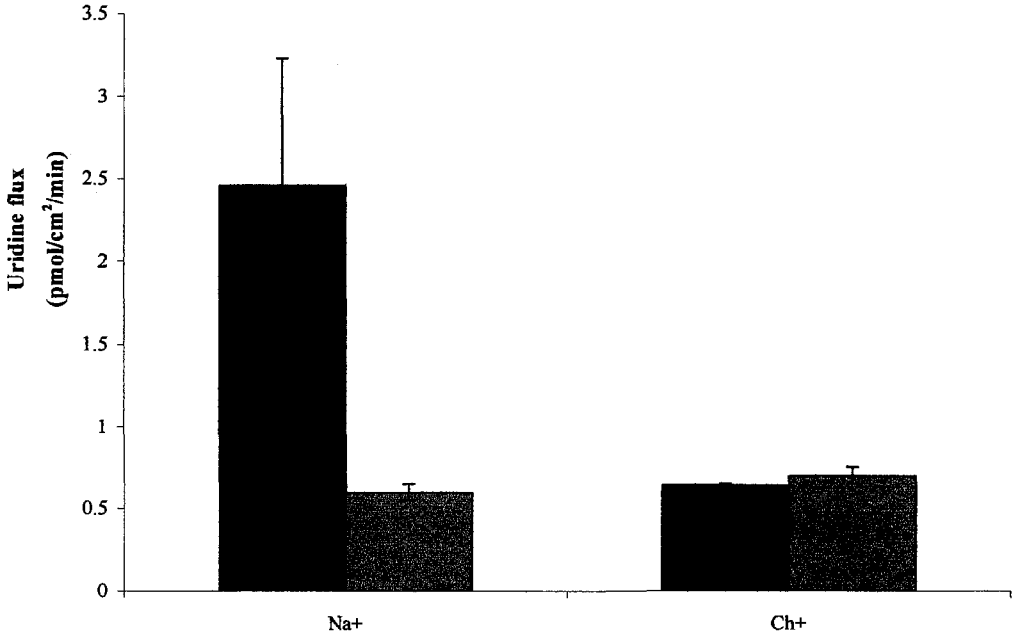

Figure 3-3 Rates of uridine transport across mouse jejunal epithelium in the presence and absence of Na^+ and competing unlabelled uridine.

The slope of ^{3}H-uridine flux as a function of time gives the rate of uridine transepithelial movement from the apical chamber to the basolateral chamber. The rates shown on the left are for mouse jejunum in Na^+ KHS medium, where the black bar is the rate before unlabelled uridine (20 mM) addition, and the grey bar is the rate after uridine application (n = 5). On the right are the corresponding rates in Ch^+ KHS medium before and after addition of uridine (20 mM) (n = 6). Uridine flux in Na^+ KHS medium in the absence of unlabelled uridine was significantly higher than in the other three conditions ($p < 0.05$) (error bars represent SEM). Data are from Figs. 3-1 and 3-2.

3.1.2 Uridine transport across different regions of mouse intestine

For comparison with data obtained for jejunum in Fig. 3-2, corresponding tissue samples from three additional regions of mouse intestine (duodenum, ileum and colon) were prepared and mounted as described in Section 2.3. Experiments were carried out under conditions identical to those detailed in Section 3.1.1 and Fig. 3-2. Apical-to-basolateral ^{3}H-uridine fluxes for all four intestinal preparations (duodenum, jejunum, ileum and colon) are depicted in Fig. 3-4.

Duodenum. Fig. 3-4A shows that ^{3}H-uridine fluxes in duodenum were low and unaffected by the addition of an excess of unlabelled uridine (20 mM was added to the apical chamber at time 50 min). Further, there was no significant difference between uridine fluxes in Na^+ KHS medium and uridine fluxes in Ch^+ KHS medium: overall fluxes in the presence (n = 6) and absence (n = 5) of Na^+ were 1.1 $\pm$ 0.2 and 0.9 $\pm$ 0.1 pmol/cm^2/min, respectively. These findings suggest that uridine fluxes in duodenum were not transporter-mediated.

Jejunum. Results for uridine fluxes in jejunum (Fig. 3-4B) are those described in detail in Section 3.1.1 and Fig. 3-2. In marked contrast to duodenum, uridine fluxes in jejunum showed marked Na^+-dependence and competition by unlabelled uridine. Comparison of Figs. 3-4A and 3-4B shows that the low fluxes of uridine in duodenum were broadly similar to the basal (i.e. non-mediated) fluxes of uridine in jejunum in the absence of Na^+ and/or presence of unlabelled uridine.

Ileum. Continuing down the intestinal tract, the next tissue region to be characterized was ileum. Ileum exhibited a similar pattern of uridine transport as jejunum, but to lesser extent. As shown in Figure 3-4C, there was a significant difference

in flux in Na^+ KHS and Ch^+ KHS media. Furthermore, in Na^+ KHS medium, the addition of excess unlabelled uridine (20 mM) resulted in a reduction in uridine transepithelial movement to a rate similar to that in Ch^+ KHS medium, which was unaffected by uridine addition. In Na^+ KHS medium, fluxes were 1.88 ± 0.19 pmol/cm^2/min (n = 6) before the addition of 20 mM unlabelled uridine and 1.08 ± 0.20 pmol/cm^2/min (n = 6) following uridine addition, a reduction of 43% ($p < 0.05$). The corresponding flux in Ch^+ KHS medium was 1.08 ± 0.14 pmol/cm^2/min (n = 5). Consequently, therefore, a component of the uridine flux in ileum, like jejunum, was both Na^+-dependent and inhibited by excess unlabelled uridine. Comparison of Figs. 3-4B and 3-4C illustrates, however, that the extent of Na^+-dependent uridine transport was less for ileum than in jejunum.

Colon. The final region to be examined for uridine transport was colon. Here, the pattern of uridine flux was similar to that in duodenum, showing no evidence of Na^+-dependence or uridine competition, and indicating, therefore, that fluxes were not transporter-mediated. Fluxes in Na^+ KHS and Ch^+ KHS media were 0.72 ± 0.12 and 0.49 ± 0.10 pmol/cm^2/min (n = 6), respectively.

Since jejunal epithelium exhibited the greatest extent of transepithelial uridine transport, this tissue region was selected for all subsequent experiments.

3.1.3 Basolateral-to-apical transport of uridine in mouse jejunum

Using an equivalent protocol (Section 2.4.4), jejunal fluxes of ^{3}H-uridine were also investigated in the opposite basolateral-to-apical direction.

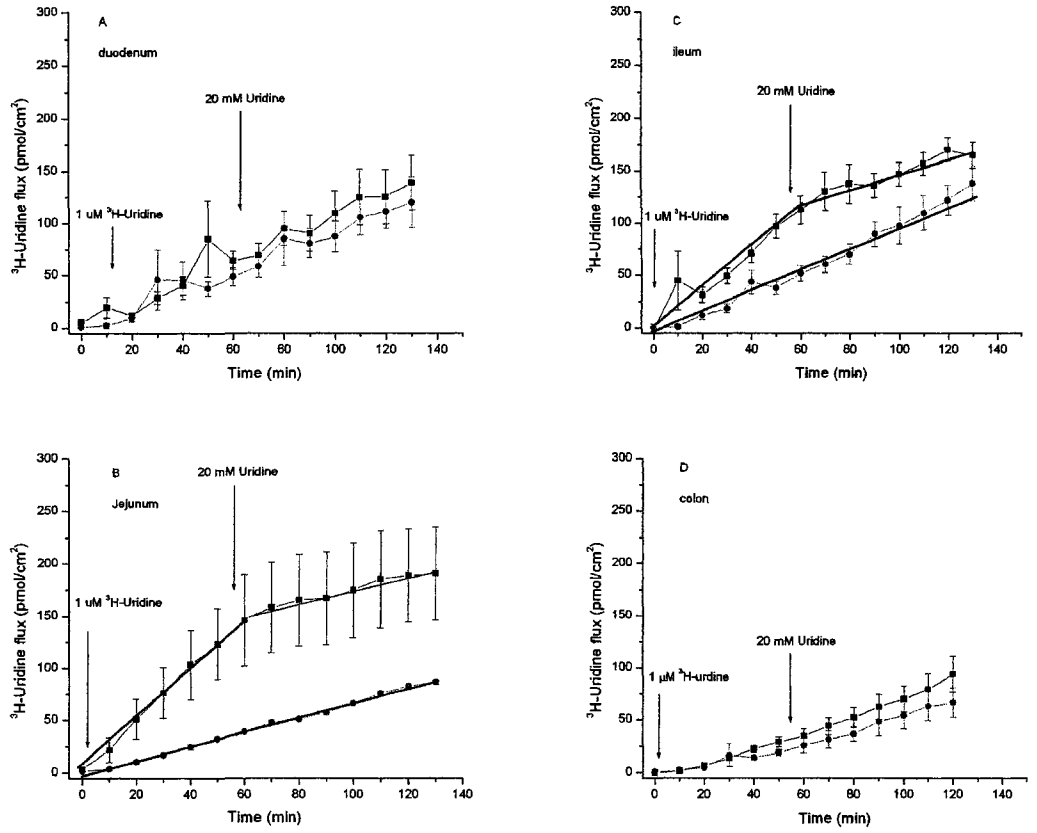

Figure 3-4 Apical-to-basolateral transport of uridine across different regions of mouse intestinal epithelium.

Transport profiles were generated by measuring the appearance of ^{3}H-uridine on the basolateral side of the tissue following addition of ^{3}H-uridine (1 µM) to the apical side. This was undertaken in both Na^{+} KHS medium (*squares*) and Ch^{+} KHS medium (*circles*). Under both conditions, excess unlabelled uridine (20 mM) was applied to the apical chamber after 50 min. (A) duodenum (B) jejunum (C) ileum (D) colon (n = 6). Significant differences are indicated in the text. (error bars represent SEM).

As shown in Fig. 3-5, fluxes were low and approximately linear with time, and there was no difference between Na^+ and Ch^+ KHS media. Furthermore, the addition of unlabelled uridine (20 mM) at 50 min did not reduce the rate of uridine flux. Fluxes in Na^+ KHS (n = 6) and Ch^+ KHS (n = 5) media were 0.53 $\pm$ 0.07 and 0.68 $\pm$ 0.07 pmol/cm^2/min, respectively.

In contrast to uridine movement in the apical-to-basolateral direction, therefore, where the majority of transepithelial fluxes were both Na^+-dependent and inhibited by excess unlabelled uridine, transfer in the opposite basolateral-to-apical direction had the characteristics of non-mediated movement of permeant across the epithelium. Fig. 3-6 depicts fluxes in the two directions, and demonstrates that the magnitude of non-mediated movement of permeant across the epithelium is similar in both directions. Mediated (Na^+-dependent) transepithelial transport of uridine was therefore vectorial in nature, whereas non-mediated movement of uridine across the epithelium was not.

3.1.4 Transepithelial movement of mannitol across mouse jejunum

Using an equivalent protocol (Section 2.4.5), apical-to-basolateral jejunal fluxes of ^{3}H-mannitol (1 μM) were also investigated to quantify the extent of paracellular movement of solute across the epithelium. As shown in Fig. 3-7, fluxes of mannitol were approximately linear with time, with no difference between Na^+ and Ch^+ KHS media. The addition of unlabelled uridine (20 mM) at 50 min did not reduce the rate of mannitol movement across the epithelium. Mannitol fluxes in Na^+ KHS and Ch^+ KHS media were 0.50 $\pm$ 0.09 and 0.38 $\pm$ 0.07 pmol/cm^2/min (n = 6), respectively.

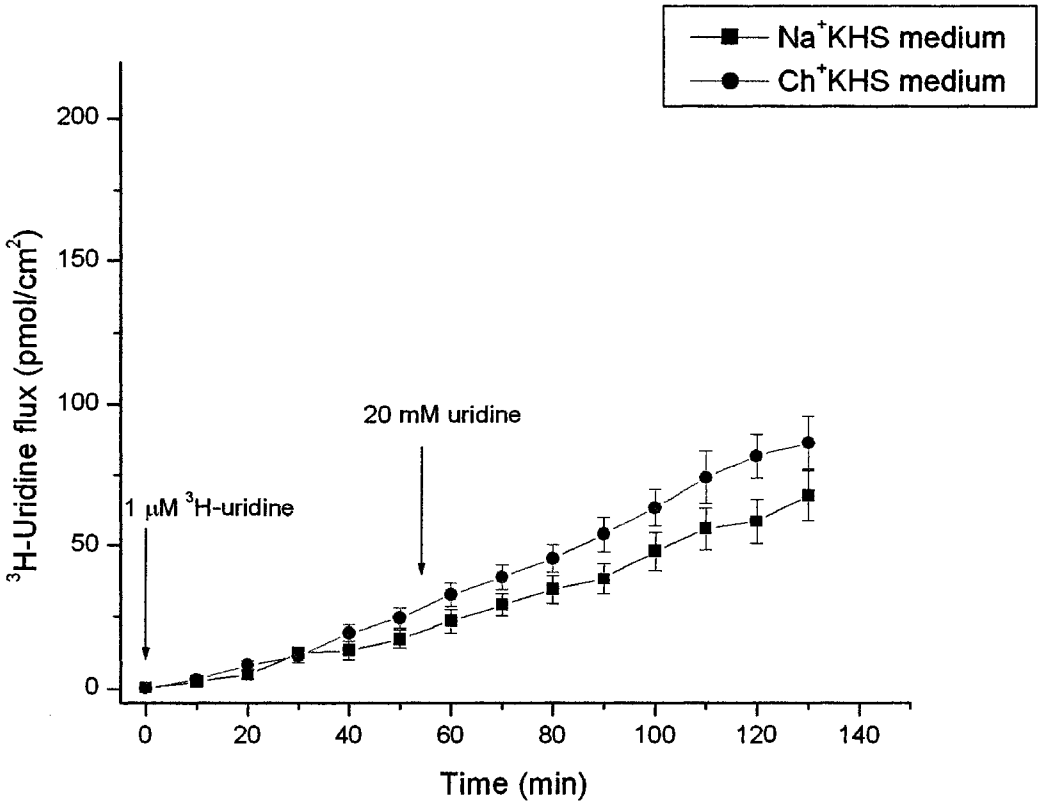

Figure 3-5 Basolateral-to-apical flux of uridine across mouse jejunal epithelium. Transepithelial fluxes were determined by measuring the appearance of ^{3}H-uridine on the apical side of the tissue following addition of ^{3}H-uridine (1 μM) to the basolateral side. This was undertaken in both Na^{+} KHS medium (*squares*) (n = 6) and Ch^{+} KHS medium (*circles*) (n = 5). Under both conditions, excess unlabelled uridine (20 mM) was applied to the basolateral chamber after 50 min. (error bars represent SEM).

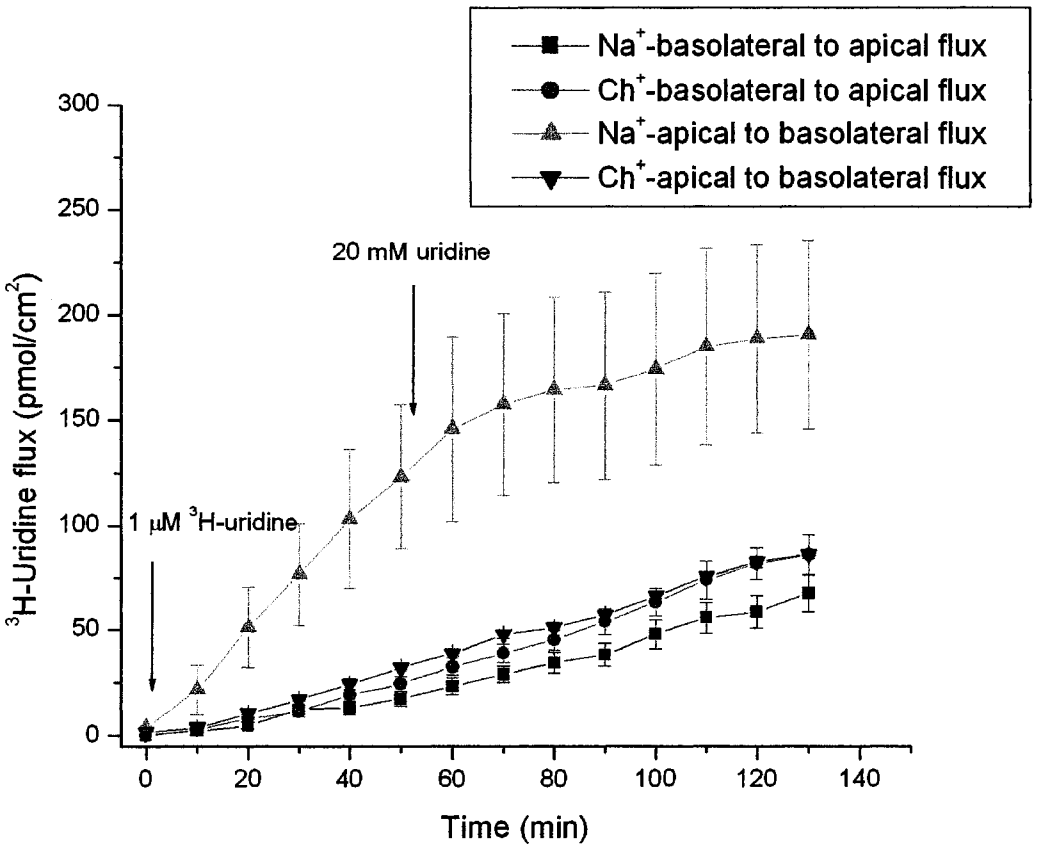

Figure 3-6 Comparison of apical-to-basolateral and basolateral-to-apical fluxes of uridine across mouse jejunal epithelium.

^{3}H-Uridine (1 μM) was applied to one chamber and samples taken from the opposite chamber (every 10 min for 2 h); at 50 min, 20 mM unlabelled uridine was applied as competing nucleoside to the same chamber as radiolabelled permeant. This was undertaken in both Na^+ KHS and Ch^+ KHS media: *(triangles)* (n = 5) and *(squares)* (n = 6), fluxes in Na^+-containing medium in the apical-to-basolateral and basolateral-to-apical directions, respectively; (*upside down triangles*) (n = 6) and (*circles*)(n = 5), corresponding fluxes in the absence of Na^+, respectively. Significant differences are indicated in the text. Data are from Figs. 3-2 and 3-5. (error bars represent SEM).

Fig. 3-7 compares these apical-to-basolateral mannitol fluxes to the corresponding fluxes of uridine in Na^+ and Ch^+ KHS media shown previously in Fig. 3-2. Clearly, mannitol fluxes in both conditions were much smaller than apical-to-basolateral fluxes of uridine in Na^+ KHS medium. To a much lesser extent, mannitol fluxes in Na^+ and Ch^+ KHS media were also smaller than those for uridine in Ch^+ KHS medium: only in the case of Ch^+ KHS medium, however, was the difference in uridine and mannitol fluxes statistically significant ($p < 0.05$). The results suggested that the majority of non-mediated movement of uridine across mouse jejunum can be accounted for by paracellular pathway(s).

3.1.5 Transepithelial Resistance

As described in Section 2.4.6, trans-epithelial resistance was calculated using Ohm's Law. Taking Fig. 2-3 as an example when 0.5 mV of potential difference was applied across jejunal epithelium, the result was an increase in I_{sc} of 2.7 μA, which corresponds to a resistance of 37 Ω/cm^2. The normal range of tissue resistance across the mouse jejunum is 20-40 Ω/cm^2 (Sandu *et al.* 2005). Values within this range are considered to indicate "normal" tissue integrity. All of the experiments reported in this thesis had tissue resistance values >20 Ω/cm^2.

3.1.6 Competing uridine concentrations

In Sections 3.1.1 to 3.1.4, an excess of unlabelled uridine was added to the same chamber as ^3H-uridine in order to block transporter-mediated fluxes. The unlabelled uridine concentration in these experiments was 20 mM, and was added 50 min after the start of the experiment. In order to establish experimental conditions that would enable

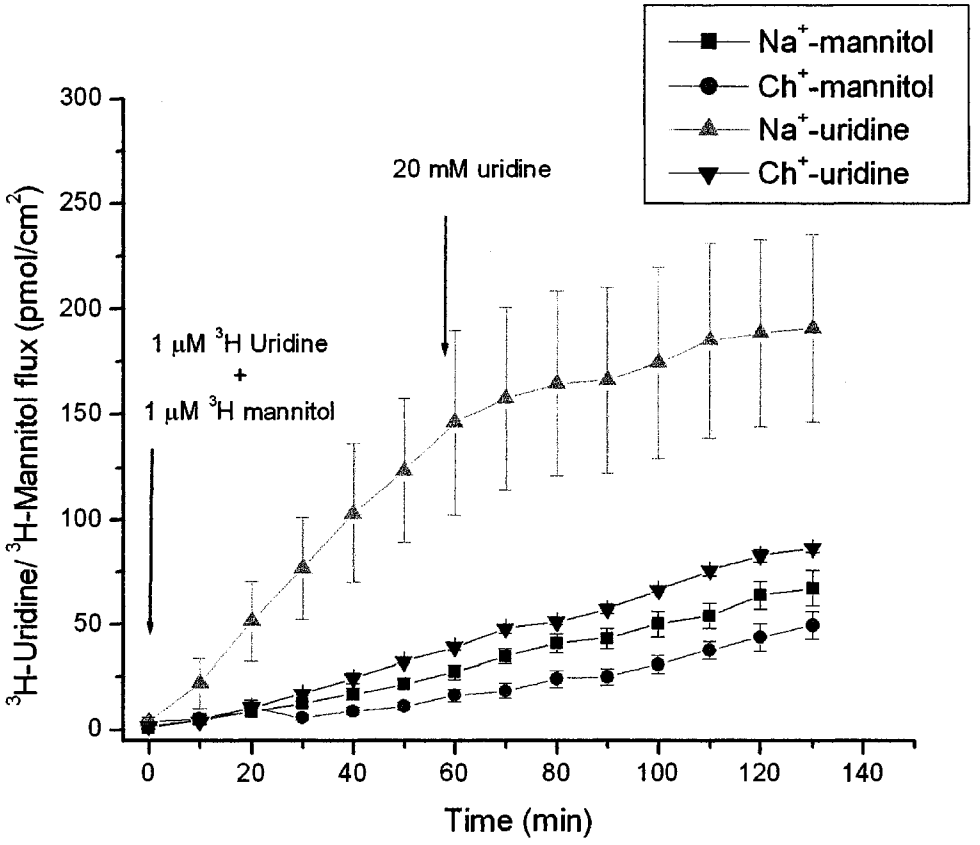

Figure 3-7 Comparison of apical-to-basolateral movement of mannitol and uridine across mouse jejunal epithelium.

Either ^{3}H-mannitol or ^{3}H-uridine (1 μM) were added to the apical chamber, and samples taken every 10 min from the basolateral chamber; unlabelled uridine (20mM) was added to the apical chamber at time 50 min. This was undertaken in both Na^+ KHS medium (*squares*) (n = 6), and in Ch^+ KHS medium *(circles)* (n = 5). Corresponding uridine fluxes in the presence and absence of Na^+ from Fig. 3-2 are indicated by *(triangles)* (n = 5) and *(inverted triangles)* (n = 6), respectively. Significant differences are indicated in the text. (error bars represent SEM).

further characterization of the mechanisms by which uridine is transported across mouse jejunal epithelium; Fig. 3-8 shows the results of experiments in Na^+ KHS medium in which varying concentrations of unlabelled uridine (1, 5 and 20 mM) were added to the apical chamber immediately prior to the time zero addition of 1 μM ^{3}H-uridine. The corresponding flux in the absence of competing unlabelled uridine is also shown. Fluxes were approximately linear with time throughout the 2 h duration of the experiment, and all three unlabelled uridine concentrations reduced ^{3}H-uridine transport to similar extents. Transepithelial ^{3}H-uridine fluxes were: 1.87 $\pm$ 0.42 pmol/cm^2/min (n = 8) for the control without unlabelled uridine added, and 0.67 + 0.17, 0.63 $\pm$ 0.12, and 0.50 $\pm$ 0.07 pmol/cm^2/min in the presence of 1, 5 and 20 mM unlabelled uridine, respectively (n = 5, $p < 0.05$ for the difference between fluxes in the presence and absence of unlabelled uridine). The rate of transepithelial movement was therefore reduced by 64 % when 1 mM unlabelled uridine was added, by 66 % in the presence of 5 mM unlabelled uridine, and by 73% in the presence of 20 mM unlabelled uridine. This confirmed that the majority of transepithelial uridine transport across mouse jejunum in the presence of Na^+ was transporter-mediated, and established that 1 mM unlabelled uridine was sufficient to block the majority of this transport activity.

3.1.7 Thymidine and inosine compete for transport with uridine in mouse jejunum

As described in Chapter 1, all three murine Na^+-dependent nucleoside transporters transport uridine: mCNT1 is pyrimidine nucleoside selective, mCNT2 is purine nucleoside-selective, but also transports uridine, while mCNT3 transports both pyrimidine and purine nucleosides. Cross-competition experiments were therefore undertaken with the mCNT1/3 permeant thymidine and the mCNT2/3 permeant inosine

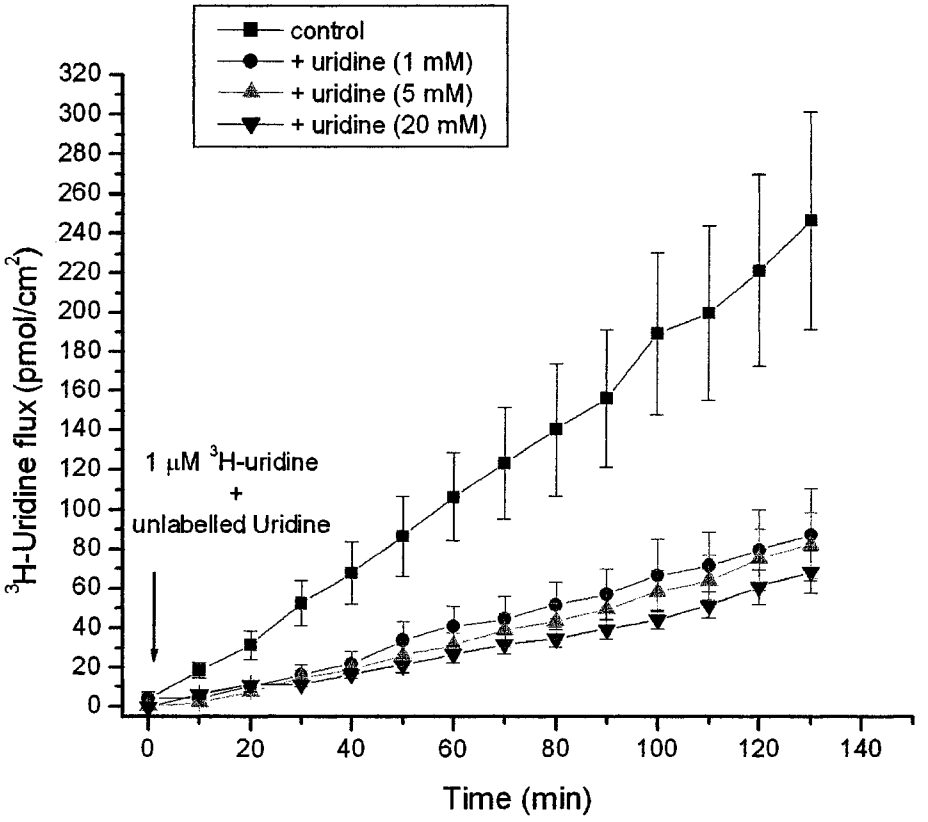

Figure 3-8 Effects of different concentrations of competing unlabelled uridine on apical-to-basolateral flux of ^{3}H-uridine across mouse jejunal epithelium.
^{3}H-uridine (1 μM) was added to the apical chamber at time zero, and samples were taken every 10 min from the basolateral chamber. Fluxes in Na^+ KHS medium were determined either in the absence of competing unlabelled uridine (*squares*) (n = 16), or when different concentrations of unlabelled uridine were added to the apical chamber immediately prior to the addition of ^{3}H-uridine; unlabelled uridine concentrations were 1 mM (*circles*), 5 mM (*triangles*) and 20 mM (*inverted triangles*) (n = 5). (error bars represent SEM).

to determine the extents to which each of these three transporters contributed to movement of ^{3}H-uridine across mouse jejunal epithelium. Similar to Fig. 3-8, the competing unlabelled nucleoside (1 mM) and ^{3}H-uridine (1 μM) were both added to the apical chamber at time zero, and fluxes were determined in both Na^+ KHS and Ch^+ KHS media. The experimental design is described in section 2.4.3. In each individual experiment there were four parallel Ussing Chamber set-ups. Two employed Na^+ KHS medium, one with and one without unlabelled competing nucleoside (1 mM) added to the apical chamber at time zero. The other two employed Ch^+ KHS medium, one with and one without 1 mM of the same competing unlabelled nucleoside.

As shown in Fig. 3-9, 1 mM unlabelled thymidine completely abolished Na^+-dependent transepithelial flux of uridine across mouse jejunum, reducing uridine transport activity in the presence of Na^+ by 76 %. In marked contrast, but as expected from uridine competition experiments, there was no effect of thymidine on the smaller Na^+-independent, non-mediated component of the uridine flux. Uridine fluxes in Na^+ KHS medium in the absence and in the presence of unlabelled thymidine were 2.63 $\pm$ 0.58 (n = 4) and 0.64 $\pm$ 0.24 pmol/cm^2/min (n = 4), respectively ($p < 0.05$), compared to 0.47 $\pm$ 0.05 (n = 16) and 0.64 $\pm$ 0.10 pmol/cm^2/min (n = 4), respectively, in Ch^+ KHS medium. These findings suggested that Na^+-dependent transepithelial movement of uridine across mouse jejunum was mediated by mCNT1 and/or mCNT3.

The corresponding effects of unlabelled inosine on transepithelial fluxes of ^{3}H-uridine across mouse jejunal epithelial tissue are shown in Fig. 3-10. In this case, substantial, but incomplete, inhibition of Na^+-dependent uridine transport was observed, unlabelled inosine reducing uridine flux in the presence of Na^+ by 46%.

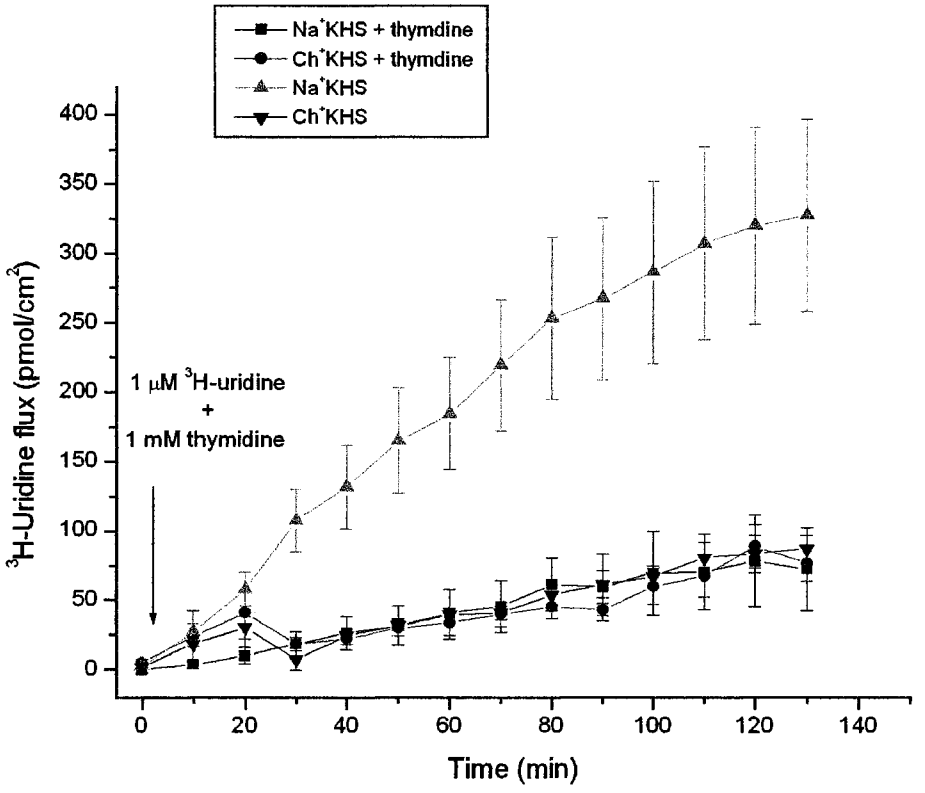

Figure 3-9 Thymidine inhibits uridine transport across mouse jejunal epithelium
^{3}H-Uridine (1 μM) was added to the apical chamber in Na^+ KHS medium with (*squares)* (n = 4) and without 1 mM unlabelled thymidine (*triangles*) (n = 4), and samples were taken from the basolateral chamber every 10 min. Corresponding fluxes with (*circles*) (n = 4) and without 1 mM thymidine (*inverted triangles*) (n = 4) were also undertaken in Ch^+ KHS medium. Significant differences are indicated in the text. (error bars represent SEM).

Similar to thymidine, there was no effect of inosine on the smaller Na^+-independent, non-mediated component of the uridine flux. Uridine fluxes in Na^+ KHS medium in the absence and presence of unlabelled inosine were 3.35 ± 0.55 (n = 4) and 1.32 ± 0.21 pmol/cm^2/min (n = 4), respectively, compared to 0.67 ± 0.09 (n = 4) and 0.61 ± 0.13 pmol/cm^2/min (n = 4), respectively, in Ch^+ KHS medium ($p < 0.05$ for the difference between the flux rate in Na^+ KHS medium in the presence of inosine and fluxes under the other three conditions). The extent of inosine inhibition of the Na^+-dependent component of transepithelial uridine flux was therefore 61%. Supporting the findings from Fig. 3-9, the results provided further evidence for involvement of mCNT1/3, with mCNT1 contributing to a maximum of 39% of the overall mCNT1/3 flux. The estimate of the mCNT1 contribution would decline if an inosine concentration of 1 mM caused only partial inhibition of mCNT3 jejunal transport activity.

3.1.8 Transepithelial transport of formycin B across mouse jejunal epithelium

The apical-to-basolateral flux of ^{3}H-formycin B (1 μM), a non-metabolized analogue of inosine, was studied using the same protocol described in Section 2.4.3 and illustrated for ^{3}H-uridine in Section 3.1.1 and Fig. 3-2. Jejunal epithelial tissue was prepared and used by the procedure described in Section 2.3. In Na^+ KHS medium, the ^{3}H-formycin B transepithelial fluxes were 1.46 ± 0.14 pmol/cm^2/min before addition of excess unlabelled uridine, and 0.46 ± 0.09 pmol/cm^2/min following addition of 20 mM uridine to the apical chamber at 50 min ($p < 0.05$) (n = 6) (Fig. 3-11). This addition of unlabelled uridine halfway through the experiment reduced the rate of ^{3}H-formycin B transepithelial flux by 68% to a value that was similar to that in Ch+ KHS medium (0.65

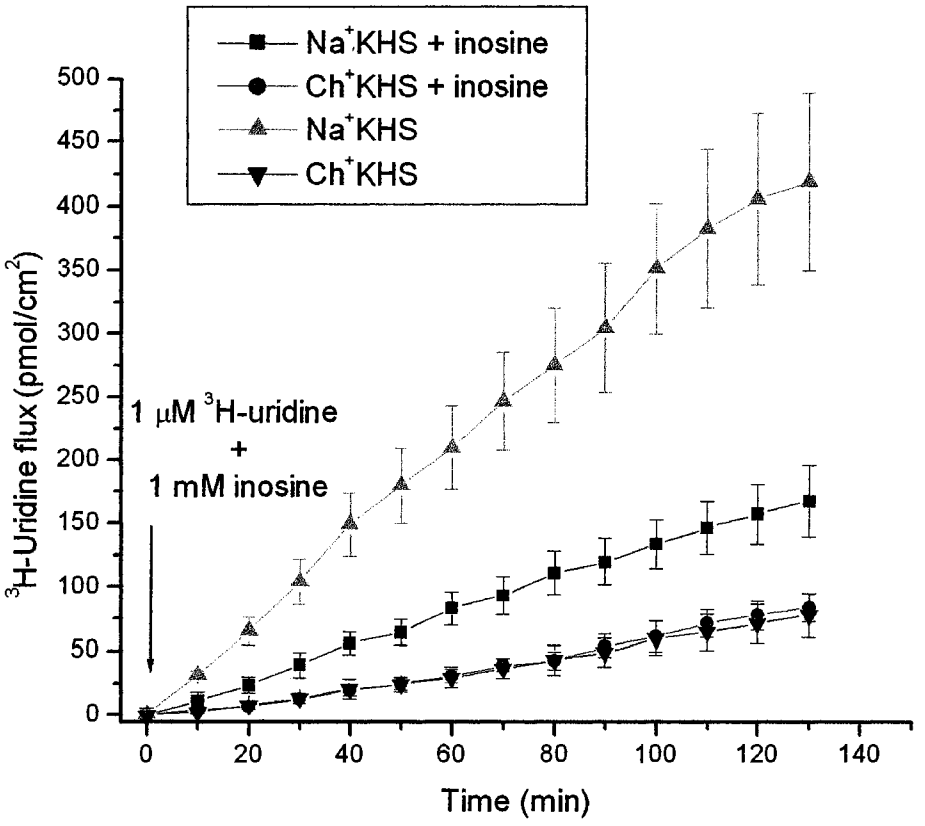

Figure 3-10 Inosine inhibits uridine flux across mouse jejunal epithelium
^{3}H-Uridine (1 μM) was added to the apical chamber in Na^+ KHS medium with *(squares)* (n = 4) and without 1 mM unlabelled inosine *(triangles)* (n = 4), and samples were taken from the basolateral chamber every 10 min. Corresponding fluxes with *(circles) (n* = 4) and without 1 mM inosine (inverted *triangles)* (n = 4) were also undertaken in Ch^+ KHS medium. Significant differences are indicated in the text. (error bars represent SEM).

$\pm$ 0.18 pmol/cm^2/min) (n = 5). Like uridine, therefore, formycin B flux across the jejunal epithelium was predominantly Na^+-dependent and transporter-mediated. Other experiments examining ^{3}H-formycin B flux across the mouse jejunum were similar in protocol to the ^{3}H-uridine transport competition experiments undertaken in Section 3.1.7. and illustrated in Fig. 3-9. The difference was that ^{3}H-formycin B (1 μM) was used as the tracer permeant rather than ^{3}H-uridine. When the analysis was carried out in Na^+ KHS medium, the ^{3}H-formycin B fluxes were 1.48 $\pm$ 0.32 and 0.36 $\pm$ 0.08 pmol/cm^2/min in the absence and in the presence of excess unlabelled thymidine (1 mM) respectively, a reduction of 76 % ($p < 0.05$) (n = 4) (Fig. 3-12). Corresponding transport rates in Ch^+ KHS medium were 0.69 $\pm$ 0.07 (n = 4) and 0.42 $\pm$ 0.07 pmol/cm^2/min (n = 3), respectively, a decrease of 39 % ($p < 0.05$) Unlike uridine, therefore, and not detected in Fig. 3-11, the results are consistent with a small but significant Na^+-independent mediated component of ^{3}H-formycin B transport. Calculated by subtraction of fluxes in the presence and absence of Na^+, the respective magnitudes of the Na^+-dependent and Na^+-independent components of mediated ^{3}H-formycin B transport were 1.48 – 0.69 = 0.79 and 0.69 – 0.42= 0.27 pmol/cm^2/min, respectively. For comparison, the magnitude of the corresponding Na^+-dependent ^{3}H-uridine transepithelial transport rate was 2.63 – 0.64 = 1.99 pmol/cm^2/min (Section 3.1.7 and Fig. 3.9).

Inhibited by the pyrimidine nucleoside thymidine, the larger Na^+-dependent component of ^{3}H-formycin B transport had characteristics consistent with involvement of mCNT3, while the smaller Na^+-independent component of transport potentially involved mENT1 and/or mENT2, each of which transports both pyrimidine and purine nucleosides.

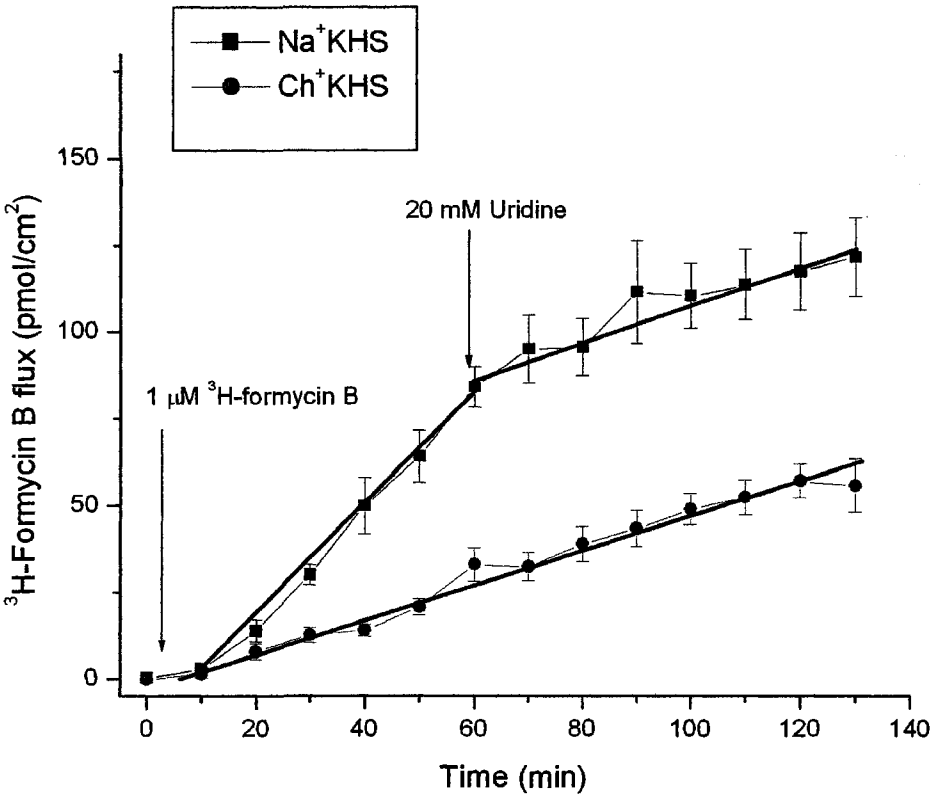

Figure 3-11 Na^+-dependent transport of formycin B across mouse jejunal epithelium. Mouse jejunum epithelial tissue was subjected to either Na^+ KHS medium (n = 6) or Ch^+ KHS medium (n = 5). In each condition, ^{3}H-formycin B (1 μM) was applied to the apical chamber and the resulting transepithelial flux measured by taking samples from the basolateral chamber every 10 min for 2 h. After 50 min, uridine (20 mM) was applied to the apical chamber. As shown by the slopes of the regression lines, formycin B flux was much greater in the presence than in the absence of Na^+, and a high concentration of unlabelled uridine blocked the Na^+-dependent component of transepithelial formycin B movement ($p < 0.05$) (error bars represent SEM).

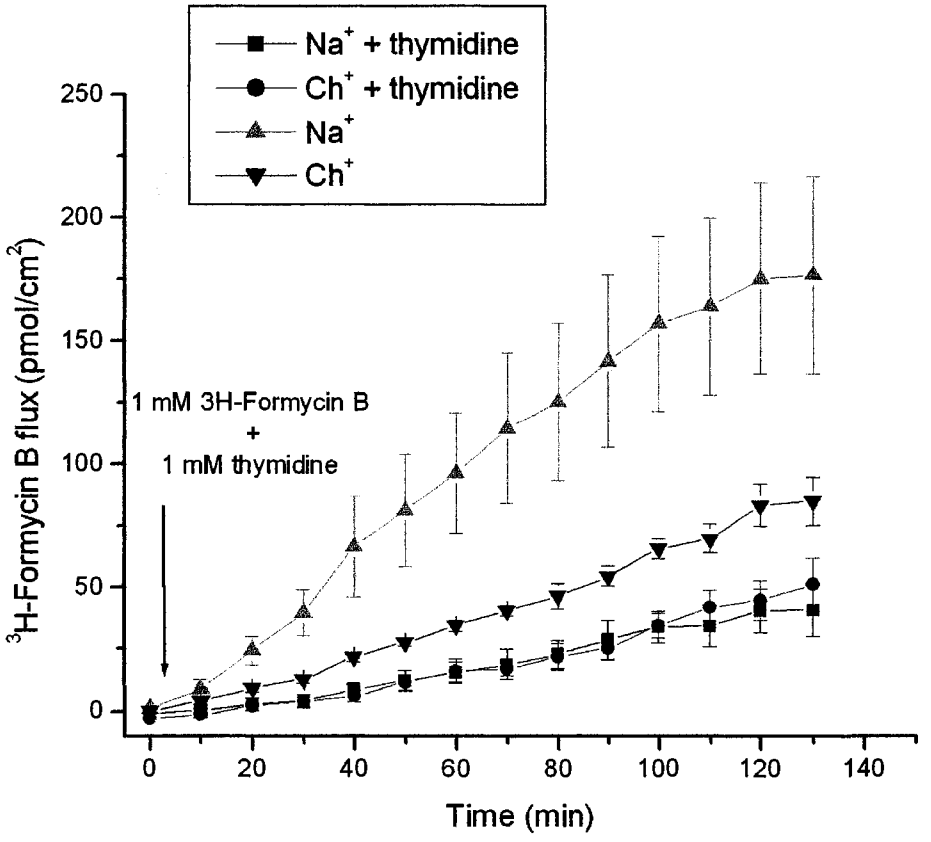

Figure 3-12 Thymidine inhibits formycin B transport across mouse jejunal epithelium. ^{3}H-Formycin B (1 μM) was added at time zero to the apical chamber in Na^{+} KHS medium with *(squares)* (n = 4) and without 1 mM unlabelled inosine *(triangles)* (n = 4), and samples taken from the basolateral chamber every 10 min. Corresponding fluxes with *(circles)* (n = 3) and without 1 mM thymidine (inverted *triangles*) (n = 4) were also undertaken in Ch^{+} KHS medium. Significant differences are indicated in the text. (error bars represent SEM).

It was not possible to resolve the latter component of transepithelial flux in Fig. 3-11: fluxes of ^{3}H-formycin B in Ch^+ KHS medium before and after uridine (20 mM) addition were not significantly different from each other (0.51 $\pm$ 0.08 and 0.44 $\pm$ 0.04 pmol/cm^2/min (n = 4), respectively).

3.1.9 Uridine transport across jejunal epithelial tissue from CNT3 (-/-) mice.

Results presented in Sections 3.1.7 and 3.1.8 implicate mCNT3 as a major contributor to uridine and formycin B movement across mouse jejunal epithelium. To determine if this is indeed the case, a final series of flux studies were undertaken in CNT3 (-/-) null mice. Animals were engineered and genotyped to confirm mCNT3 gene disruption as detailed in Section 2.5. Experiments were performed as described in Section 2.4.3 using jejunal epithelial tissue prepared as outlined in Section 2.3.

Fig. 3-13 shows plots of apical-to-basolateral transepithelial movement of ^{3}H-uridine across the jejunum epithelium of CNT3 (-/-) mice in both Na^+ KHS and Ch^+ KHS media, together with corresponding reference data from wild-type Balb/c mice, which are presumably CNT3 (+/+) (Section 3.1.7 and Fig. 3-9), as well as confirmatory results from a representative control wild-type FVB/N mouse which was determined experimentally to be CNT3 (+/+) and is therefore termed CNT3 (+/+) hereafter. The data for CNT3 (-/-) and CNT3 (+/+) mice showing, in addition, the effects of time zero addition of 1 mM unlabelled uridine, are also presented in Figs. 3-14A & B.

In Na^+ KHS and Ch^+ KHS media, CNT3 (-/-) tissue gave similar ^{3}H-uridine fluxes of 0.95 $\pm$ 0.15 and 0.87 $\pm$ 0.26 pmol/cm^2/min (n = 5), respectively, suggesting total

loss of Na^+-dependent transport function (Fig. 3-13). In comparison, the corresponding transepithelial fluxes of ^{3}H-uridine in wild-type animals in the presence and in the absence of Na^+ were 2.63 $\pm$ 0.58 and 0.64 $\pm$ 0.24 pmol/cm^2/min (n = 4), respectively, for Balb/c mice, and 2.91 and 0.78 pmol/cm^2/min (n = 1), respectively, for CNT3 (+/+) mice ($p < 0.05$ for the reduced Na^+ KHS uridine flux rate in CNT3 (-/-) versus control Balb/c mice).

Fig. 3-14A shows the effects of excess unlabelled uridine (1 mM) on ^{3}H-uridine transepithelial movement in CNT3 (-/-) mice. Uridine fluxes in Na^+ KHS medium in the absence and in the presence of unlabelled uridine were 0.95 $\pm$ 0.15 and 0.52 $\pm$ 0.11 pmol/cm^2/min (n = 5) ($p < 0.05$), respectively, compared to 0.87 $\pm$ 0.26 and 0.79 $\pm$ 0.19 pmol/cm^2/min (n = 5), respectively, in Ch^+ KHS medium. Therefore, the addition of excess unlabeled uridine resulted in a modest reduction in fluxes in Na^+ KHS medium that was not seen in Ch^+ KHS medium. Although uninhibited ^{3}H-uridine fluxes in the presence and absence of Na^+ were indistinguishable, this suggests that CNT3 (-/-) mice might have a small residual component of Na^+-dependent transport remaining, even with mCNT3 absent.

3.2 Gene expression of nucleoside transporters in mouse jejunum epithelial tissue

TaqMan™ quantitative real time RT-PCR was performed in order to assess nucleoside transporter transcript levels in mouse jejunum according to procedures described in Section 2.4. Results were expressed as $1/\Delta Ct$, where ΔCt was calculated as the Ct (cycle threshold) value for a particular nucleoside transporter minus that for GAPDH. The resulting parameter ΔCt, which is the transcript level normalized to

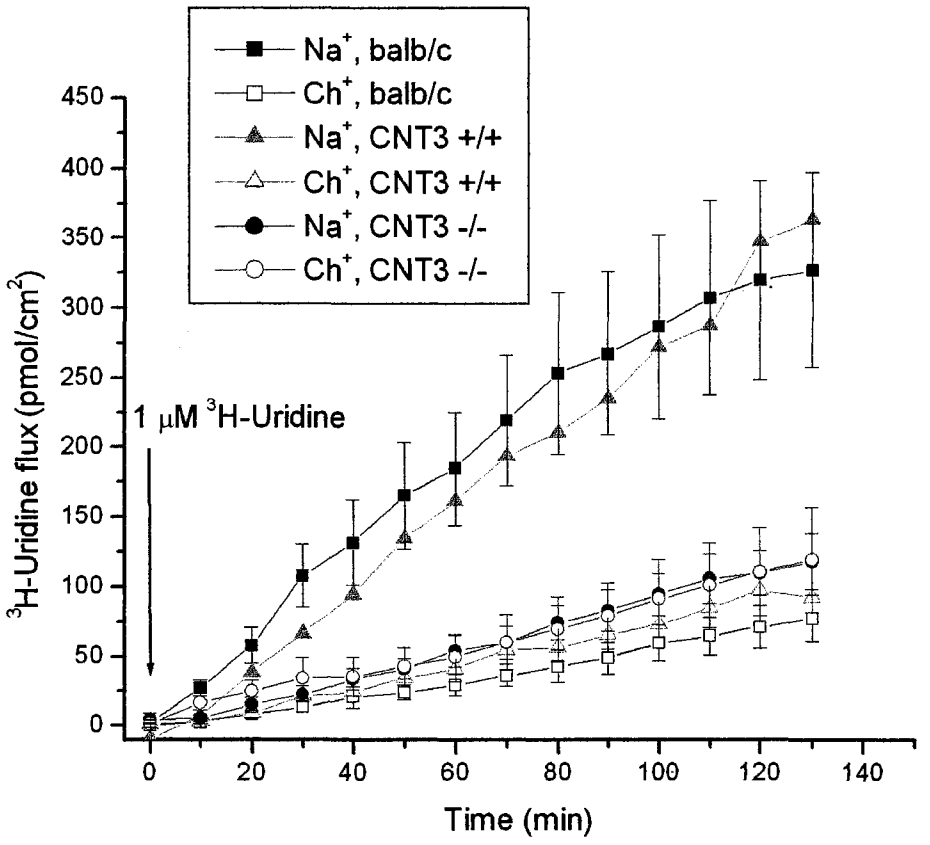

Figure 3-13 Effects of loss of Na^+-dependent uridine transport function on transepithelial fluxes in jejunal epithelium.

At time zero, ^{3}H-uridine (1 μM) was added to the apical chamber in either Na^+ KHS or Ch^+ KHS medium (*closed* and *open* symbols, respectively), and samples taken from the basolateral chamber every 10 min for 2 h: (i) CNT3 (-/-) mice (*circles*) (n = 5), (ii) control wild-type Balb/c mice (*squares*) (n = 4), and (iii) a representative wild-type FVB/N CNT3 (+/+) mouse (n = 1) (*triangles*). Significant differences are indicated in the text. Data for wild-type Balb/c mice are from Fig. 3-9. (error bars represent SEM).

A

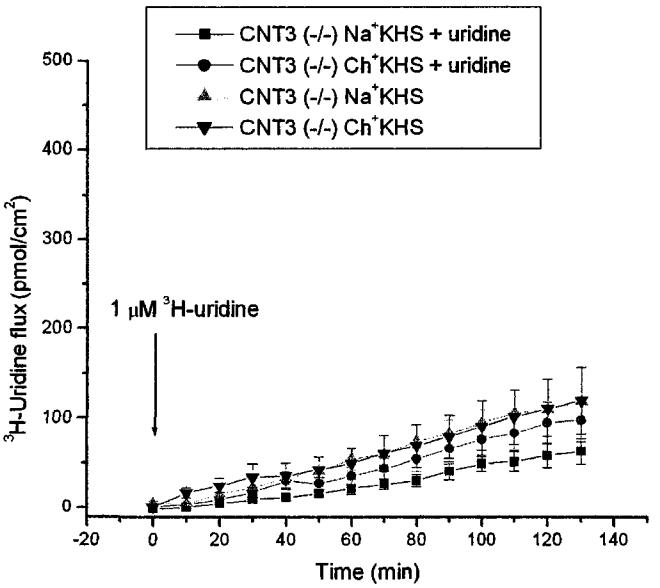

B

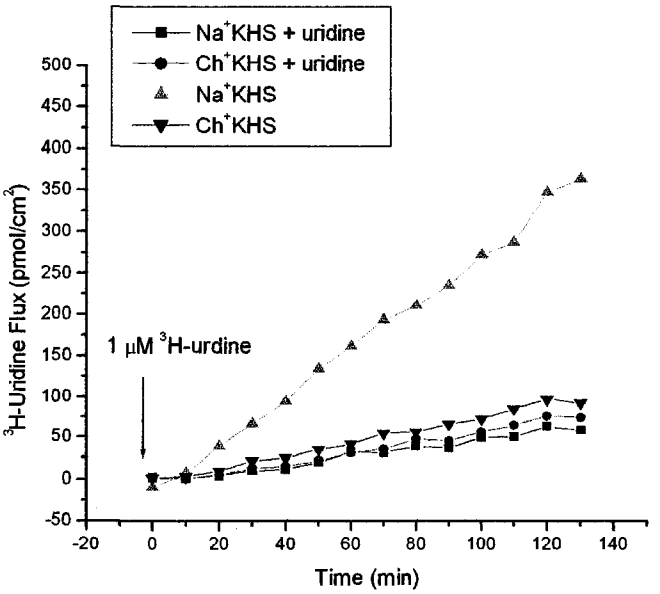

Figure 3-14 Uridine transport across CNT3 (-/-) and CNT3 (+/+) mouse jejunal epithelium

^{3}H-Uridine (1 μM) was added at time zero to the apical chamber in Na^+ KHS medium with (*squares)* and without (*triangles*) 1 mM unlabelled uridine, and samples were taken from the basolateral chamber every 10 min. Corresponding fluxes with (*circles)* and without 1 mM inosine (inverted *triangles*) were also determined in Ch^+ KHS medium. (A) CNT3 (-/-) mice (n = 5) (error bars represent SEM); (B) a representative CNT3 (+/+) mouse (n = 1). Fluxes in the absence of competing unlabelled uridine are also presented in Fig. 3-13.

GAPDH, enabled comparison between different samples, provided that all expressed GAPDH to similar extents. As an illustrative example, Fig. 3-15 provides a representative real time fluorescence recording for mouse jejunal epithelium, comparing amplification of mCNT3 relative to GAPDH. Because a low ΔCt value indicates a high amount of transcript expression, different transporters were compared as 1/ ΔCt, such thatthe nucleoside transporter/tissue sample exhibiting the greatest transcript abundance also had the highest 1/ ΔCt value. Fig. 3-16 compares transcript levels for all seven nucleoside transporters (mCNT1, mCNT2, mCNT3, mENT1, mENT2, mENT3 and mENT4) in jejunal epithelium prepared as described in Section 2.3 from both wild-type (Balb/c) and CNT3 (-/-) null mice. For mCNT1 the 1/ΔCt values were 0.147 ± 0.004 and 0.187 ± 0.010 for wildtype (Balb/c) and CNT3 (-/-) null mice, respectively ($p<0.05$, $n = 3$). Corresponding values for mCNT2 were 0.245 ± 0.021 and 0.280 ± 0.025, respectively. For mCNT3, transcript levels were 0.114 ± 0.005 for Balb/c, and zero (not detectable) for CNT3 (-/-). These results verify the gene knockout in CNT3 (-/-) null mice, and suggest a small, but significant, compensatory increase in expression of transcripts for mCNT1, but not mCNT2. The rank order of relative transcript abundance was mCNT2 > mCNT1 > mCNT3.

Relative mENT1-4 transcript abundance was similar to mCNT3, and none of the ENTs showed significant differences between wildtype (Balb/c) and CNT3 (-/-) null mice. Respective 1/ΔCt values were: ENT1 (0.094 ± 0.003; 0.109 ± 0.005), ENT2 (0.081 ± 0.001; 0.084 ± 0.0006), ENT3 (0.082 ± 0.004; 0.094 ± 0.0008) and ENT4 (0.075 ± 0.004; 0.082 ± 0.001) ($n = 3$).

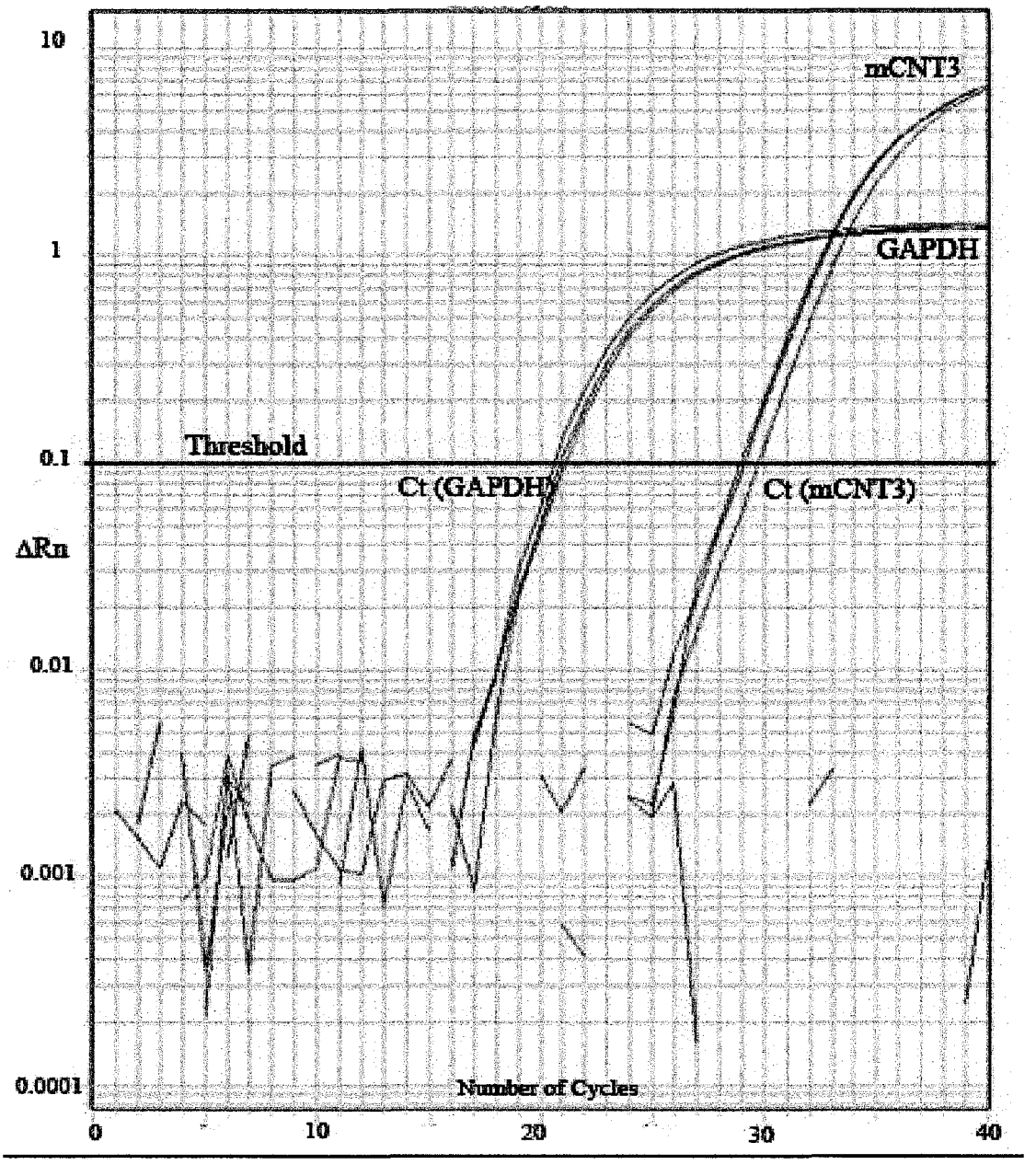

Figure 3-15 Real time RT-PCR amplification of mCNT3 transcripts.
Quantitative real time RT-PCR was performed on wild-type (Balb/c) mouse jejunal epithelium tissue using mCNT3 and GAPDH probes and primers. ΔRn (change in reporter fluorescence normalized to the signal from a passive reference dye) is plotted against the number of cycles in the PCR reaction. Ct values, which were used to designate transcript levels, were determined by the number of cycles needed to reach a certain ΔRn (threshold). The threshold was set in the exponential phase of the PCR reaction. The difference between the Ct value for CNT3 and GAPDH denotes the normalized expression level of the transporter (ΔCt). This analysis was also undertaken for each of the other six nucleoside transporters, comparing transcript levels in both wild-type (Balb/c) and CNT3 (-/-) null mice (Fig. 3-16).

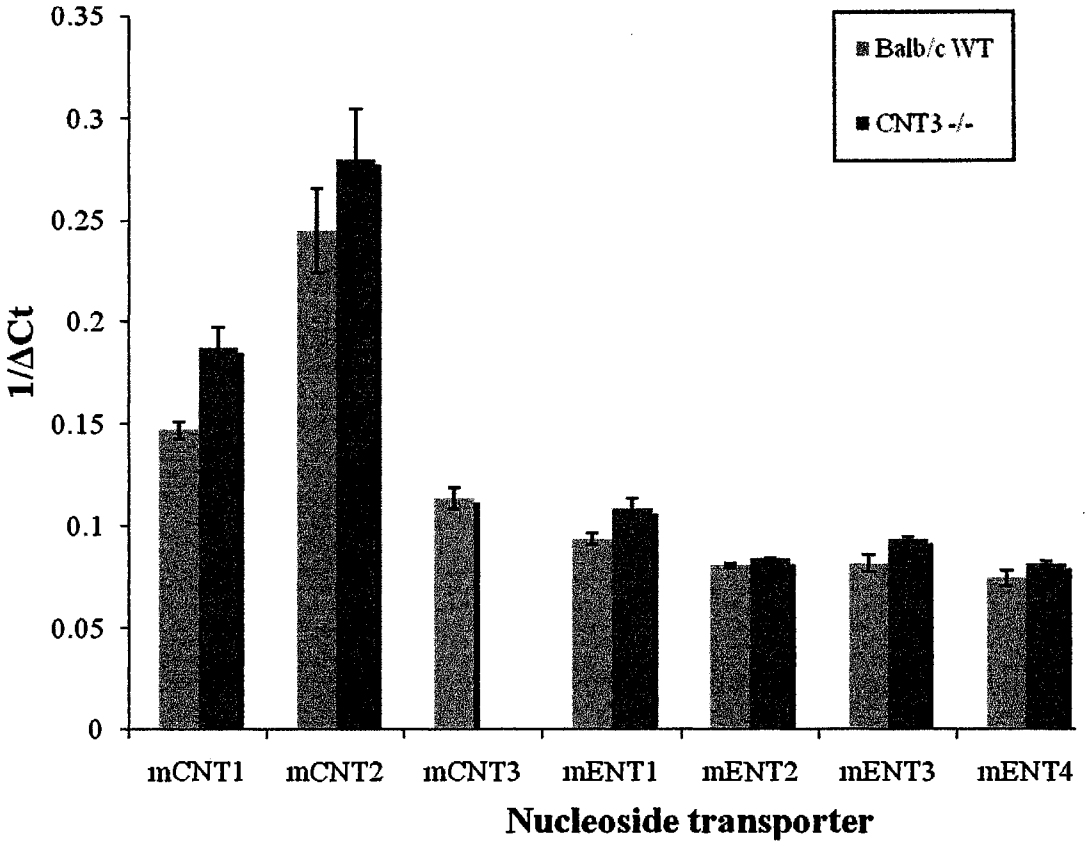

Figure 3-16 Gene expression of nucleoside transporters in mouse jejunal epithelium. Quantitative real time RT-PCR was performed on mouse jejunum tissue, with the transcript level for each transporter compared to that for GAPDH as shown in Fig. 3-15. Transcript level was determined by the cycle threshold (Ct) value, which is the number of cycles required to reach a certain level of fluorescence. The Ct value for each nucleoside transporter had the corresponding Ct value of GAPDH subtracted from it, giving ΔCt. Different transporters were then compared as 1/ΔCt. This was performed using probes and primers specific for each nucleoside transporter in both wild-type (Balb/c) and CNT3 (-/-) null mice (n = 3). Significant differences are indicated in the text.

3.3 Immunohistochemistry of mCNT3 in mouse jejunum

Immunohistochemistry images for wild-type CNT3 (+/+) mouse jejunum were collected as described in Section 2.7. As indicated by the arrows, Fig. 3-17A shows specific $mCNT3_{61-84}$ polyclonal antibody staining that was largely confined to brush border membranes, and was absent when no primary antibody was added (Fig. 3-17B), or when the $mCNT3_{61-84}$ antibody was in competition with excess exogenous mCNT3 $peptide_{61-84}$ (Fig. 3-17C).

3.4 Uridine metabolism in mouse jejunal epithelial cells

The metabolism of uridine as it crossed the jejunal epithelium was assessed by thin layer chromatography (TLC). Ussing chamber samples collected from the basolateral medium after incubation of jejunal epithelium in Na^+ KHS medium for 2 h with 1 μM apical ^{3}H-uridine were spotted onto cellulose TLC plates alongside standards containing ^{3}H-uridine and ^{14}C-uracil as described in Section 2.8, and the amounts of radioactivity (counts per minute, CPM) present in 1 cm sections of the chromatograms were determined. Positions of peak radioactivity from the origin divided by the distance traveled by the solvent front enabled calculation of the retention factor (Rf) of the transported species. Fig. 3-18 shows representative sample and standard chromatograms from the same TLC plate. ^{3}H in the sample ran as a single peak with an Rf value of 0.86, compared to 0.88 for standard ^{3}H-uridine and 0.79 for ^{14}C-uracil. The putative identity of ^{3}H in the sample as unmetabolized uridine was confirmed by reruns of the same sample spiked either with ^{14}C-uracil (Fig. 3-19) or ^{14}H-uridine (Fig.3-20). In the same solvent system, UMP was retained at the origin (data not shown).

A

B

C

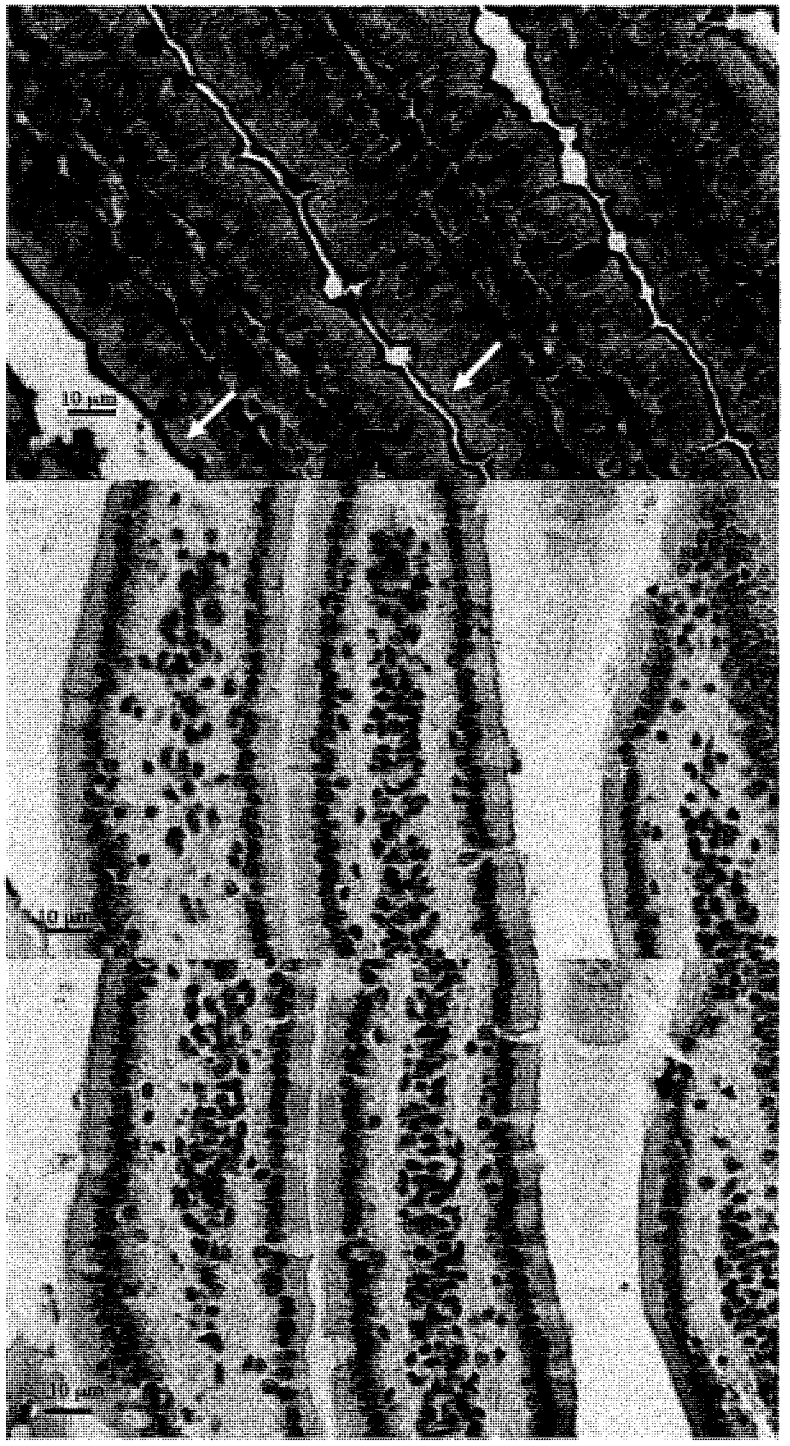

Figure 3-17 Immunohistochemistry of mouse jejunum stained for mCNT3
(A) Jejunum stained with polyclonal mCNT3$_{61-84}$ antibodies (1/10 dilution), (B) control lacking primary antibodies, and (C) control pre-incubated with excess mCNT3 peptide$_{61-84}$. Images were taken at 40X magnification, and show strong specific staining along the brush boarder membrane (indicated by the white arrows).

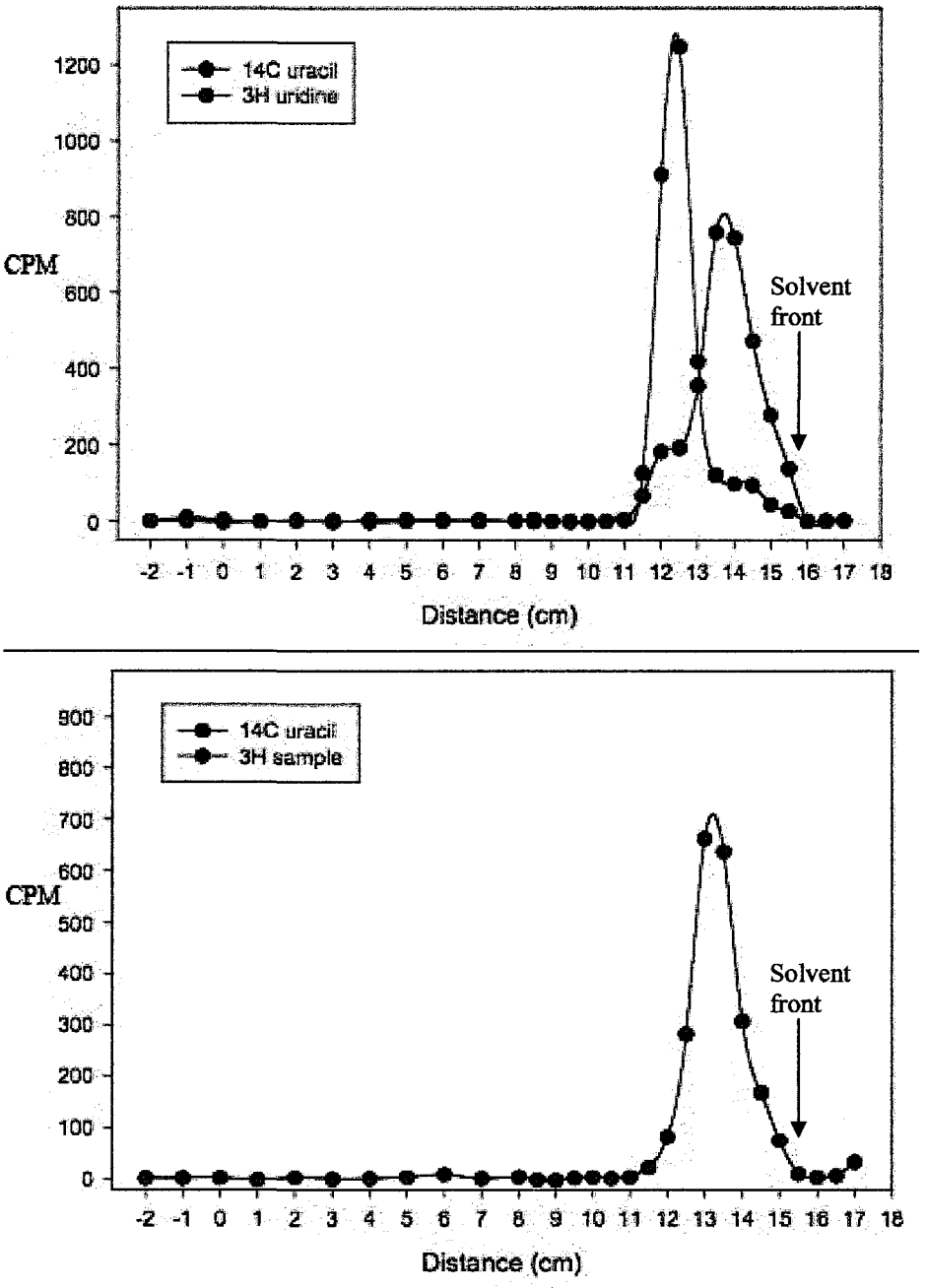

Figure 3-18 Thin layer chromatography of a basolateral Ussing chamber sample following incubation of mouse jejunal epithelium with apical ^{3}H-uridine.
Thin layer chromatography was performed on cellulose TLC plates with LiCl/formic acid as solvent. The graphs show the amounts of radioactivity in 1 cm sections of the chromatograms, where the baseline that the samples were spotted is set at zero, and the solvent front is indicated by the arrow. (*top*) standard chromatogram containing known quantities of both ^{3}H-uridine and ^{14}C-uracil. (*bottom*) basolateral sample chromatogram. Rf values were calculated from the distance traveled from the origin divided by the distance traveled by the solvent front. Note: the minor shoulder peak of ^{3}H-uridine in the top panal is an artifact of scintillation counter spillover from ^{14}C-uracil in the same run.

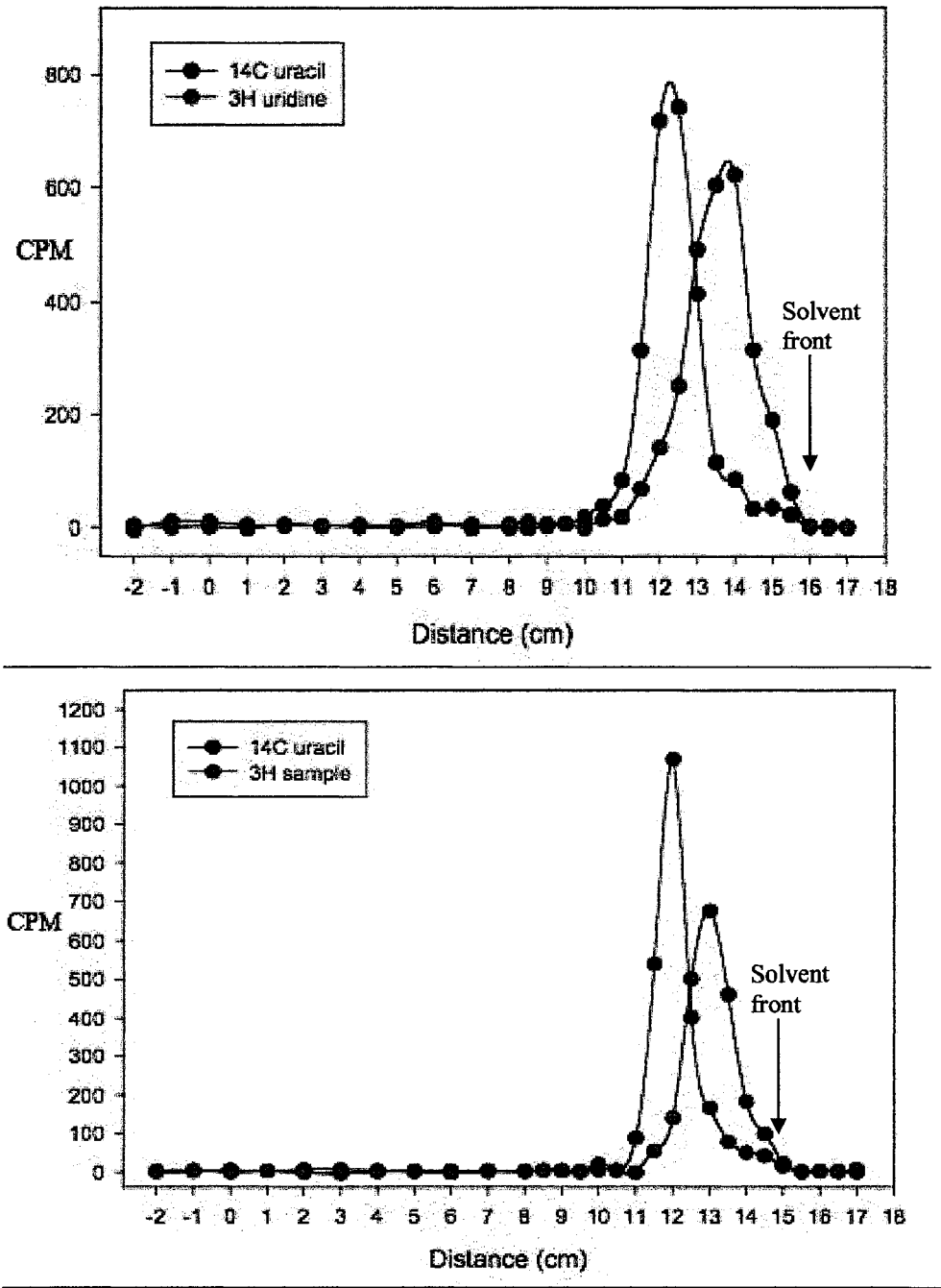

Figure 3-19 Thin layer chromatography of a basolateral Ussing chamber sample spiked with ^{14}C-uracil.

Thin layer chromatography was performed on cellulose TLC plates with LiCl/formic acid as solvent. The graphs show the amounts of radioactivity in 1 cm sections of the chromatograms, where the baseline that the samples were spotted is set at zero, and the solvent front is indicated by the arrow. (*top*) standard chromatogram containing known quantities of both ^{3}H-uridine and ^{14}C-uracil. (*bottom*) chromatogram of a basolateral sample overlaid with ^{14}C-uracil.

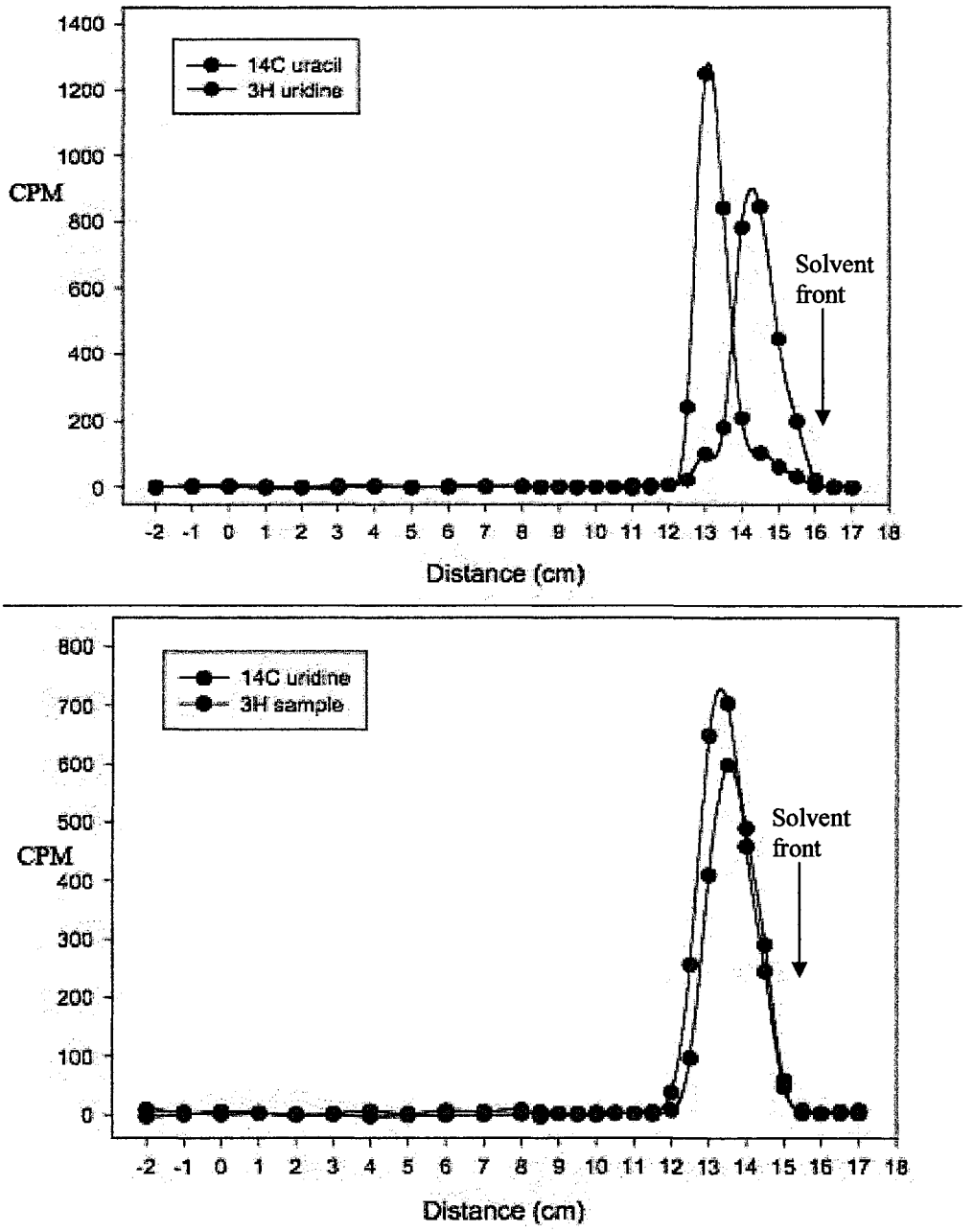

Figure 3-20 Thin layer chromatography of a basolateral Ussing chamber sample spiked with ^{14}C uridine.

Thin layer chromatography was performed on cellulose TLC plates with LiCl/formic acid as solvent. The graphs show the amounts of radioactivity in 1 cm sections of the chromatograms, where the baseline that the samples were spotted is set at zero, and the solvent front is indicated by the arrow. (*top*) standard chromatogram containing known quantities of both ^{3}H-uridine and ^{14}C-uracil. (*bottom*) chromatogram of a basolateral sample overlaid with ^{14}C-uridine. Note: the minor shoulder peak of ^{3}H-uridine in the top panel is an artifact of scintillation counter spillover from ^{14}C-uracil in the same run.

3.5 Tissue accumulation of uridine in mouse jejunal epithelial cells

At the end of apical-to-basolateral ^{3}H-uridine transepithelial flux experiments in Na^+ KHS and Ch^+ KHS media in the absence of added unlabelled nucleoside, the jejunum epithelial tissue was collected and counted for radioactivity as described in Section 2.9. The amount of ^{3}H-uridine trapped in the epithelium after 2 h in Na^+ KHS medium was 210 ± 45 pmol/cm^2, compared to a lower, but not significantly different, value of 159 ± 39 pmol/cm^2 in Ch^+ KHS medium (n = 7). The corresponding amounts of ^{3}H-uridine that crossed the jejunum and appeared on the basolateral side of the tissue in the same experiments were 369 ± 56 pmol/cm^2 in Na^+ KHS medium, and 89 ± 7 pmol/cm^2 in Ch^+ KHS medium (n = 7) ($p < 0.05$). In Na^+ KHS medium, therefore, the majority of ^{3}H-uridine taken up by the tissue was transported across the epithelium, whereas in Ch^+ KHS medium most of the ^{3}H-uridine taken up was retained.

The same analysis was also undertaken for ^{3}H-formycin B. The amount of ^{3}H-formycin B trapped in the epithelium was 69 ± 22 pmol/cm^2 in Na^+ KHS medium, compared to a lower, but not significantly different, value of 51 ± 11 pmol/cm^2 in Ch^+ KHS medium (n = 7). The corresponding amounts of ^{3}H-formycin B that crossed the jejunum and appeared on the basolateral side of the tissue in the same experiments were 175 ± 39 pmol/cm^2 in Na^+KHS medium, and 84 ± 8 pmol/cm^2 in Ch^+ KHS medium (n = 7) ($p < 0.05$). As a metabolically resistant analogue of inosine, therefore, the amounts of ^{3}H-formycin B retained by the tissue were less than for ^{3}H-uridine, and most of the ^{3}H-formycin B taken up by the tissue either in the presence or absence of Na^+ was transported across the epithelium.

Chapter 4 Discussion

Despite its physiological, metabolic and pharmacological significance (Young *et al.*, 2001), and in contrast to the situation with respect to kidney (Elwi *et al.*, 2006), there has been only limited investigation of nucleoside transport in the intestine. Most of these studies have examined either isolated enterocytes, brush border and basolateral membrane vesicles, or recombinant intestinally derived transporters produced in *Xenopus* oocytes (Vijayalakshmi and Belt, 1988; Jarvis, SM., 1989; Betcher *et al.*, 1990; Roden *et al.*, 1991; Huang *et al.*, 1993, 1994; Patil and Unadkat, 1997). Under these conditions, the polarized nature of the intact epithelium was eliminated and, in consequence, the potential for apically- and basolaterally-located nucleoside transporters to contribute to transepithelial movement of nucleosides and nucleoside drugs across the tissue was not fully addressed. Transwell and other monolayer cell culture systems employing, for example, human colonic Caco-2 and rat small intestinal IEC-6 cells are of limited value in this regard because of issues of polarity, differentiation status, and resultant uncertainty that they fully express the correct types and relative activities of apical and basolateral transporters (Jakobs and Paterson, 1986; Jakobs *et al.*, 1990; He *et al.*, 1994; Ward and Tse, 1999; Mun *et al.*, 1998; Aymerich *et al.*, 2004).

Conventionally, the Ussing chamber apparatus is employed in the electrophysiological characterization of transepithelial ion fluxes (Schultheiss and Diener, 1998; Li *et al.*, 2004; Duta *et al*, 2006), and has been used with some success in this regard in intestine (Lam *et al*, 2003; Lam *et al*, 2004; Hayashi *et al.*, 2007; Matos *et al.*, 2007; Zhang *et al.*, 2007a). Such investigations have been greatly facilitated by the

use of a tissue preparation in which the smooth muscle layer attached to the basolateral surface of the intestinal epithelium is dissected away, leaving only the intact epithelium itself to be mounted into the Ussing chamber aperture (Lam *et al*, 2003, Lam *et al*, 2004; Kato *et al*., 2006; Hayashi *et al*., 2007; Zhang *et al*., 2007a). This thesis investigates the use of the same apparatus and tissue preparation in studies of transepithelial fluxes of radiolabelled nucleosides across the mouse intestinal epithelium.

4.1 Transepithelial uridine transport across mouse jejunal epithelium is Na^+-dependent and transporter-mediated

The jejunum is generally considered to be the primary site of nutrient, including nucleosides, absorption from the diet (Young *et al*., 2001). In the present study, it was verified in initial experiments that uridine was primarily moved from the apical side of mouse jejunal epithelium to the basolateral side through transporter-mediated processes. ^{3}H-Uridine (1 μM) was added to the apical side of the Ussing chamber at the start of the experiment, and halfway through (after 50 min) an excess of unlabelled uridine (20 mM) was also added to the apical chamber. As shown in Figure 3-1, the addition of unlabelled uridine substantially reduced the rate of ^{3}H-uridine flux across the jejunal epithelium. Furthermore, this effect was only observed in the presence of Na^+ (Na^+ KHS medium) and not when the experiment was performed under Na^+-free conditions (Ch^+ KHS medium) (Figs. 3-2 and 3-3). The poorly metabolized inosine analog, formycin B, was moved across jejunal epithelium in a similar Na^+-dependent manner (Fig. 3-11).

Uridine is a universal permeant for all human and other mammalian CNTs and ENTs, including murine (m) CNT1-3 and ENT1-4, with apparent transporter affinities in

the μM – low mM range (Section 1.3): therefore, ^{3}H-uridine has the potential to report all possible nucleoside transport activities in the tissue, and self-competition by excess unlabelled uridine will eliminate all transporter-mediated ^{3}H-nucleoside fluxes (Baldwin *et al.*, 2004; Gray *et al.*, 2004). The Na^+-dependent nature of the transepithelial fluxes shown for uridine and formycin B in Figs. 3-2, 3-3 and 3-11 potentially implicate one or more of the three CNTs (mCNT1, mCNT2 and mCNT3) in the process. In these and subsequent experiments, the ^{3}H-uridine concentration investigated was 1 μM, a value below the mCNT3 uridine apparent K_m value 18 μM (Drs. SK Loewen and SY Yao, personal communication) (Section 1.3).

For uridine, the residual Na^+-independent component of transepithelial transport was unaffected by excess unlabelled uridine (Fig. 3-3), a finding consistent with non-mediated paracellular movement across the epithelium. Two components therefore contribute to transepithelial uridine fluxes in jejunum: (i) a major transporter-mediated component that is Na^+-dependent, and (ii) a minor Na^+-independent component that is non-mediated. The relative contributions of these two pathways is clearly illustrated in Fig. 3-2, where the transepithelial movement of ^{3}H-uridine in Ch^+ KHS medium in the presence or absence of excess unlabelled uridine exhibited a time course that was parallel to that of the self-inhibited flux of uridine in Na^+ KHS medium. The lack of effect of unlabelled uridine on uridine movement in Ch^+ KHS medium suggests little, if any, apical involvement of mENTs operating in parallel to CNTs in transepithelial uridine transport in jejunum.

A similar situation exists for formycin B, as illustrated in Fig. 3-12. As discussed subsequently in Section 4-5, however, a small additional component of transepithelial

flux that was transporter-mediated, but Na^+-independent was detected for formycin B in experiments where the competing nucleoside was added to the apical chamber at the same time as permeant (Figs. 3-12 and 3-14). This suggests possible operation of a secondary ENT-mediated component of transport.

4.2 The CNT- mediated process occurs at the apical membrane of mouse jejunal epithelium

Evidence that the CNT activity described in Section 4.2 is located at the apical membrane comes from the finding that transepithelial movement of ^3H-uridine in the opposite basolateral-to-apical direction was independent of Na^+, and unaffected by unlabelled uridine (Fig. 3-5). Furthermore, the magnitude of this flux was similar to that of non-mediated, Na^+-independent movement of ^3H-uridine in the opposite apical-to-basolateral direction (Fig. 3-6). The symmetry of this flux in the apical-to-basolateral and basolateral-to-apical directions suggests that the pathway may be paracellular in nature (see also next Section).

Consequently, therefore, Na^+ is required on the apical side of the epithelium for transporter-mediated nucleoside movement across mouse jejunum. Further evidence that the CNT activity involved in transepithelial transport of uridine is apically located comes from immunohistochemistry results shown in Fig. 3-17 (Section 4.6).

4.3 The paracellular component of jejunal uridine flux

To further investigate the nature of the Na^+-independent, non-mediated component of transport, the flux of ^3H-mannitol across the jejunal epithelium was

investigated. Slightly smaller in molecular weight than uridine (182 versus 244), mannitol is the molecule of choice when investigating non-mediated paracellular permeability pathways in epithelia (Pappenheimer, 1990; van Meeteren *et al.*, 1998; Shah *et al.*, 2007). Fig. 3-7 demonstrated that the ^{3}H-mannitol flux across jejunal epithelium was unaffected by the different media used (Na^+ KHS and Ch^+ KHS), was unaltered in the presence of uridine, was much lower in magnitude than the apical-to-basolateral ^{3}H-uridine flux in Na^+ KHS medium, but closely similar to that in Ch^+ KHS medium. It is therefore likely that paracellular movement accounts for the majority of Na^+-independent, non-mediated nucleoside flux observed in Ussing chamber experiments. Passive diffusion of nucleosides across the apical and basolateral membranes of enterocytes may contribute secondarily to non-mediated flux of nucleosides since there was a small, but statistically significant, difference in uridine-Ch^+ KHS and mannitol-Ch^+ KHS transepithelial transfer rates. This difference was not apparent, however, when comparing uridine-Ch^+ KHS and mannitol-Na^+ KHS transepithelial transfer rates, so the contribution of passive diffusion fluxes to overall transepithelial movement, if any, is minor.

Mannitol fluxes also allowed an assessment of tissue integrity. Whether or not the rates of ^{3}H-mannitol and non-mediated ^{3}H-uridine transfer seen in the present experiments correspond in magnitude to the rates of paracellular movement *in vivo*, it is clear from Fig. 3-7, for example, that tissue integrity was sufficient to enable the demonstration and subsequent characterization of trans-cellular fluxes of radiolabelled nucleosides across the intestinal epithelium. This isotopic measure of tissue integrity is in addition to, and independent of that provided by measurements of short circuit current (I_{sc}) and transepithelial resistance (TER), both of which were monitored continuously

throughout flux assay experiments, but which alone may be insufficient to fully predict tissue integrity (Mukherjee *et al.*, 2004).

4.4 Uridine transport across the mouse intestinal epithelium occurs primarily at the jejunum

The investigations discussed above focused on movement of uridine and formycin B across the jejunal epithelium, considered to be the primary region from which nucleosides are absorbed from the intestinal lumen (Roden *et al.*, 1991; Young *et al.*, 2001). This was confirmed in experiments which, for the first time, systematically compared uridine fluxes across epithelium prepared from mouse duodenum, jejunum, ileum and colon (Fig. 3-4). Of the four tissue regions examined, only two, jejunum and the adjoining ileum exhibited detectable Na^+-dependent transport function, with jejunum > ileum. Subsequent studies to further explore the mechanism(s) of transepithelial nucleoside transport therefore focused on jejunum.

4.5 Nucleoside transport across mouse jejunal epithelium is largely mCNT3-mediated

4.5.1 Thymidine and inosine inhibit transepithelial uridine flux

It has already been established that a CNT-mediated process at the apical membrane of mouse jejunal epithelial tissue is responsible for the majority of transepithelial uridine flux. The identity of the specific transporter or transporters responsible for this Na^+-dependent transport capability was examined in cross-competition experiments in which apical-to-basolateral transport of ^{3}H-uridine or ^{3}H-formycin B in the presence or absence of Na^+ was determined in the presence of a

competing unlabelled nucleoside also added to the apical chamber. The concentration of the competing unlabelled nucleoside used was 1 mM. Consistent with the mCNT3 uridine apparent K_m values of 18 μM determined by kinetic analysis of the recombinant transporters produced in *Xenopus* oocytes (Drs. SK Loewen and SY Yao, personal communication) (Section 1.3), uridine self-inhibition studies established that this concentration of uridine was sufficient to cause essentially complete inhibition of jejunal Na^+-dependent transport function, and was equally effective as 5 and 20 mM uridine in this regard (Fig. 3-8). Selection of a concentration of 1 mM for cross-competition experiments avoided possible low-affinity inhibition of transporters for which the selected nucleoside competitor was not a physiological permeant. At high concentrations, for example, cells expressing purine nucleoside-selective mCNT2 also transport the pyrimidine nucleoside cytidine (Nagai *et al.*, 2006).

By means of these cross-competition experiments, it was established that unlabelled thymidine completely blocked Na^+ dependent ^{3}H-uridine transport across mouse jejunal epithelium (Fig. 3-9). Inosine was also inhibitory, but incompletely and a small fraction of Na^+ dependent ^{3}H-uridine transport activity remained in the presence of 1 mM inosine (Fig. 3-10). CNT1, CNT2 and CNT3 have affinity for uridine, whereas CNT2 and CNT3 have affinity for inosine, and CNT1 and CNT3 have affinity for thymidine (Griffith and Jarvis, 1996; Young *et al.*, 2001; Gray *et al.*, 2004; Kong *et al.*, 2004). Taken together, therefore, the observed cross-inhibition of Na^+ dependent ^{3}H-uridine transport activity by thymidine and inosine indicate major involvement of mCNT3 (that component of Na^+ dependent ^{3}H-uridine transport inhibited by both thymidine and inosine), with possible minor participation of mCNT1 (that fraction of

thymidine-sensitive ^{3}H-uridine transport that was not inhibited by inosine). Since it has been reported that inosine is extensively metabolized by intestinal epithelial cells (Roden *et al.*, 1991), it is also possible that local concentrations of inosine at the apical surface were insufficient to cause complete inhibition of mCNT3 function. If this were the case, the already major contribution of mCNT3 to overall Na^{+} dependent ^{3}H-uridine transport activity would be even greater.

Complementary to these ^{3}H-uridine cross-inhibition experiments, the ability of mouse jejunal epithelium to transport ^{3}H-formycin B was also examined. Formycin B is an analog of the purine nucleoside inosine, and is therefore transported by CNT2 and/or CNT3 (Young *et al.*, 2001; Gray *et al.*, 2004; Zhang *et al.*, 2005). Formycin B was used in preference to inosine, because formycin B is not phosphorylated or degraded by mammalian cells (Vijayalakshmi and Belt, 1988; Plagemann and Woffendin, 1989; Roden *et al.*, 1991). As discussed previously in Section 4.1, and shown in Figs. 3-11 and 3-12, the overall characteristics of ^{3}H-formycin B transport were similar to those of ^{3}H-uridine. In particular, there was a component of the transepithelial flux of ^{3}H-formycin B that was both Na^{+}-dependent and transporter-mediated (*i.e.* inhibited in the presence of excess (20 mM) unlabelled uridine) (Fig. 3-11). Consistent with mCNT3 involvement, this flux was also inhibited by 1 mM thymidine (Fig. 3-12). Additionally, thymidine inhibition revealed a small component of the ^{3}H-formycin B transepithelial flux in Ch^{+} KHS medium that was also transporter-mediated, indicating possible operation of a secondary ENT-mediated component of transport. This latter component of transport was not evident in experiments where the competing nucleoside was added at the mid-way point of the experiment (e.g. Fig. 3-11), and was only evident in circumstances such

as Fig. 3-12 where full 2h time courses of permeant uptake (± competing unlabelled nucleoside) were undertaken in parallel.

In conclusion, therefore, the results of experiments discussed in this section are consistent with major apical involvement of mCNT3, with possible minor apical contributions from mCNT1 and mENT1 and/or mENT2. As a correlate to these studies, *cib*-type (*i.e.* CNT3) functional activity was the major component of nucleoside transport activity found in *Xenopus* oocytes microinjected with mRNA extracted from rat jejunal epithelial scrapings (Huang *et al.*, 1993), and the cDNA encoding rat (r) CNT1 was first isolated from a jejunal cDNA library (Huang *et al.*, 1994).

4.5.2 Lack of Na^+-dependent transport activity in CNT3(-/-) null mice

A caveat of cross-inhibition studies such as those undertaken in the present study is that the observed inhibition of transepithelial fluxes might reflect events at the internal aspect of the basolateral membrane of the enterocyte instead of externally at the cell's apical membrane. For example, apical mCNT1 and mCNT2 might functionally combine to accumulate thymidine and inosine within enterocytes, which might then block mENT1/2-mediated exit of ^{3}H-uridine or ^{3}H-formycin B across the basolateral membrane of the cell. Previous studies of isolated mouse enterocytes in which both *cit* (mCNT1) and *cif* (mCNT2) functional activities were demonstrated (Vijayalakshmi and Belt, 1988) support such an interpretation. Independent evidence in support of the conclusion that most nucleoside flux was through mCNT3 came from transepithelial ^{3}H-uridine flux experiments in CNT3 (-/-) null mice, which exhibited a complete absence of Na^+-dependent transport function, with the possible exception of a minor residual component of mCNT1 activity (Figs. 3-13 and 3-14).

Most of the wild-type experiments undertaken in the present study used Balb/c mice. Figs. 3-13 and 3-14 include a control CNT3 (+/+) mouse with the same FVB/N genetic background as the mCNT3 (-/-) null mice to confirm that wild-type Balb/c and FVB/N mice exhibit similar transport characteristics. mCNT3 is therefore established to be a primary participant in trans-cellular transport of nucleosides across mouse jejunal epithelium.

The reason(s) for the discrepancy between the previous study of isolated mouse enterocytes (Vijayalakshmi and Belt, 1988), which implicated mCNT1 and mCNT2 in Na^+-dependent thymidine and formycin B transport activities, and the present findings is not known, although the former study predates the discovery of the *cib* (later CNT3) transporter (Wu *et al.*, 1992; Belt *et al.*, 1993; Huang *et al.*, 1993). In a more recent study, rat small intestinal IEC-6 cultured cells have similarly been reported to express rCNT1/2 functional activity (Aymerich *et al.*, 2004).

4.6 CNT and ENT transcripts in mouse jejunal epithelium

Fig. 3-16 displays real time RT-PCR results for all seven nucleoside transporters in Balb/c wild-type and CNT3 (-/-) null mouse jejunal epithelia. Transcripts for the four ENTs and the three CNTs were present at significant levels, with mCNT2 > mCNT1 > mCNT3 and mENT1-4. mCNT transcript levels did not therefore correlate with functional activity, except in the case of mCNT3 (-/-) null mice, where no mCNT3 message, as expected, was present. The high level of mCNT2 transcripts shown in Fig. 3-16 for isolated jejunal epithelium was consistent with previous reports of nucleoside transporter gene expression in intact intestinal tissue (Lu *et al.*, 2004; Kim *et al.*, 2007).

Other than a very modest increase in mCNT1 transcripts, there was no evidence that loss of mCNT3 function was compensated by increased expression of any of the genes encoding the other nucleoside transporters.

4.7 Apical expression of mCNT3 protein in mouse jejunal enterocytes

The vectorial nature of transepithelial Na^+-dependent ^3H-uridine transport shown in Figs. 3-5 and 3-6 locates mCNT3 to the apical membrane of mouse jejunal enterocytes. Immunohistochemistry confirmed this conclusion (Fig. 3-17). In this thesis, therefore, mouse jejunal enterocytes have been shown to possess (i) apically expressed mCNT3 functional activity, (ii) mCNT3 transcript, and (iii) apically expressed mCNT3 protein.

4.8 Metabolism of uridine during transepithelial transport

During the Ussing chamber ^3H-uridine flux assay experiments described in this thesis, samples were taken from the opposite side of the epithelium from where the ^3H-urdine was added. It was possible that the ^3H collected in the basolateral chamber following apical-to-basolateral transfer was no longer ^3H-uridine as the result of intracellular metabolism within jejunal epithelial cells. To investigate this possibility, ^3H samples from the basolateral side of the Ussing chamber experiments were analyzed by thin layer chromatography (TLC), and compared to the relative mobilities of uridine and the uridine metabolites uracil and UMP (as a representative of uridine phosphorylation products). Figs. 3-18 – 3-20 show that basolateral ^3H migrated as a single symmetrical peak with an R_f value consistent with unmetabolized uridine. While clearly not phosphorylated or in the form of uracil, the fact that sample ^3H co-chromatographed with

authentic uridine, but close to the solvent front, requires verification by other TLC (or HPLC) protocols (Williams *et al.*, 1989; Williams and Jarvis, 1991; Huang *et al.*, 1993; Errasti-Murugarren *et al.*, 2007). The finding that uridine likely crosses the jejunal epithelium intact, implies the presence of basolateral mENT1 and/or mENT2 to facilitate exit across the basolateral membrane. The ability of formycin B, a metabolically resistant analog of inosine, to also cross the epithelium supports this conclusion. In previous studies, 70% of uridine taken up by isolated enterocytes was recovered as uracil (Vijayalakshmi and Belt, 1988). Uracil was similarly the major product detected on the basolateral side of cultured Caco-2 intestinal cells following apical application of uridine (He *et al.*, 1994). The intact epithelium, therefore, likely preserves the metabolic integrity of uridine to a greater extent than isolated cell systems.

At the end of apical-to-basolateral ^{3}H-uridine and ^{3}H-formycin B flux experiments, the epithelium was collected and counted for ^{3}H trapped within the tissue. The results showed that in Na^{+} KHS medium, approximately two-thirds of all ^{3}H-uridine taken up by the tissue was released to the basolateral side, with one-third trapped inside the epithelial cells in an unknown form. The chemical nature of this ^{3}H was not examined. Lower levels of tissue accumulation were found for ^{3}H-formycin B, and for both permeants there was no significant difference in tissue accumulation in the presence and absence of Na^{+}. Because it is poorly metabolized, tissue levels of ^{3}H-formycin B are more likely to reflect nucleoside analogue levels within the enterocyte interior. If so, and because steady-state accumulation reflects the interplay of transport across both apical and basolateral membranes, it is not necessarily to be expected that Na^{+} would lead to elevated concentrations of permeant within the cell.

4.9 Future Directions

The main goals of the experiments described in this thesis were (i) to establish the utility of the Ussing chamber apparatus to investigate the nature of transepithelial fluxes of radiolabelled nucleosides across the intestinal epithelium, and (ii) to initiate investigation of the mechanisms involved. Both these goals have been achieved. Contrary to expectations from the literature (*e.g.* Vijayalakshmi and Belt, 1988), but in parallel with recent findings in human kidney (Damaraju *et al.*, 2007; Elwi *et al.*, 2008), the broadly selective pyrimidine and purine nucleoside transporter mCNT3 has been shown to play a major role in the process. Cation-coupled and apically located, this transporter functions to complete the first half of the translocation process and transport luminal nucleosides across the enterocyte apical membrane into the cell interior. Completion of the translocation processs requires participation of other transporters located in the basolateral membrane. Driven by Na^+ (and in the case of CNT3, H^+) electrochemical gradients, CNTs function as concentrative inwardly-directed transporters, whereas ENTs are bidirectional, transporting nucleosides down their concentration gradients. ENTs, and especially ENT1 and/or ENT2, are therefore the likely basolateral partners in the process, a suggestion supported by studies on enterocyte basolateral membrane vesicles (Williams *et al.*, 1989; Betcher *et al.*, 1990). This can be readily tested in the Ussing chamber system in a number of ways. For example, NBMPR, an inhibitor of mENT1 (Yao *et al.*, 1997; Sundaram et al., 2001a; Baldwin *et al.*, 2004), could be applied to the basolateral surface during mouse jejunal apical-to-basolateral flux assay experiments. Similarly, dipyridimole, an inhibitor of both mENT1

and mENT2 (Kiss *et al.*, 2000), could be applied to the basolateral surface during flux assay experiments. Basolateral membrane function could be isolated in such experiments either by use of membrane-impermeant nucleoside transport inhibitors (Visser *et al.*, 2007), or by permeablization of the apical membrane (Gross *et al.*, 2001). To confirm the roles of ENTs, mENT1 (-/-) and mENT2 (-/-) null mice are now available (Drs. CE Cass and JD Young, personal communication). Since ENTs are a likely obligatory component to transepithelial nucleoside fluxes, it is probable that mENT1 (-/-) and/or mENT2 (-/-) null mice will exhibit transepithelial transport phenotypes equally as severe as that demonstrated in this thesis for deletion of mCNT3. Since the genes for mCNT3, mENT1 and mENT2 are located on different chromosomes, there is also the possibility of studying transport in tissue from mice with different knockout combinations. The possible presence of secondary mENT activity in the apical membrane also merits further investigation, as does the chemical identity of nucleosides trapped within the epithelium.

In this way, and by incorporating parallel studies of other pyrimidine and purine nucleosides, it will be possible to fully unravel the molecular mechanisms of transepithelial intestinal nucleoside transport and, in so doing, provide insight into the relative importance of intestinal nucleoside transporters for enterocyte metabolic needs and whole body pyrimidine and purine homeostasis. Finally, the Ussing chamber apparatus is ideally suited to the investigation of intestinal anticancer and antiviral nucleoside drug transport and metabolism. As reviewed in Section 1.4 a number of such drugs are administered orally, but their mechanisms of absorption are poorly understood.

4.10 Conclusions

This study is the first to analyze transepithelial fluxes of nucleosides across the intact intestinal epithelium of mice. Using the Ussing Chamber apparatus, it was shown that radiolabelled uridine and formycin B apical-to-basolateral fluxes were transporter mediated and mostly Na^+-dependent. It was also demonstrated that transport was most prominent in jejunum, and vectorial in nature. Multiples lines of evidence, including studies of mCNT3 (-/-) null mice, implicated apical mCNT3 in the process. The CNT3 transporter isoform is ideally suited for this purpose, having (i) a broad permeant selectivity for both purine and pyrimidine nucleosides (*i.e.* functionally equivalent to CNT1 and CNT2 combined), (ii) an enhanced thermodynamic ability to drive nucleoside entry across the enterocyte apical membrane (2:1 Na^+:nucleoside coupling stoichiometry versus 1:1 for CNT1/2), and (iii) an ancillary ability to couple nucleoside uptake to the H^+ electrochemical gradient (enterocytes experience an acidic apical microenvironment) (Ritzel *et al.*, 2001; Damaraju *et al.*, 2005).

By demonstrating trans-cellular transport of poorly metabolized formycin B and by providing evidence that uridine is likely transported across the intestinal epithelium intact, there is presumptive evidence for the presence of the ENT transporter isoforms ENT1 and/or ENT2 within the enterocyte basolateral membrane. Both ENTs transport a broad range of pyrimidine and purine nucleosides, ENT2 having the additional capability of transporting nucleobases in addition to nucleosides (Section 1.3) (Yao *et al.*, 2002). It must be noted that mENT2 was found not to be permeable to pyrmidine nucleobases, but only to purine nucleobases (Nagai *et al.*, 2007). Evidence consistent with the possible presence of a minor component of apical ENT activity was also presented.

Quantitatively, trans-cellular nucleoside transport exceeded paracellular uridine transport by a margin of 3:1.

The advances reported here exhibit remarkable parallels to recent findings concerning the roles of h/mCNT3 and other nucleoside transporters in human kidney proximal tubule epithelial cells (Damaraju *et al.*, 2007; Elwi *et al.*, 2008). Using radiolabelled uridine and formycin B as illustrative examples, the present study provides proof-of-principle that Ussing chamber methodology, particularly when used in conjunction with genetic approaches, has considerable potential in studies of the intestinal absorption of nutrients and orally administered drugs, including nucleoside analogues used in cancer and viral chemotherapy.

References

Aymerich I, Duflot S, Fernández-Veledo S, Guillén-Gómez E, Huber-Ruano I, Casado FJ, Pastor-Anglada M. "The concentrative nucleoside transporter family (SLC28): new roles beyond salvage?" *Biochem Soc Trans.* 3, no. 1 (2005): 216-9.

Aymerich I, Pastor-Anglada M, Casado FJ. "Long term endocrine regulation of nucleoside transporters in rat intestinal epithelial cells." *J Gen Physiol.* 124, no. 5 (2004): 505-12.

Baldwin SA, Beal PR, Yao SY, King AE, Cass CE, Young JD. "The equilibrative nucleoside transporter family, SLC29." *Pflugers Arch. Eur. J. Physiol.* 447, no. 5 (2004): 735-43.

Baldwin SA, Yao SY, Hyde RJ, Ng AM, Foppolo S, Barnes K, Ritzel MW, Cass CE, Young JD. "Functional characterization of novel human and mouse equilibrative nucleoside transporters (hENT3 and mENT3) located in intracellular membranes." *J Biol Chem.* 280, no. 16 (2005): 15880-7.

Barnes, K., Dobrzynski, H., Foppolo, S., Beale, P.R., Ismat, F., Scullion, E.R., Sun, L., Tellez, J., Ritzel, M.W., Claycomb, W.C., Cass, C.E., Young, J.D., Billeter-Clark, R., Boyett, M.R. and Baldwin, S.A. Distribution and functional characterization of equilibrative nucleoside transporter-4, a novel cardiac adenosine transporter activated at acidic pH. *Circ. Res.* 99 (2006): 510-519.

Belt JA, Marina NM, Phelps DA, Crawford CR. "Nucleoside transport in normal and neoplastic cells." *Adv Enzyme Regul.* 33 (1993): 235-52.

Betcher SL, Forrest JN Jr, Knickelbein RG, Dobbins JW. "Sodium-adenosine cotransport in brush-border membranes from rabbit ileum." *Am J Physiol. 1990* 259, no. 3 pt. 1 (1990): G504-10.

Bronk JR, Hastewell JG. "The transport and metabolism of naturally occurring pyrimidine nucleosides by isolated rat jejunum." *J Physiol.* 395 (1988): 349-61.

Cao D, Leffert JJ, McCabe J, Kim B, Pizzorno G. "Abnormalities in uridine homeostatic regulation and pyrimidine nucleotide metabolism as a consequence of the deletion of the uridine phosphorylase gene." *J Biol Chem.* 280, no. 22 (2005): 21169-75.

Cass CE, Young JD, Baldwin SA. "Recent advances in the molecular biology of nucleoside transporters of mammalian cells." *Biochem Cell Biol.* 76, no. 5 (1998): 761-70.

Che M, Ortiz DF, Arias IM. "Primary structure and functional expression of a cDNA encoding the bile canalicular, purine-specific Na(+)-nucleoside cotransporter." *J Biol Chem.*, no. 270 (1995): 13596-9.

Cheng H, Bjerknes M. "Whole population cell kinetics and postnatal development of the mouse intestinal epithelium." *Anat Rec* 211, no. 4 (1985): 420-6.

Crawford CR, Cass CE, Young JD, Belt JA. "Stable expression of a recombinant sodium-dependent, pyrimidine-selective nucleoside transporter (CNT1) in a transport-deficient mouse leukemia cell line." *Biochem Cell Biol.* 76, no. 5 (1998): 843-51.

Damaraju S, Zhang J, Visser F, Tackaberry T, Dufour J, Smith KM, Slugoski M, Ritzel MW, Baldwin SA, Young JD, Cass CE. "Identification and functional characterization of variants in human concentrative nucleoside transporter 3, hCNT3 (SLC28A3), arising from single nucleotide polymorphisms in coding regions of the hCNT3 gene." *Pharmacogenet Genomics.* 15, no. 3 (2005): 173-82.

Damaraju VL, Elwi AN, Hunter C, Carpenter P, Santos C, Barron GM, Sun X, Baldwin SA, Young JD, Mackey JR, Sawyer MB, Cass CE. "Localization of broadly selective equilibrative and concentrative nucleoside transporters, hENT1 and hCNT3, in human kidney." *Am J Physiol Renal Physiol.* 293, no. 1 (2007): F100-11.

Damaraju, V.L., Damaraju, S., Young, J.D., Baldwin, S.A., Mackey, J.R., Sawyer, M.B. and Cass, C.E. "Nucleoside anticancer drugs: the role of nucleoside transporters in resistance to cancer chemotherapy". *Oncogene.* 22 (2003) :7524-7536.

Dobbins JW, Laurenson JP, Forrest JN Jr. "Adenosine and adenosine analogues stimulate adenosine cyclic 3', 5'-monophosphate-dependent chloride secretion in the mammalian ileum." *J Clin Invest.* 74, no. 3 (1984): 929-35.

Duta V, Duta F, Puttagunta L, Befus AD, Duszyk M. "Regulation of basolateral Cl(-) channels in airway epithelial cells: the role of nitric oxide." *J Membr Biol.* 213, no. 3 (2006): 165-74.

Elwi AN, Damaraju VL, Baldwin SA, Young JD, Sawyer MB, Cass CE. "Renal nucleoside transporters: physiological and clinical implications." *Biochem Cell Biol.* 84, no. 6 (2006): 844-58.

Elwi AN, Damaraju VL, Kuzma ML, Baldwin SA, Young JD, Sawyer MB, Cass CE. "Human concentrative nucleoside transporter 3 is a determinant of fludarabine transportability and cytotoxicity in human renal proximal tubule cell cultures." *Cancer Chemother Pharmacol.* , May 24 2008 [Epub ahead of print].

Errasti-Murugarren E, Pastor-Anglada M, Casado FJ. "Role of CNT3 in the transepithelial flux of nucleosides and nucleoside-derived drugs." *J Physiol.* 582, no. 3 (2007): 1249-60.

Gati WP, Misra HK, Knaus EE, Wiebe LI. "Structural modifications at the 2'- and 3'-positions of some pyrimidine nucleosides as determinants of their interaction with the mouse erythrocyte nucleoside transporter." *Biochem Pharmacol.* 33, no. 22 (1984): 3325-31.

Gati WP, Paterson AR, Belch AR, Chlumecky V, Larratt LM, Mant MJ, Turner AR. "Es nucleoside transporter content of acute leukemia cells: role in cell sensitivity to cytarabine (araC)." *Leuk Lymphoma.* 32, no. 1-2 (1998): 45-54.
Gerstin KM, Dresser MJ, Wang J, Giacomini KM. "Molecular cloning of a Na+-dependent nucleoside transporter from rabbit intestine." *Pharm Res.* 17, no. 8 (2000): 906-10.

Ghanem E, Lövdahl C, Daré E, Ledent C, Fredholm BB, Boeynaems JM, Van Driessche W, Beauwens R. "Luminal adenosine stimulates chloride secretion through A1 receptor in mouse jejunum." *Am J Physiol Gastrointest Liver Physiol.* 288, no. 5 (2005): G972-7.

Graham KA, Leithoff J, Coe IR, Mowles D, Mackey JR, Young JD, Cass CE. "Differential transport of cytosine-containing nucleosides by recombinant human concentrative nucleoside transporter protein hCNT1." *Nucleosides Nucleotides Nucleic Acids.* 19, no. 1-2 (2000): 415-34.
Gray JH, Owen RP, Giacomini KM. "The concentrative nucleoside transporter family, SLC28." *Pflugers Arch. Eur. J. Physiol.* 447, no. 5 (2004): 728-34.

Griffith DA, Jarvis SM. "Nucleoside and nucleobase transport systems of mammalian cells." *Biochim Biophys Acta.* 1286, no. 3 (1996): 153-81.

Griffiths M, Beaumont N, Yao SY, Sundaram M, Boumah CE, Davies A, Kwong FY, Coe I, Cass CE, Young JD, Baldwin SA. "Cloning of a human nucleoside transporter implicated in the cellular uptake of adenosine and chemotherapeutic drugs." *Nat Med.* 3, no. 1 (1997a): 89-93.

Griffiths M, Yao SY, Abidi F, Phillips SE, Cass CE, Young JD, Baldwin SA. "Molecular cloning and characterization of a nitrobenzylthioinosine-insensitive (ei) equilibrative nucleoside transporter from human placenta." *Biochem J.* 328, no. 3 (1997b): 739-43.

Gross E, Abuladze N, Pushkin A, Kurtz I, Cotton CU. "The stoichiometry of the electrogenic sodium bicarbonate cotransporter pNBC1 in mouse pancreatic duct cells is 2 HCO(3)(-):1 Na(+)." *J Physiol.* 531, no. 2 (2001): 375-82.

Hamilton SR, Yao SY, Ingram JC, Hadden DA, Ritzel MW, Gallagher MP, Henderson PJ, Cass CE, Young JD, Baldwin SA. "Subcellular distribution and membrane topology of the mammalian concentrative Na+-nucleoside cotransporter rCNT1." *J Biol Chem.* 276, no. 30 (2001): 27981-8.

Hayashi M, Kita K, Ohashi Y, Aihara E, Takeuchi K. "Phosphodiesterase isozymes involved in regulation of HCO3- secretion in isolated mouse duodenum in vitro." *Biochem Pharmacol.* 74, no. 10 (2007): 1507-13.

He Y, Sanderson IR, Walker WA. "Uptake, transport and metabolism of exogenous nucleosides in intestinal epithelial cell cultures." *J Nutr.* 124, no. 10 (1994): 1942-9.

Huang QQ, Harvey CM, Paterson AR, Cass CE, Young JD. "Functional expression of Na(+)-dependent nucleoside transport systems of rat intestine in isolated oocytes of Xenopus laevis. Demonstration that rat jejunum expresses the purine-selective system N1 (cif) and a second, novel system N3 having broad specific." *J Biol Chem.* 268, no. 27 (1993): 20613-9.

Huang QQ, Yao SY, Ritzel MW, Paterson AR, Cass CE, Young JD. "Cloning and functional expression of a complementary DNA encoding a mammalian nucleoside transport protein." *J Biol Chem.* 269, no. 27 (1994): 17757-60.

Jakobs ES, Paterson AR. "Sodium-dependent, concentrative nucleoside transport in cultured intestinal epithelial cells." *Biochem Biophys Res Commun.* 140, no. 3 (1986): 1028-35.

Jakobs ES, Van Os-Corby DJ, Paterson AR. "Expression of sodium-linked nucleoside transport activity in monolayer cultures of IEC-6 intestinal epithelial cells." *J Biol Chem.* 265, no. 36 (1990): 22210-6.

Jarvis SM, Griffith DA. "Expression of the rabbit intestinal N2 Na+/nucleoside transporter in Xenopus laevis oocytes." *Biochem J.* 278, no. 2 (1991): 605-7.

Jarvis, SM. "Characterization of sodium-dependent nucleoside transport in rabbit intestinal brush-border membrane vesicles." *Biochim Biophys Acta.* 979, no. 1 (1989): 132-8.

Kato Y, Sugiura M, Sugiura T, Wakayama T, Kubo Y, Kobayashi D, Sai Y, Tamai I, Iseki S, Tsuji A. "Organic cation/carnitine transporter OCTN2 (Slc22a5) is responsible for carnitine transport across apical membranes of small intestinal epithelial cells in mouse." *Mol Pharmacol.* 70, no. 3 (2006): 829-37.

Kim HR, Park SW, Cho HJ, Chae KA, Sung JM, Kim JS, Landowski CP, Sun D, Abd El-Aty AM, Amidon GL, Shin HC. "Comparative gene expression profiles of intestinal transporters in mice, rats and humans." *Pharmacol Res.* 56, no. 3 (2007): 224-36.

King AE, Ackley MA, Cass CE, Young JD, Baldwin SA. "Nucleoside transporters: from scavengers to novel therapeutic targets." *Trends Pharmacol Sci. ad* 27, no. 8 (2006): 416-25.

Kiss A, Farah K, Kim J, Garriock RJ, Drysdale TA, Hammond JR. "Molecular cloning and functional characterization of inhibitor-sensitive (mENT1) and inhibitor-resistant

(mENT2) equilibrative nucleoside transporters from mouse brain." *Biochem J.* 352, no. 2 (2000): 363-72.

Kolachala VL, Obertone TS, Wang L, Merlin D, Sitaraman SV. "Adenosine 2b receptor (A2bR) signals through adenylate cyclase (AC) 6 isoform in the intestinal epithelial cells." *Biochim Biophys Acta.* 760, no. 7 (2006): 1102-8.

Kong W, Engel K, Wang J. "Mammalian nucleoside transporters." *Curr Drug Metab.* 5, no. 1 (2004): 63-84.

Lam RS, App EM, Nahirney D, Szkotak AJ, Vieira-Coelho MA, King M, Duszyk M. "Regulation of Cl- secretion by alpha2-adrenergic receptors in mouse colonic epithelium." *J Physiol.* 548 (2003): 475-84.

Lam RS, Shaw AR, Duszyk M. "Membrane cholesterol content modulates activation of BK channels in colonic epithelia." *Biochim Biophys Acta.* 1667, no. 2 (2004): 241-8.

Li H, Sheppard DN, Hug MJ. "Transepithelial electrical measurements with the Ussing chamber." *J Cyst Fibros* 3, no. Suppl 2 (2004): 123-6.

Lostao MP, Mata JF, Larrayoz IM, Inzillo SM, Casado FJ, Pastor-Anglada M. "Electrogenic uptake of nucleosides and nucleoside-derived drugs by the human nucleoside transporter 1 (hCNT1) expressed in Xenopus laevis oocytes." *FEBS Lett.* 481, no. 12 (2000): 137-40.

Lu H, Chen C, Klaassen C. "Tissue distribution of concentrative and equilibrative nucleoside transporters in male and female rats and mice." *Drug Metab Dispos.* 32, no. 12 (2004): 1455-61.

Mackey JR, Yao SY, Smith KM, Karpinski E, Baldwin SA, Cass CE, Young JD. "Gemcitabine transport in xenopus oocytes expressing recombinant plasma membrane mammalian nucleoside transporters." *J Natl Cancer Inst.* 91, no. 21 (1999): 1876-81.

Mahony WB, Domin BA, McConnell RT, Zimmerman TP. "Acyclovir transport into human erythrocytes." *J Biol Chem.* 263, no. 19 (1988): 9285-91.

Matos JE, Sausbier M, Beranek G, Sausbier U, Ruth P, Leipziger J. "Role of cholinergic-activated KCa1.1 (BK), KCa3.1 (SK4) and KV7.1 (KCNQ1) channels in mouse colonic Cl- secretion." *Acta Physiol (Oxf).* 89, no. 3 (2007): 251-8.

Mukherjee T, Squillantea E, Gillespieb M, Shao J. "Transepithelial electrical resistance is not a reliable measurement of the Caco-2 monolayer integrity in Transwell." *Drug Deliv.* 11, no. 1 (2004): 11-8.

Mun EC, Tally KJ, Matthews JB. "Characterization and regulation of adenosine transport in T84 intestinal epithelial cells." *Am J Physiol.* 274, no. 2 Pt. 1 (1998): G261-9.

Nagai K, Nagasawa K, Koma M, Hotta A, Fujimoto S. "Cytidine is a novel substrate for wild-type concentrative nucleoside transporter 2." *Biochem Biophys Res Commun.* 327, no. 2 (2006): 439-43.

Nagai K, Nagasawa K, Kyotani Y, Hifumi N, Fujimoto S. "Mouse equilibrative nucleoside transporter 2 (mENT2) transports nucleosides and purine nucleobases differing from human and rat ENT2." *Biol Pharm Bull.* 30, no. 5 (2007): 979-81.

Ngo LY, Patil SD, Unadkat JD. "Ontogenic and longitudinal activity of Na(+)-nucleoside transporters in the human intestine." *Am J Physiol Gastrointest Liver Physiol.* 283, no. 3 (2001): G475-81.

PappenheimerJR. "Paracellular intestinal absorption of glucose, creatinine, and mannitol in normal animals: relation to body size." *Am J Physiol.* 259, no. 2 pt 1 (1990): G290-9.

Pastor-Anglada M, Errasti-Murugarren E, Aymerich I, Casado FJ. "Concentrative nucleoside transporters (CNTs) in epithelia: from absorption to cell signaling." *J Physiol Biochem.* 63, no. 1 (2007): 97-110.
Patel DH, Crawford CR, Naeve CW, Belt JA. "Cloning, genomic organization and chromosomal localization of the gene encoding the murine sodium-dependent, purine-selective, concentrative nucleoside transporter (CNT2)." *Gene.* 242, no. 1-2 (2000): 51-8.

Patil SD, Ngo LY, Glue P, Unadkat JD. "Intestinal absorption of ribavirin is preferentially mediated by the Na+-nucleoside purine (N1) transporter." *Pharm Res.* 15, no. 6 (1998): 950-2.

Patil SD, Unadkat JD. "Sodium-dependent nucleoside transport in the human intestinal brush-border membrane." *Am J Physiol.* 272, no. 6 pt. 1 (1997): G1314-20.

Plagemann PG, Woffendin C. "Use of formycin B as a general substrate for measuring facilitated nucleoside transport in mammalian cells." *Biochim Biophys Acta.* 1010, no. 1 (1989): 7-15.

Podgorska M, Kocbuch K, Pawelczyk T. "Recent advances in studies on biochemical and structural properties of equilibrative and concentrative nucleoside transporters." *Acta Biochim Pol.* 52, no. 4 (2005): 749-58.

Polentarutti BI, Peterson AL, Sjöberg AK, Anderberg EK, Utter LM, Ungell AL. "Evaluation of viability of excised rat intestinal segments in the Ussing chamber: investigation of morphology, electrical parameters, and permeability characteristics." *Pharm Res.* 16, no. 3 (1999): 446-54.

Ritzel MW, Ng AM, Yao SY, Graham K, Loewen SK, Smith KM, Ritzel RG, Mowles DA, Carpenter P, Chen XZ, Karpinski E, Hyde RJ, Baldwin SA, Cass CE, Young JD. "Molecular identification and characterization of novel human and mouse concentrative

Na+-nucleoside cotransporter proteins (hCNT3 and mCNT3) broadly selective for purine and pyrimidine nucleosides (system cib)." *J Biol Chem.* 276, no. 4 (2001a): 2914-27.

Ritzel MW, Yao SY, Ng AM, Mackey JR, Cass CE, Young JD. "Molecular cloning, functional expression and chromosomal localization of a cDNA encoding a human Na+/nucleoside cotransporter (hCNT2) selective for purine nucleosides and uridine." *Mol Membr Biol.* 15, no. 4 (1998): 203-11.

Frizzell RA, Schultz SG. "Models of electrolyte absorption and secretion by gastrointestinal epithelia." *Int Rev Physiol.* (1979): 205-25.

Roden M, Paterson AR, Turnheim K. "Sodium-dependent nucleoside transport in rabbit intestinal epithelium." *Gastroenterology* 100, no. 6 (1991): 1553-62.

Sanderson IR, He Y. "Nucleotide uptake and metabolism by intestinal epithelial cells." *J Nutr.* 124, no. 1 Suppl. (1994): 131S-137S.

Sandu C, Rexhepaj R, Grahammer F, McCormick JA, Henke G, Palmada M, Nammi S, Lang U, Metzger M, Just L, Skutella T, Dawson K, Wang J, Pearce D, Lang F. "Decreased intestinal glucose transport in the sgk3-knockout mouse." *Pflugers Arch.Eur. J. Physiol* 451 (2005): 437-444.

Schang LM, Coccaro E, Lacasse JJ. "Cdk inhibitory nucleoside analogs prevent transcription from viral genomes." *Nucleosides Nucleotides Nucleic Acids. 2005;24(5-7):829-37.* 24, no. 5-7 (2005): 829-37.

Schultheiss G, Diener M. "K+ and Cl- conductances in the distal colon of the rat." *Gen Pharmacol.* 31, no. 3 (1998): 337-42.

Schultz SG, Hudson RL, Lapointe JY. "Electrophysiological studies of sodium cotransport in epithelia: toward a cellular model". *Ann N Y Acad Sci.* no. 456 (1985):127-35.

Shah PJ, Jogani VV, Mishra P, Mishra AK, Bagchi T, Misra AR. "Role of 99mTc-mannitol and 99mTc-PEG in the assessment of paracellular integrity of cell monolayers." *Nucl Med Commun* 28, no. 8 (2007): 653-9.

Smith KM, Slugoski MD, Cass CE, Baldwin SA, Karpinski E, Young JD. "Cation coupling properties of human concentrative nucleoside transporters hCNT1, hCNT2 and hCNT3." *Mol Membr Biol.* 24, no. 1 (2007): 53-64.

Stehr W, Mercer TI, Bernal NP, Erwin CR, Warner BW. "Opposing roles for p21(waf1/cip1) and p27(kip1) in enterocyte differentiation, proliferation, and migration." *Surgery* 138, no. 2 (2005): 187-94.

Stow RA, Bronk JR. "Purine nucleoside transport and metabolism in isolated rat jejunum." *J Physiol.* 468 (1993): 311-24.

Sundaram M, Yao SY, Ng AM, Cass CE, Baldwin SA, Young JD. "Equilibrative nucleoside transporters: mapping regions of interaction for the substrate analogue nitrobenzylthioinosine (NBMPR) using rat chimeric proteins." *Biochemistry.* 40, no. 27 (2001): 8146-51.

Sundaram, M., Yao, S.Y.M., Ingram, J.C., Berry, Z.A., Abidi, F., Cass, C.E., Baldwin, S.A. and Young, J.D. Topology of a human equilibrative, nitrobenzylthioinosine (NBMPR)-sensitive nucleoside transporter (hENT1) implicated in cellular uptake of adenosine and anti-cancer drugs. *J. Biol. Chem.* 276, (2001) :45270-45275.

Toan SV, To KK, Leung GP, de Souza MO, Ward JL, Tse CM. "Genomic organization and functional characterization of the human concentrative nucleoside transporter-3 isoform (hCNT3) expressed in mammalian cells." *Pflugers Arch.* 447, no. 3 (2003): 195-204.

Uauy R, Stringel G, Thomas R, Quan R. "Effect of dietary nucleosides on growth and maturation of the developing gut in the rat." *J Pediatr Gastroenterol Nutr.* 10, no. 4 (1990): 497-503.

Ungell AL, Nylander S, Bergstrand S, Sjöberg A, Lennernäs H. "Membrane transport of drugs in different regions of the intestinal tract of the rat." *J Pharm Sci.* 87, no. 3 (1998): 360-6.

Ussing HH, Zerahn K. "Active transport of sodium as the source of electric current in the short-circuited isolated frog skin." *Acta. Physiol. Scand.* 23 (1951): 110-127.

Valdés R, Ortega MA, Casado FJ, Felipe A, Gil A, Sánchez-Pozo A, Pastor-Anglada M. "Nutritional regulation of nucleoside transporter expression in rat small intestine." *Gastroenterology* 119, no. 6 (2000): 1623-30.

van de Kerkhof EG, Ungell AL, Sjöberg AK, de Jager MH, Hilgendorf C, de Graaf IA, Groothuis GM. "Innovative methods to study human intestinal drug metabolism in vitro: precision-cut slices compared with ussing chamber preparations." *Drug Metab Dispos.* 34, no. 11 (2006): 1893-902.

van Meeteren ME, van Bergeijk JD, van Dijk AP, Tak CJ, Meijssen MA, Zijlstra FJ. "Intestinal permeability and contractility in murine colitis." *Mediators Inflamm* 7, no. 3 (1998): 163-8.

Vijayalakshmi D, Belt JA. "Sodium-dependent nucleoside transport in mouse intestinal epithelial cells. Two transport systems with differing substrate specificities." *J Biol Chem.* 263, no. 36 (1988): 19419-23.

Visser F, Sun L, Damaraju V, Tackaberry T, Peng Y, Robins MJ, Baldwin SA, Young JD, Cass CE. "Residues 334 and 338 in transmembrane segment 8 of human equilibrative nucleoside transporter 1 are important determinants of inhibitor sensitivity, protein folding, and catalytic turnover." *J Biol Chem.* 289, no. 19 (2007): 14148-57.

Wang J, Su SF, Dresser MJ, Schaner ME, Washington CB, Giacomini KM. "Na(+)-dependent purine nucleoside transporter from human kidney: cloning and functional characterization." *Am J Physiol.* 273, no. 6 Pt. 2 (1997): 1058-65.

Ward JL, Tse CM. "Nucleoside transport in human colonic epithelial cell lines: evidence for two Na+-independent transport systems in T84 and Caco-2 cells." *Biochim Biophys Acta.* 1419, no. 1 (1999): 15-22.

Williams TC, Doherty AJ, Griffith DA, Jarvis SM. "Characterization of sodium-dependent and sodium-independent nucleoside transport systems in rabbit brush-border and basolateral plasma-membrane vesicles from the renal outer cortex." *Biochem J.* 264 (1989): 223-231.

Williams TC, Jarvis SM. "Multiple sodium-dependent nucleoside transport systems in bovine renal brush-border membrane vesicles." *Biochem. J.* 274 (1991): 27-33.
Wright AM, Paterson AR, Sowa B, Akabutu JJ, Grundy PE, Gati WP. "Cytotoxicity of 2-chlorodeoxyadenosine and arabinosylcytosine in leukaemic lymphoblasts from paediatric patients: significance of cellular nucleoside transporter content." *Br J Haematol.* 116, no. 3 (2002): 528-37.

Wu X, Yuan G, Brett CM, Hui AC, Giacomini KM. "Sodium-dependent nucleoside transport in choroid plexus from rabbit. Evidence for a single transporter for purine and pyrimidine nucleosides." *J Biol Chem.* 267, no. 13 (1992): 8813-8.

Yao SY, Ng AM, Muzyka WR, Griffiths M, Cass CE, Baldwin SA, Young JD. "Molecular cloning and functional characterization of nitrobenzylthioinosine (NBMPR)-sensitive (es) and NBMPR-insensitive (ei) equilibrative nucleoside transporter proteins (rENT1 and rENT2) from rat tissues." *J Biol Chem.* 272, no. 45 (1997): 28423-30.

Yao SY, Ng AM, Ritzel MW, Gati WP, Cass CE, Young JD. "Transport of adenosine by recombinant purine- and pyrimidine-selective sodium/nucleoside cotransporters from rat jejunum expressed in Xenopus laevis oocytes." *Mol Pharmacol.* 50, no. 6 (1996): 1529-35.

Yao, S.Y.M., Ng, A.M.L., Sundaram, M., Cass, C.E., Baldwin, S.A. and Young, J.D. Transport of antiviral 3'-deoxy-nucleoside drugs by recombinant human and rat equilibrative, nitrobenzylthioinosine (NBMPR)-insensitive (ENT2) nucleoside transporter proteins produced in *Xenopus* oocytes. *Mol. Membr. Biol.* 18 (2001): 161-167.

Yao SY, Ng AM, Vickers MF, Sundaram M, Cass CE, Baldwin SA, Young JD. "Functional and molecular characterization of nucleobase transport by recombinant human and rat equilibrative nucleoside transporters 1 and 2. Chimeric constructs reveal a role for the ENT2 helix 5-6 region in nucleobase translocation." *J Biol Chem.* 277, no. 28 (2002): 24938-48.

Young, JD., Cheeseman, CI, Mackey, J., Cass, CE, Baldwin, SA. "Molecular mechanisms of nucleoside and nucleoside drug transport." In *Current Topics in Membranes*, 329-358. 2001.

Zhang H, Ameen N, Melvin JE, Vidyasagar S. "Acute inflammation alters bicarbonate transport in mouse ileum." *J Physiol. 2007* 581, no. 3 (2007a): 1221-33.

Zhang J, Smith KM, Tackaberry T, Visser F, Robins MJ, Nielsen LP, Nowak I, Karpinski E, Baldwin SA, Young JD, Cass CE. "Uridine binding and transportability determinants of human concentrative nucleoside transporters." *Mol Pharmacol.* 68, no. 3 (2005): 830-9.

Zhang J, Smith KM, Tackaberry T, Visser F, Robins MJ, Nielsen LP, Nowak I, Karpinski E, Baldwin SA, Young JD, Cass CE. "Uridine binding and transportability determinants of human concentrative nucleoside transporters." *Mol Pharmacol.* 68, no. 3 (2005): 830-9.

Zhang, J., Visser, F., King, K.M., Baldwin, S.A., Young, J.D. and Cass, C.E. The role of nucleoside transporters in cancer chemotherapy with nucleoside drugs. *Cancer Metastasis Rev.* 26 (2007b): 85-110.